Inhibition of Free fatty acid-Induced Insulin Resistance by Rosemary Extract: Investigation of the Mechanisms Involved

Filip Vlavcheski, BSc (Honours)

Submitted in partial fulfillment of the requirements for the degree

Master of Science in Applied Health Sciences

(Health Sciences)

Faculty of Applied Health Sciences

Brock University

St. Catharines, ON

© December 2017

Abstract

Excess of plasma free fatty acids (FFA) are highly associated with insulin resistance and are a major risk factor for the development of type 2 diabetes mellitus. This thesis investigates the effect of rosemary extract and rosemary extract polyphenols carnosic acid (CA), rosmarinic acid (RA) and carnosol (COH) on recovering/blunting FFA-induced insulin resistance in skeletal muscle cells and the mechanism(s) involved. Exposure of L6 myotubes with the FFA palmitate significantly reduced the insulin-stimulated glucose uptake. Most importantly, the insulin-stimulated glucose uptake was restored in the presence of RE and its polyphenols CA, RA and COH. Furthermore, treatment with palmitate increased serine phosphorylation of IRS-1 and significantly decreased the insulin-stimulated phosphorylation of Akt. These effects were completely abolished in the presence of rosemary extract. Additionally, we investigated the effect of palmitate and rosemary extract on the phosphorylation and of JNK, mTOR, P70S6K and AMPK kinases. Our results indicate that palmitate treatment increased the phosphorylation of JNK, mTOR, p70S6K whereas rosemary extract completely abolished this effect. Additionally, rosemary extract increased the phosphorylation of AMPK even in the presence of palmitate. The expression levels of these proteins were not affected by any of the treatments. These results indicate that treatment with rosemary extract attenuated the palmitate-induced phosphorylation of the serine residues of IRS-1, mTOR, p70 S6K and JNK while increasing the phosphorylation of AMPK. Additionally, treatment with RE restored the insulin-stimulated glucose uptake in palmitate-induced insulin resistant cells.

Acknowledgements:

First of all, I would like to express my sincere gratitude to my supervisor Dr. Evangelia Tsiani for her continuous support, patience and guidance through this entire journey. Her encouragement and knowledge contributed immensely towards the quality of my education. I would also like to thank my committee members Dr. Huidi Wang and Dr. Rebecca MacPherson for their valuable comments, advice and suggestions, I truly enjoyed working with both of you. Finally, I would like to thank my amazing friends and family especially my parents and my sister Marija and cousin Katerina for their constant support, inspiration and encouragement. Thank you to my fellow graduate students and to the people working in Litsa's lab, past and present, Hesham Shamshoum, Jessy Moore, Yannis Vlachogiannis, Pauline De Mython, Alina Jaglanian and Mark Megaly. I am beyond grateful to be surrounded by all of you.

Table of Contents:

CHAPTER1: BACKGROUND INFORMATION 1
1.1 Insulin and insulin signaling cascade 1
1.1.1 Insulin 1
1.1.2 Role of insulin in glucose homeostasis 1
1.1.3 Insulin signaling cascade 2
1.1.4 Insulin receptor 5
1.1.5 Insulin receptor substrate 6
1.1.6 Importance of Phosphatidylinositiol-3-kinase in Insulin Signaling 7
1.1.7 Importance of Protein Kinase B (Akt /PKB) in Insulin Signaling 9
1.1.8 Importance of AS160 in Insulin Signaling 10
1.2 Insulin Resistance 12
1.2.1 Muscle Insulin Resistance 13
1.3 Mechanisms Underlying Insulin Resistance 16
1.3.1 Serine phosphorylation of IRS-I and insulin resistance 16
1.3.2 The Glycogen synthase kinase-3 (GSK3) pathway 18
1.3.3 Insulin Resistance and c-Jun N-terrninal Kinase (JNK) 20
1.3.4 Protein Kinase C (PKC) and Insulin Resistance in Skeletal Muscle 22
1.3.5 IKK-NFkB Pathway and Insulin Resistance in Skeletal Muscle 24
1.3.6 mTOR and p70 S6K Pathway and Insulin Resistance in Skeletal Muscle 25
1.3.7 Free Fatty Acids (FFA)-Induced Skeletal Muscle Insulin Resistance 28
1.4 AMP-activated Protein Kinase Pathway (AMPK) 30
1.5 Rosemary and its phenolic compounds 33
1.5.1 Evidence of Anti-Diabetic Effects of Rosemary Extract: In Vitro Studies 35
1.5.2 Evidence of Anti-Diabetic Effects of Rosemary Extract: In Vivo Studies 39
1.5.3 Evidence of Anti-Hyperglycemic Effects of Rosemary: Human studies 45
1.6 Rational 47
1.7 Hypothesis 48
CHAPTER 2: METHODOLOGY 51
2.1 Materials 51

2.2 Cells 51
2.3 Cell Culture Technique 53
2.4 Preparation of Palmitate Stock 55
2.5 Preparation of Rosemary Extract (RE) 55
2.6 Cell Treatment 56
2.7 Glucose Uptake Assay 56
2.8 Preparation of Cell Lysates for Western Blotting 57
2.9 Protein Assay 57
2.10 Western Blot Analysis 58
2.11 Statistical Analysis 58
CHAPTER 3: RESULTS 59
3.1 Rosemary extract restores the insulin-stimulated glucose uptake in palmitate treated muscle cells 59
3.2 Rosemary extract prevents the palmitate-induced Ser307 and Ser636/639 phosphorylation of IRS-1. 60
3.3 Rosemary extract restores the insulin-stimulated Akt phosphorylation in palmitate treated myotubes 63
3.4 Rosemary extract prevents the palmitate-induced phosphorylation of JNK in L6 66
myotubes 66
3.5 Rosemary extract prevents the palmitate-induced phosphorylation of mTOR in L6..... 69
myotubes 69
3.6 Rosemary extract prevents the palmitate-induced phosphorylation of p70 S6K in L6..... 71
Myotubes..... 71
3.7 Rosemary extract stimulates the phosphorylation of AMPK in the presence of palmitate.. 73
3.8 Carnosic acid, a polyphenol in rosemary extract, restores the insulin-stimulated glucose uptake in palmitate treated muscle cells 75
3.9 Rosmarinic acid, a polyphenol found in rosemary extract restores the insulin-stimulated glucose uptake in palmitate treated muscle cells 76
3.10 Carnosol, a polyphenol found in rosemary extract restores the insulin-stimulated glucose uptake in palmitate treated muscle cells 78
CHAPTER 4: DISCUSSION 79
4.1 Rosemary extract ameliorates palmitate-induced insulin resistance 79
4.2 Investigating the Mechanism of Action of RE and its Polyphenols in Insulin Resistant Myotubes..... 80
4.3 Summary/Conclusion 91

4.4 Future Directions 92
REFERENCE:..... 94
Appendix:..... 119

LIST OF TABLES

Table 1: Kinases involved in different serine phosphorylation sites of IRS-1 18

Table 2: Anti-diabetic effects of RE and its main polyphenolic constituents: *in vitro* studies 38

Table 3: Anti-diabetic effects of RE and its main polyphenolic constituents: *in vivo* studies 43

Table 4: Anti-diabetic and antioxidant properties of RE: Human studies 46

LIST OF FIGURES

Figure 1: The effect of insulin on its target tissues to regulate blood glucose homeostasis 2

Figure 2: Insulin signaling pathway leading to translocation of GLUT4 to the plasma membrane in skeletal muscle 4

Figure 3: Proposed mechanism of FFA-induced insulin resistance in skeletal muscle 14

Figure 4: Rosemary extract restores insulin-stimulated glucose uptake in palmitate treated muscle cells 60

Figure 5: Effects of palmitate and RE on IRS-l expression and Ser307, Ser636/639 phosphorylation. 63

Figure 6: Effects of palmitate and RE on Akt expression and Ser473 and Thr308 phosphorylation. 66

Figure 7: Effects of palmitate and RE on JNK expression and phosphorylation. 69

Figure 8: Effects of palmitate and RE on mTOR expression and phosphorylation. 71

Figure 9: Effects of palmitate and RE on p70 S6K expression and phosphorylation 73

Figure 10: Effects of palmitate and RE on AMPK expression and phosphorylation. 75

Figure 11: Carnosic acid, a polyphenol in rosemary extract, restores insulin-stimulated glucose uptake in palmitate treated muscle cells. 76

Figure 12: Rosmarinic acid, a polyphenol in rosemary extract, restores insulin-stimulated glucose uptake in palmitate treated muscle cells. 77

Figure 13: Carnosol, a polyphenol in rosemary extract, restores insulin-stimulated glucose uptake in palmitate treated muscle cells. 79

List of Abbreviations:

ACC: acetyl CoA carboxylase

AICAR: 5-Aminoimidazole-4-carboxamide ribonucleotide 5’

AMP: adenosine monophosphate

AMPKK: AMPK kinase

AMPK: AMP-activated kinase

CA: carnosic acid

CaMKK: Ca2+/calmodulin kinase kinase

CAT: catalase

COH: carnosol

DAG: diacylglycerol

EGP: endogenous glucose production

ELISA: enzyme-linked immunoassorbant assay

ER: Endoplasmic reticulum

FFA: free fatty acid

G6Pase: glucose-6-phosphatase

Gab-1: GRB2-associated-binding protein 1

GDM: gestational diabetes mellitus

GLUTs: glucose transporters

GPx: glutathione peroxidase

GSK3: glycogen synthase kinase 3

GSV: storage vesicle

GU: Glucose uptake

HFF: high fat fed

HFR: high fructose fed

HSL: hormone sensitive lipase

IGF-1,-2: insulin-like growth factors-1, -2

IGT: impaired glucose tolerance

IKK: inhibitor Iκβ Kinase

IL-6: interleukin-6

IR: insulin resistance

IRS: insulin receptor substrate

JNK: c-Jun-N-terminal kinase

LCACoAs: long chain fatty acyl CoAs

LKB1: liver kinase B1

MAPK: mitogen activated protein kinase

MDA: malonadialdehyde

MEFs: mouse embryonic fibroblasts

mTOR: mammalian target of rapamycin

NOS: nitric oxide synthase

p70S6K: p70S6 ribosomal protein kinase

PDK1: 3-phosphoinositide dependent protein kinase-1

PH: pleckstrin homology

PI3K: phosphatidylinositol-4,5-bisphosphate-3-kinase

PIP2: Phosphatidylinositol 4,5-bisphosphate

PIP3: Phosphatidylinositol (3,4,5)-triphosphate

PKA: protein kinase B (Akt)

PKC: protein kinase C

PGC-1: Peroxisome proliferator-activated receptor-gamma coactivator-1

PL: pancreatic lipase

PP1: protein phosphatase 1

PPARγ: peroxisome proliferator-activated receptors (PPARs)

RA: rosmarinic acid

RE: rosemary extract

siRNA: small interference RNA technique

SH2: Src homology 2

SOD: superoxide dismutase

STZ: streptozotocin

T1DM: type 1 diabetes mellitus

T2DM: type 2 diabetes mellitus

TSC1/2: tuberous sclerosis complex 1/2

CHAPTER1: BACKGROUND INFORMATION

1.1 Insulin and insulin signaling cascade

1.1.1 Insulin

Insulin is a pleiotropic protein hormone mainly involved in maintaining glucose homeostasis and lowering postprandial glucose elevations by endorsing fat and skeletal muscle tissue glucose uptake from the circulation in addition to inhibiting endogenous glucose production (EGP) by the liver (1) (Figure 1). It was first discovered by Banting and Best in 1922 at the University of Toronto, Canada (2). Insulin is produced by the pancreatic β-cells in the islets of Langerhans. The half-life of insulin is around 5 minutes and is cleared by receptor-mediated endocytosis and degraded by lysosomal insulinase. After insulin is secreted and delivered to its target tissues, it binds its receptors located in the plasma membrane leading to activation of signaling cascades that result in the hormone's effect.

1.1.2 Role of insulin in glucose homeostasis

Insulin plays a critical role in maintaining blood glucose homeostasis (Figure 1). After meal ingestion, there is a rise in blood glucose. This increase in blood glucose is sensed by the β cells of the islets of Langerhans in the pancreas and leads to insulin secretion into the blood circulation. Circulating insulin then binds to its receptors located on the plasma membrane of insulin target tissues such as skeletal muscle, adipose and hepatic tissue restoring physiologically normal levels of blood glucose (euglycemia). In skeletal muscle and adipose tissue, insulin promotes transport and utilization of glucose as well as storage in the form of glycogen and triglycerides respectively (3,4). On the

other hand, in the liver, insulin inhibits endogenous glucose production by inhibiting gluconeogenesis and glycogenolysis (Figure 1). The end result of the insulin actions is to maintain and restore plasma glucose levels within a physiological range of 4-7 millimolar (mM).

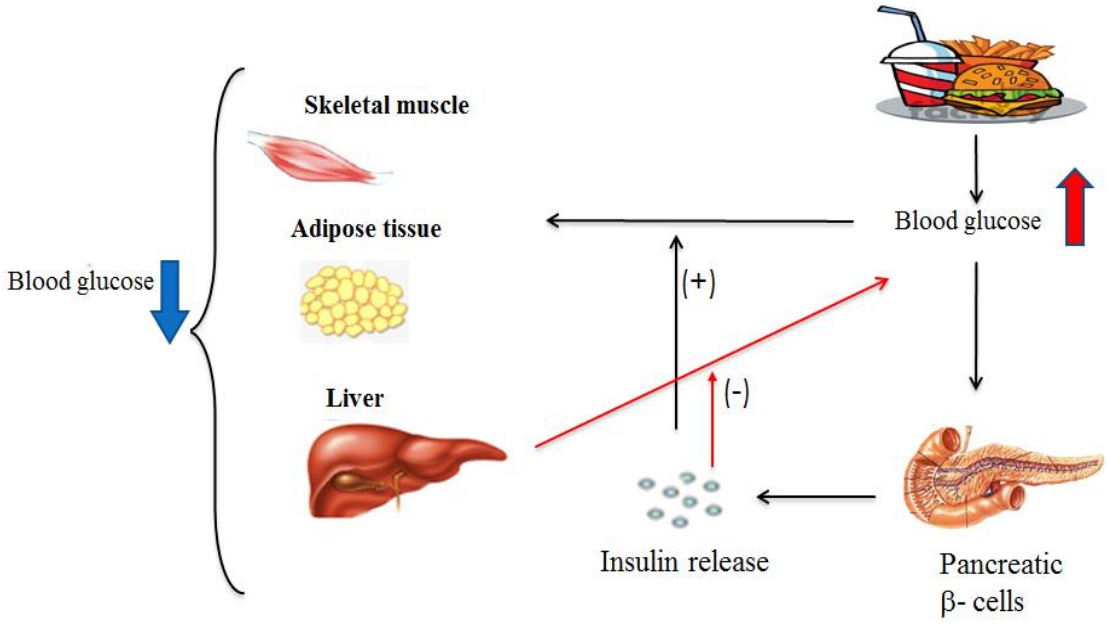

Figure 1: The effect of insulin on its target tissues to regulate blood glucose homeostasis

1.1.3 Insulin signaling cascade

Insulin action is initiated by insulin binding to its receptor leading to an increase in the receptor's tyrosine kinase activity towards intracellular substrates. When insulin binds to the α subunit of the receptor, it causes a conformational change allowing for autophosphorylation of the β subunit leading to an increase in the intrinsic tyrosine kinase activity domain of the receptor. The activation of the insulin receptor leads to phosphorylation of numerous intracellular substrates on tyrosine residues which includes

members of the insulin receptor substrate family (IRS) (Figure 2). Furthermore, the p85 regulatory subunit of phosphatidylinositol-4,5-bisphosphate-3-kinase (PI3K) binds to tyrosine phosphorylated residues of IRS resulting in increased activity of its catalytic subunit p110. Activation of PI3K leads to generation of lipid phosphatidylinositol 3,4,5-triphosphate (PIP3) from phosphatidylinositol 4,5-diphosphate (PIP2). Increased levels of PIP3 bind to phosphatidylinositol-3,4,5-phosphate-dependent kinase-1 (PDK-1) and protein kinase B (PKB/Akt) (5). PKB/Akt and PDK-1 proximate to the cell plasma membrane allowing phosphorylation of PKB/Akt on threonine308 by PDK-1 (5). Glucose uptake, glycolysis, glycogen/ protein synthesis and other insulin actions are mediated by PKB/Akt (6,7). The established substrates of PKB/Akt include a) glycogen synthase kinase-3; b) the Rab GTPase activating protein AS160/TBC1D4 involved in glucose transport and glucose transporters (GLUT) translocation to the cell membrane. c) Rheb GTPase activating tumor suppressor complex (1/2) (TSC1/2) involved in protein synthesis and a regulator of mammalian target of rapamycin (mTOR); d) Transcription factors Forkhead box protein (FoxO) mainly involved in the regulation of gluconeogenic genes (8,9). Insulin-stimulated phosphorylation of Akt leads to downstream phosphorylation of its substrate AS160 which causes inhibition of its Rab-GTPase activating protein (Rab-GAP) activity and has been established as a key component necessary for the GLUT4 translocation from an intracellular compartment to the plasma membrane (9,10) (Figure 2). Therefore, exposure of muscle and adipocytes to insulin leads to dramatic increase in GLUT4 translocation from the intracellular vesicles to the cell membrane via exocytosis and reducing GLUT4 internalization. The end result of this process is GLUT4 translocation to the cell membrane providing a route for glucose entry

down the concentration gradient via facilitated diffusion. Once transported inside the cell, glucose is converted to glucose-6-phosphate by the action of hexokinase following isomerization of glucose-6-phosphate to glucose-1-phosphate and activation to uridine-5-diphosphate glucose which is later turned into glycogen by glycogen synthase. Insulin mediates glycogen deposition by synchronized transport of glucose and glycogen synthesis. Insulin leads to glycogen synthase activation in liver by dephosphorylation through inhibition of kinases including protein kinase A (PKA) and glycogen synthase kinase 3 (GSK3) and activation of protein phosphatase 1 (PP1) (11).

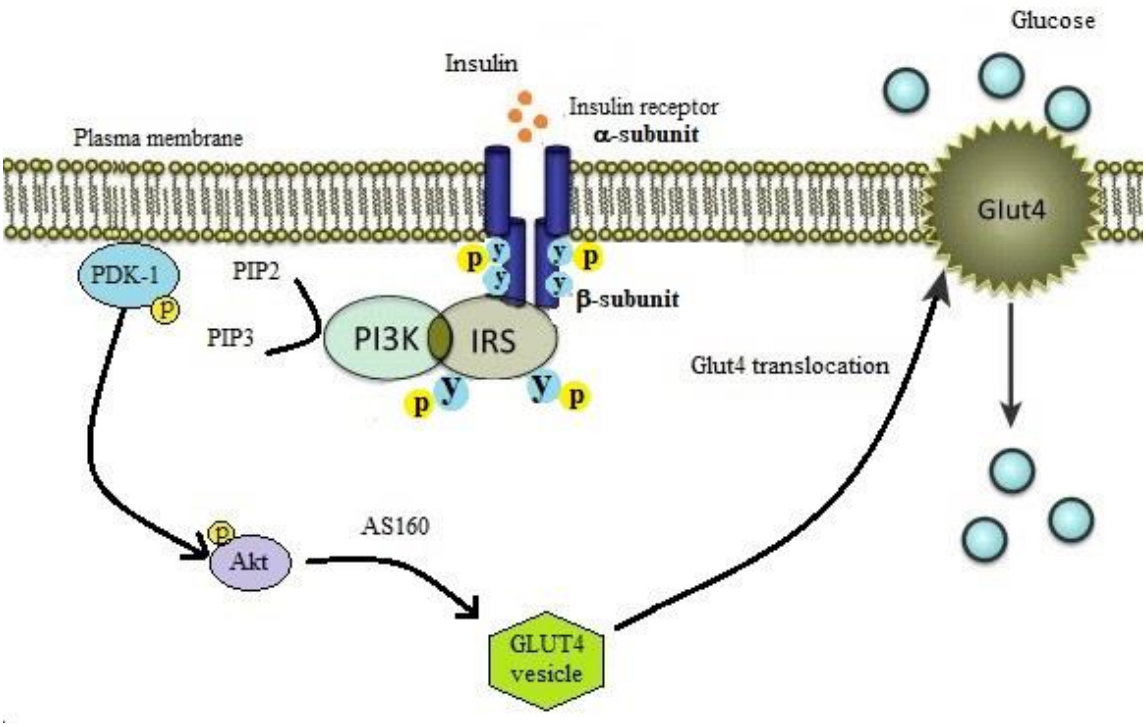

Figure 2: Insulin signaling pathway leading to translocation of GLUT4 to the plasma membrane in skeletal muscle

1.1.4 Insulin receptor

The binding of insulin to its receptor leads to activation of multiple intracellular molecules/ proteins that communicate the signaling downstream within the cell and lead to an induction of insulin-stimulated response. The insulin receptor has an intrinsic tyrosine kinase activity belonging to a large family of cell surface receptors called tyrosine kinases which also includes the insulin-like growth factor receptors (IGFR) (12). The structure of insulin receptor comprises of two extracellular α subunits which contain the insulin binding domain and two transmembrane β subunits each including: an extracellular, a transmembrane and a cytosolic domain (13) (Figure 2). The cytosolic domain contains an ATP binding consensus sequence along with three clusters of tyrosine residues that may be phosphorylated as a result of insulin signalling (13). The tyrosine residue clusters are found a) proximal to the cell surface in the juxtamembrane domain, b) in the catalytic region which is located in the centre of the β subunit and c) in the COOH-tail region (12). Insulin binding to the α subunit of the receptor causes a conformational change of the receptor, resulting in autophosphorylation of the β subunit tyrosine residues, leading to increases in the tyrosine kinase activity (12). A total of 13 tyrosine residues have been identified in the β subunit with Y953, Y960, and Y972 being the key residues in the juxtamembrane region, Y1146, Y1151, and Y1152 in the catalytic domain, and Y1316, and Y1322 in the COOH-terminal domain. The catalytic domain corresponds to approximately 50% of the receptor's autophosphorylation activity, 30-35% of the activity corresponds to the COOH-terminal domain and 15% corresponds to the juxtamembrane domain (13). Studies have indicated that upon point mutation of

substitution of the tyrosine residues, located in different domains, with phenylalanine the insulin stimulated action is inhibited (13,14). Additionally, removal of the tyrosine residues (1146, 1151 and 1152) that lie on the catalytic subunit resulted in complete abolishment of the insulin-stimulated effects (13).

1.1.5 Insulin receptor substrate

The insulin receptor substrate (IRS) is a family of proteins consisting of at least four isoforms (IRS-1 to -4) (15). The expression of IRS-1 (180kDa) is mostly in adipose and skeletal muscle tissue and is involved in regulation of metabolic processes such as protein synthesis and glucose transport. IRS-2 (185 kDa) is mainly expressed in the liver, skeletal muscle and adipose tissue. IRS-3 is expressed in adipose and IRS-4 in neuroendocrine tissue and is suggested to be predominantly exerting negative regulation of the IRS-1 and IRS-2 (15). Appropriate IRS-1 signaling is crucial for insulin action and any disturbances in the IRS-1 expression could severely impair the insulin effects in its target tissues. Overexpression of IRS-1 in L6 skeletal rat muscle cells significantly increase basal and insulin-induced glucose uptake and increase the GLUT4 trafficking to the cellular membrane indicating that IRS-1 plays a major part in the insulin signaling pathway (16). Additionally, insulin-induced PI3K activity associated with IRS-1 was increased in these cells compared to control. On the other hand, silencing the IRS-1 gene using small interfering RNA (siRNA) showed significant reduction in insulin-stimulated glucose uptake and GLUT4 translocation in L6 muscle cells (16). In addition, knockdown of the IRS-1/2 gene in mice has led to the development of insulin resistance and T2DM indicating that IRS plays a crucial role in the insulin signaling *in vivo* (17,18). In primary skeletal muscle cells isolated from prediabetic patients (patients with an impaired insulin

tolerance) the insulin-stimulated glucose uptake was reduced by 30-50% compared to the healthy control and this reduction was associated with lower phosphorylation of IRS-2, reduced downstream signaling and activation of PI3K in response to insulin (19). In another study, skeletal muscle biopsies obtained from T2DM patients showed no reduction in protein expression levels of the IRS-1 or p85 subunit of PI3K, however they displayed significant reduction in the insulin-induced tyrosine phosphorylation of IRS-1 and its downstream effector PI3K (20). Furthermore, significant reduction of insulin-stimulated IRS-1 phosphorylation and PI3K activity along with a decrease of 2-deoxyglucose uptake (53% compared to control) was seen in intact muscle strips from obese patients (21). Another study found that in skeletal muscle from lean type 2 diabetic subjects the insulin-stimulated IRS-1 phosphorylation and PI3K activation was significantly reduced in comparison to healthy individuals (22). It is important to note that the total IRS-1 protein levels were not reduced and were similar between all the groups (22). In normoglycemic subjects having a family history of type 2 diabetes, examination of skeletal muscle revealed insulin resistance that was associated with lower insulin-stimulated IRS-1 tyrosine phosphorylation and reduced IRS-1 associated PI3K activity (23). The current evidence indicate that significantly lower IRS tyrosine phosphorylation and IRS associated PI3K activity, resulting in decreased insulin-stimulated glucose uptake in skeletal muscle.

1.1.6 Importance of Phosphatidylinositiol-3-kinase in Insulin Signaling

Phosphatidylinositol-3-kinase (PI3K) consists of a p110 catalytic subunit and a p85 regulatory subunit that has two SH2 domains which interact with specific phosphotyrosine-containing motifs, pYMXM and pYXXM, in the IRS proteins (5,6). The

PI3K family entails 14 members that are divided into four classes. Class I, II, and III belong to the lipid kinases group and class IV are related protein kinases (5). It should be noted that only class I family of heterodimeric p85/p110 PI3K are responsive to insulin (3). There are a few isoforms of p85 regulatory subunit such as p85α, p55α, p85β, and p55γ. Treatment of 3T3-L1 adipocytes with LY294002 (inhibitor of PI3K) completely inhibited GLUT4 translocation to the plasma membrane and blocked insulin-induced glucose uptake (24). Another study investigated the effect of wortmannin, another inhibitor of PI3K, and found that it completely abolished insulin-stimulated PI3K activation and glucose uptake in rat adipocytes (25). Inhibition of PI3K activity either by LY294002 or wortmannin blocks insulin-stimulated glucose uptake in skeletal muscle cells indicating that PI3K plays a crucial role in the action of insulin (26). Overexpressing of p110α led to 1.4 fold increase of basal glucose transport in comparison to the control group and increased translocation of GLUT4 in 3T3-L1 adipocytes (27). These studies clearly indicate that the PI3K and particularly p110 catalytic subunit is critical for GLUT4 translocation *in vitro.* A study investigating mice with heterozygous loss of p110α +/- p110β+/- showed 40% reduction in insulin-induced IRS-1 associated PI3K activity along with 50% decrease in PI3K activity and showed hyperinsulinemia and mild glucose intolerance compared to control (28). Furthermore, mice lacking p85α and p85β regulatory subunits of PI3K showed impaired PI3K signaling in muscle, insulin resistance and glucose intolerance (29). On the other hand, skeletal muscle cells obtained from T2DM subjects showed decreased IRS-1 tyrosine phosphorylation, decreased association of PI3K with IRS-1 and PI3K activity in response to insulin in comparison to skeletal muscle cells obtained from healthy individuals (30). The above mentioned *in*

vitro and *in vivo* studies provide evidence of the importance of PI3K in basal and insulin-stimulated glucose uptake.

1.1.7 Importance of Protein Kinase B (Akt /PKB) in Insulin Signaling

Protein Kinase B (PKB/Akt) is a serine/threonine kinase which includes the three mammalian isoforms Akt1, Akt2, and Akt3. Akt1 is universally expressed in mammalian tissues while Akt2 is widely expressed in insulin target tissues including skeletal muscle, adipose and liver tissue. Akt3 is expressed in low levels in mammalian tissue excluding testes and brain. In order for Akt to be activated, phosphorylation of the threonine (Thr308) and serine residue (Ser473) is required (5). Inactivated Akt is mostly located in the cytoplasm however upon PI3K activation, Akt translocate to the cell membrane where it is phosphorylated by PDK resulting in its activation. In the absence of insulin, constitutively active Akt stimulated glucose uptake and GLUT4 translocation in 3T3-L1 adipocytes (31). Similarly, constitutively active Akt1 increased glucose uptake in 3T3-L1 GLUT4 overexpressing adipocytes and Chinese hamster ovary cells (32). Additionally, the study showed that inhibition of Akt using small interference RNA (siRNA) significantly lowered insulin-induced glucose uptake (32). In another study performed in Akt2-null adipocytes derived from immortalized mouse embryo fibroblasts (MEFs) the insulin-induced glucose uptake along with GLUT4 translocation were markedly decreased (33). Additionally, when Akt2 action was restored via re-expression the effect was reversed (33). Other studies found similar effect in muscle cells indicating abolishment of insulin-induced glucose uptake as a result to impaired Akt action (34,6,35). Mice that underwent homozygous deletion of Akt2 showed fasting hyperglycemia and impairment in the insulin-induced glucose uptake in muscle tissue *in*

vitro (36). Similarly, impaired insulin action in addition to hyperglycemia was observed in Akt2-null mice (37). Furthermore, decrease in insulin-induced glucose uptake (60%) and phosphorylation and activation of Akt was observed in adipocytes that were isolated from T2DM in comparison to adipocytes from healthy controls (38). Therefore, from the above mentioned studies it can be noted that Akt plays a critical role in insulin-stimulated GLUT4 trafficking to the cell membrane and loss of Akt function leads to insulin resistance and T2DM. From the *in vitro* and *in vivo* studies present in the literature it is already established that IRS, PI3K and Akt are important proteins involved in the action of insulin and glucose homeostasis and altering the levels of these protein in different experimental models has a serious impact on the insulin-induced glucose uptake.

1.1.8 Importance of AS160 in Insulin Signaling

The Akt substrate of 160kDa originally known as TBC1 domain family member 4 (TBC1D4) is a protein containing a Rab-GAP (GTPase-activating protein) domain located at the COOH terminus and two phosphotyrosine-binding (PTB) domains located at the NH2 terminus (39). The presence of a Rab-GAP domain formed a hypothesis that Akt-mediated phosphorylation of AS160 may be involved in the regulation of GLUT4 trafficking to the plasma membrane through the GAP activity towards Rab proteins. Therefore, it was suggested that Rab-GAP activity of AS160 endorses hydrolysis of GTP to GDP of Rab located on the GLUT4 storage vesicle (GSV) and that the GSV-bound Rabs in their inactive GDP-bound form are unable to undergo GLUT4 translocation. Upon AS160 phosphorylation by insulin, there is inactivation of the Rab-GTPase activity therefore the GSV-associated Rabs would become loaded with GTP which promotes the GLUT4 release and translocation to the plasma membrane (10). This hypothesis has been

tested in 3T3-L1 adipocytes where the phosphorylation sites of AS160 (Ser318, Ser588, Thr642, Ser751) were mutated to alanine (AS160-4P) and were coexpressed with GLUT4. The AS160-4P significantly reduced the insulin-stimulated GLUT4 translocation to the cell membrane by 80% in comparison to the control (wild type) (40). This may suggest that the GAP activity in AS160-4P is unrestrained and cannot be attenuated by insulin-stimulated phosphorylation which would keep the GLUT4 vesicle Rab in its inactive GDP form thus preventing GLUT4 translocation to the cell membrane. In addition, the AS160-4P-induced effect is dependent on an intact Rab-GAP domain. Mutation of the putative GAP domain in AS160-4P (arginine 973 residue to lysine) abolished the inhibitory effect on GLUT4 translocation (40). Similarly, the insulin stimulated translocation of GLUT4 was inhibited by expression of the AS160-4P mutant in L6 muscle cells (41). A study found that insulin stimulation leads to AS160 phosphorylation in isolated rat epitrochlearis skeletal muscle in a PI3K-sensitive manner (42). Moreover, other stimuli that were previously found to induce GLUT4 translocation including contraction and AICAR, stimulated AS160 phosphorylation (42) which indicates that AS160 is not a substrate for Akt alone but also for other kinases such as AMP-activated protein kinase (AMPK). Furthermore, in tibialis anterior muscle from mice overexpressing AS160-4P mutant, the insulin-stimulated glucose uptake was reduced by 30% compared to the vector expression control. Additionally, the contraction-induced glucose uptake was reduced by 40%. This inhibitory effect of the AS160-4P was abolished in response to insulin and contraction when Arg973 was replaced with Lys in muscle (41). Taken together these studies provide evidence of the importance of the downstream substrate of Akt (AS160) in the insulin-stimulated glucose uptake.

1.2 Insulin Resistance

Insulin resistance is a state in which there is a diminished responsiveness to normal circulating levels of insulin in the major insulin target tissues such as skeletal muscle, adipose and hepatic. Normal circulating levels of insulin in human plasma between meals range from 57–79 pmol/L (43). Alternatively, it can be defined as a failure of insulin target tissues to appropriately respond to normal physiological levels of insulin present in the blood. The state of insulin resistance is associated with elevated circulating free-fatty acids, obesity, inactive (sedentary) lifestyle, aging and genetic predisposition (5). Studies showed that the earliest metabolic defect in T2DM is impaired glycogen synthesis in muscle tissue as a consequence to reduced glycogen synthase activity (44,45). In an insulin resistant state, insulin-induced glucose uptake, utilization and storage of glucose as muscle glycogen is compromised (5,6). In adipose tissue insulin action to promote glucose uptake and storage as triglycerides as well as inhibiting hormone sensitive lipase (HSL) in order to supress lipolysis is compromised (46). Additionally, inhibition of liver gluconeogenesis and glycogenolysis in insulin resistant state is also compromised (46). As a consequence to skeletal muscle, adipose and liver tissue insulin resistance there is a chronic elevation of blood plasma glucose levels resulting in hyperglycemia. The side effect of chronically elevated glucose in the blood (hyperglycemia) may lead to short-term effects such as diabetic ketoacidosis, a metabolic state caused by breakdown of fatty acids in order to create energy thereby creating ketone bodies that significantly impair the blood buffering system or long-term effects such as cardiovascular damage that could lead to the development of cardiovascular disease, macrovascular/microvascular damage, nephropathy, neuropathy and retinopathy and

severe complications including infections and amputations (35,47). The pathophysiology of the above-mentioned conditions is complex and the exact etiology is often difficult to identify. However, people affected by diabetes are frequently affected by high levels of inflammation, oxidative stress and dyslipidemia that can result in cellular damage, atherosclerosis, high blood pressure and other conditions that lead to damaging the vasculature and other vital organs (35,47). Additionally, it should be noted that chronic hyperglycemia aggravates target tissue insulin resistance and it is a major contributor to pancreatic β cell exhaustion and loss of function.

1.2.1 Muscle Insulin Resistance

Skeletal muscle accounts for 75% to 80% of postprandial glucose uptake and is quantitatively the most important tissue involved in maintaining glucose homeostasis (3). As a result, skeletal muscle insulin resistance is a major contributor to imbalances in the blood glucose levels which will lead to hyperglycemia, decreased glucose tolerance and T2DM. Studies have confirmed that individuals suffering from T2DM are severely insulin resistant compared to weight-, age- and sex-matched controls (48). Additionally, as result to muscle insulin resistance there is an impairment in 85-90% of the total body glucose disposal (48). Evidence has shown that skeletal muscle insulin resistance precedes hepatic insulin resistance and insulin deficiency from dysfunctional pancreatic β-islet cells by decades. 75-80% of insulin-induced glucose clearance is converted to glycogen in the muscle cells and the rest 25-20% is converted to carbon dioxide and water (49). In the case of muscle insulin resistance, recent evidence has indicated that impairment in the insulin-induced glucose transport is the main contributor to decreased

glycogen content and decrease in the phosphorylation activity contributes in much smaller extent (50).

There are several mechanisms in which insulin-stimulated glucose uptake may be decreased including reduced expression of the insulin receptor, decreased tyrosine phosphorylation of the insulin receptor or IRS-1 as a result to reduced tyrosine kinase activity of the receptor, diminished downstream activation/phosphorylation of Akt and GLUT4 translocation to the cell membrane (51). Studies have shown, that serine phosphorylation of IRS-1 leads to impairment in the insulin signaling pathway which in turns leads to significant decrease in insulin-stimulated glucose uptake (52–54). Insulin resistance is strongly associated with obesity which is a major risk factor for the development of type 2 diabetes, cardiovascular disease and metabolic syndrome (51). Insulin-stimulated glucose uptake in muscle has shown to be significantly reduced in obese individuals and patients with type 2 diabetes (51). Additionally, reduced expression and tyrosine phosphorylation levels of IRS-1 were found in 30% of high risk subjects for type 2 diabetes including obese subjects and first-degree relatives of type 2 diabetic individuals (55). Signaling molecules such as mTOR (56,57), p70 S6K (58,59), GSK3 (60), c-Jun N-terminal kinase (JNK) (61) and PKC's (62) have been implicated to be involved in the serine phosphorylation of IRS-1 protein which leads to reduction in the insulin-stimulated glucose uptake in skeletal muscle and adipose tissue (51) (Figure 3). Multiple studies have found that elevated saturated free fatty acids (FFA) levels lead to insulin resistance by affecting the above mentioned molecules (56,59,61–64). The following section describes in detail the signaling molecules involved in insulin resistance.

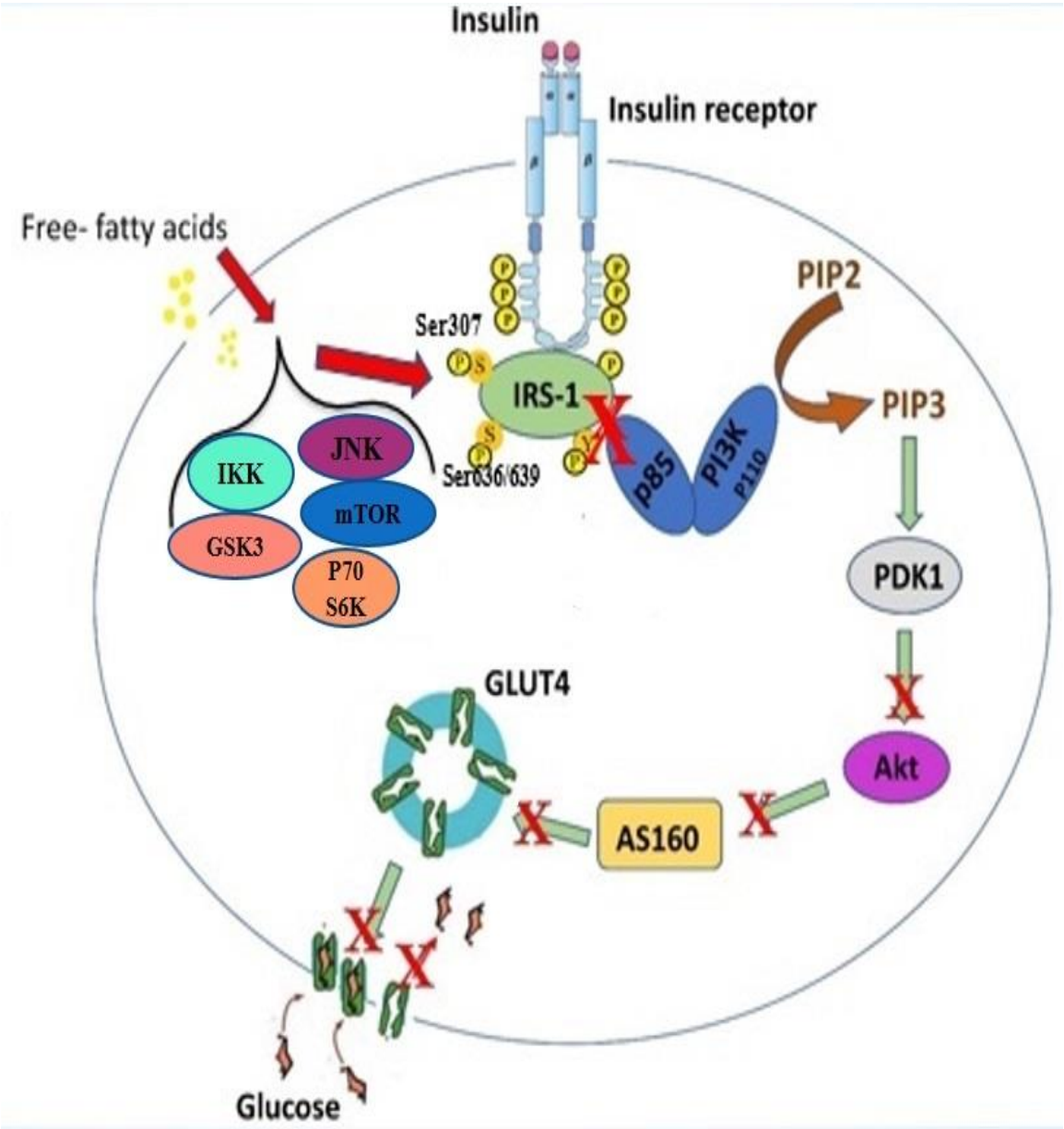

Figure 3: Proposed mechanism of FFA-induced insulin resistance in skeletal muscle

1.3 Mechanisms Underlying Insulin Resistance

1.3.1 Serine phosphorylation of IRS-I and insulin resistance

The involvement of the serine phosphorylation of IRS-1 in insulin resistance was first demonstrated a few decades ago when 17 okadaic acid was used in skeletal muscle cells and 3T3-L1 adipocytes. Okadaic acid significantly reduced insulin-stimulated GLUT4 translocation and glucose uptake by inhibiting tyrosine phosphorylation of IRS-1 and its downstream effectors such as PI3K (64,65) (Table 1). The exact mechanism of the inhibition was not known at the time however it was later discovered that okadaic acid increases the Ser307 phosphorylation of IRS-1 (65,55). Moreover, prolonged exposure to insulin (hyperinsulinemia) has shown to increase serine phosphorylation of IRS-1 in skeletal muscle and adipocytes indicating that negative feedback mechanism may be involved in the uncoupling of IRS-1 protein from its upstream/downstream members and prevents normal functioning of the insulin signaling (66).

The mechanism behind the serine phosphorylation of IRS-1 was also investigated in L6 muscle cells. Although these cells exhibit high basal serine phosphorylation of IRS-1 in comparison to healthy human skeletal muscle (67), they are extensively used due to being the most feasible *in vitro* skeletal muscle model and having the ability to respond to insulin. The increased serine phosphorylation of IRS-1 is clearly correlated to reduced tyrosine phosphorylation leading to decreased glucose uptake (68). Numerous cytokines and protein kinases lead to an increased levels of serine phosphorylation of IRS-1 and at the same time diminish the insulin-stimulated phosphorylation of IRS-1 on its tyrosine residues. Hyperphosphorylation of the serine residues of IRS-1 makes a poor substrate for

the insulin receptor leading to inhibition of its downstream effects. For instance, diabetogenic agents may cause serine/threonine protein kinase activation or they may lead to inactivation of serine/threonine phosphatases which would lead to an increase of serine phosphorylation of IRS-1 and diminished insulin action (53) (Table 1). In different rodent models of obesity including rats and mice inhibiting seine phosphorylation of IRS-1 led to improved tyrosine phosphorylation and insulin sensitivity.

Phosphorylation of different serine residues located on IRS-1 has been correlated to decreased downstream effector activation such as PI3K association and Akt phosphorylation/activity and ultimately glucose uptake. The end of phospho The insulin resistance phenomenon remains complex tyrosine binding (PTB) domain contains Ser307 which moderates the interaction of IRS-1 with the insulin receptor (69). The proinflammatory cytokine TNF-α has been implicated in the development of insulin resistance therefore several studies have investigated the effect of TNF-α on IRS-1 phosphorylation. Increase in TNF-α ιs linked to increase of Ser307 phosphorylation on IRS-1 in adipose, liver and muscle tissue (69,70,64,71). Additionally, stimuli such as increased levels of FFA are also implicated in serine phosphorylation of IRS-1. Increased levels of Ser307 phosphorylation were observed in mice fed with high fat diet (72). Additionally, a study found that decreased phosphorylation of Ser612 by mitogen activated protein kinase (MAPK) is associated to improved insulin-induced tyrosine phosphorylation of IRS-1 in mice (73). Similarly, HFD fed mice lacking 4E-BPs showed an increase Ser636/639 phosphorylation of IRS-1 (74). Ob/ob and K/KA^{y} mice fed with HFD also exhibited increased phosphorylation of Ser307 and Ser636/639 (59). Furthermore, there was a hyperphosphorylation of the serine residues (632/639) of IRS-1

in hepatocytes treated with 0.4 mM palmitate for 22 hours (56). Moreover, increase of Ser1101 phosphorylation on IRS-1 decreased the insulin-stimulated tyrosine phosphorylation of IRS-1 and downstream effector proteins such as Akt in C2C12 muscle cells (75). The studies above indicate that exposure to FFA leads to phosphorylation of Ser307, Ser636/639 as well as Ser1101 on IRS-1 which is highly correlated with reduced insulin action and induction of insulin resistance (Table 1).

Table 1: Kinases involved in different serine phosphorylation sites of IRS-1

Reference	Stimuli	Upstream kinases	Serine Residue of IRS-1	Tissue	Effect on Insulin Signaling
Aguire et al. (69) Gual et al. (55) Brustel. et al. (64)	FFA Okadaic acid TNF-α	mTOR p70 S6K JNK PKCθ GSK3	307 337	Muscle Adipose Liver	Decreased action
Tanaguchi et al.(76)	FFA	ERK mTOR	612	Muscle Liver	Decreased action
Le Bo (74) Gual et al. (55)	FFA	mTOR p70 S6K	636/639	Muscle Adipose Liver	Decreased action
Li et al. (62) Tremblay et. (75)	FFA	PKCθ	1101	Muscle Adipose Liver	Decreased action

1.3.2 The Glycogen synthase kinase-3 (GSK3) pathway

Glycogen synthase kinase-3 (GSK3) is a 51 kDa serine/threonine protein kinase predominantly involved in the regulation of glycogen synthesis by inactivating glycogen synthase. Additionally, GSK3 is also involved in the regulation of blood glucose homeostasis and is correlated with the development of insulin resistance (77).

GSK3α and GSK3β are the 2 isoforms expressing high levels of homology in regards to biological function and structure (78). The GSK3 isoforms have both an inhibitory serine phosphorylation site (Ser21 for GSK3α and Ser9 for GSK3β) and a catalytic tyrosine activation site (Y279 for α, and Y216 for β) (77). GSK3 is nearly always active therefore Akt or other stimuli can cause serine phosphorylation of GSK3 leading to inhibition of its activity (77).

Correlation between type 2 diabetes and GSK3 has been reported in patients with type 2 diabetes and both isoforms were significantly elevated in skeletal muscle tissues of these subjects (77). Furthermore, GSK3 elevation in expression and activity levels was found to have an inverse relationship to insulin action in type 2 diabetes patients undergoing hyperinsulinemic/euglycemic clamp test (79). Studies conducted in 3T3-L1 adipocytes have demonstrated that GSK3 activation leads to serine phosphorylation of IRS-1 which in turns attenuates insulin-induced tyrosine phosphorylation of IRS-1 (80). A study suggested that phosphorylation of the Ser332 on IRS-1 by GSK3 significantly attenuated insulin signaling in C2C12 muscle cells (81). Additionally, in muscle obtained from individuals that were classified as having metabolic syndrome, activation of GSK3 was associated with an increased phosphorylation of Ser337 on IRS-1 (82).Moreover, it was indicated that Ser332 is a GSK3 site of phosphorylation and Ser336 acts as a "priming" site required for GSK3 action (81). In summary, GSK3 is one of the key regulators involved in glucose homeostasis and may be one of the players involved in the development of insulin resistance.

1.3.3 Insulin Resistance and c-Jun N-terrninal Kinase (JNK)

JNK is a stress activated serine/ threonine kinase and a member of the MAPK family (83). JNK isoforms include JNKI (46kDa), JNK2 (54kDA), and JNK3 (54kDA). JNK1 and JNK2 are found to be commonly expressed in majority of tissues however JNK3 is mostly expressed in the brain, heart and testes (83). Stimulation of JNK1 is assumed to be involved in the pathology involving obesity and type 2 diabetes. Activation of JNK leads to the formation of a dimer and translocation to the nucleus where it causes phosphorylation of transcription factors such as c-Jun thereby mediating gene transcription (84). Phosphorylation of Thr183/Tyr185 residue of JNK is considered a site for activation (85).

JNK may be activated by different environmental stressors including FFA, radiation, growth factors, cytokines like tumor necrosis factor alpha (TNF-α) or interleukin-1β (IL-β) (3) (54). *In vitro* studies performed in HEK293T hepatocytes have shown that JNK1 and JNK2 have similar affinity and activity in regards to Ser307 phosphorylation of IRS-1 (84). Existing evidence indicate that JNK may be a major mediator involved in the development of insulin resistance. The increase in JNK activation was associated with Ser307 phosphorylation of IRS-1 in skeletal muscle and liver (83). Studies showed that TNF-α leads to stimulation of JNK which in turn causes phosphorylation of Ser307 residues on IRS-1 in adipose and liver and muscle (69,70,64,71). Mutation of Ser307 to alanine abolishes IRS-1 phosphorylation by JNK and attenuates the inhibitory effect of TNF-α on IRS-1 (69).

In comparison to high saturated fat diet where insulin resistance was established and confirmed by a hyperinsulinemic-euglycemic clamp, JNK phosphorylation was not increased in normal diet fed controls rats in both muscle and liver tissue (83). A study has shown that JNK-interacting protein 1 (JIP1) responsible for binding of JNK signaling pathway components is needed for JNK activation and inhibition of IRS-1 in the adipose tissue of obese mice (86,55). Furthermore, in JIP-1 deficient mice insulin-induced tyrosine phosphorylation was increased and IRS-1 (Ser 307) was decreased in epidydimal fat pads (86,55).

Moreover, continuous JNK activation was observed in primary pancreatic J3 cells and mouse hepatocytes from HFD fed and STZ-induced insulin resistant mice (87). Additionally, targeted mutation of the JNK1 locus in mice abolished JNK expression and showed to prevent HFD-induced insulin resistance (87). In agreement with the previous studies Solinas et al 2006 found that phosphorylation of the Ser307 residues on IRS-1 is the main mechanism involving JNK-mediated induction of insulin resistance in this study (70,87). In rodent *in vivo* models of obesity insulin sensitivity is significantly improved by inhibiting serine phosphorylation of IRS-1 together with improvement in the impaired tyrosine phosphorylation of IRS-1 in $Jnk1^{-/-}$ and $Jnk2^{-/-}$ C57BL/6J mice (61).

Studies have also investigated the differences between the JNK1 and JNK2 involvement in high-fat diet induced insulin resistance and obesity *in vivo*. Mice lacking JNK1 have significantly improved insulin sensitivity and exhibited protective effect against high fat-induced insulin resistance in liver. Mice lacking JNK2 on the other hand, did not have any effect on the insulin sensitivity. As a result, JNK2 was ruled out as a key mediator of establishing insulin resistance, type 2 diabetes and obesity (84). It is very

interesting to note that JNK2 and not JNK1 deficient mice exhibited protective effects against type 1 diabetes and atherosclerosis. As a result, it can be concluded that both isoforms may play a role in influencing the pathology of diabetes (84). JNK activation has been inhibited by rosiglitazone, an antidiabetic drug belonging to the family of thizolidinediones, leading to normalizing blood glucose levels in insulin resistant mice (88). Rosiglitazone given to high fat fed obese mice with an established insulin resistance significantly inhibited JNK activation and reduced insulin resistance (89).

1.3.4 Protein Kinase C (PKC) and Insulin Resistance in Skeletal Muscle

PKC is a large class of serine/threonine protein kinases consisting of approximately 10 different isoforms. PKC's are involved in variety of cellular processes including cellular growth differentiation and cell signaling pathways (90,91). The PKC family is classified in 3 major subgroups including conventional PKC's (cPKC) referring to calcium and diacylglycerol-dependent PKC's (PKC α, β I-II, and γ), novel calcium-independent PKC's (nPKC) which includes PKC, δ, ε, η and θ and atypical PKC's (aPKC) including PKCζ and ι/λ (92).

The insulin resistance phenomenon remains complex and there is evidence for PKC's involvement. A study found that PKCθ was involved in the Ser1101 phosphorylation of IRS-1 in 3T3-L1 adipocytes and C2C12 skeletal muscle cells thus preventing the downstream effect of insulin and glucose uptake (62). Additionally, phosphorylation Ser1101 on IRS-1 was also increased though nutrient (amino acids infusion) and hormonal (insulin) stimulation of p706SK in obese mice (75).

Increase in muscle PKCθ activity in skeletal muscle seen in rats that underwent lipid infusion resulting in high circulating levels of FFA resulted in 50% decrease in IRS-1 associated PI3K activity and insulin-stimulated IRS-1 tyrosine phosphorylation as well as increased muscle ser307 on IRS-1 (93). Additionally, PKCθ can activate IKK which in turn leads to Ser307 phosphorylation of IRS-1 (93). Moreover, lipid infusion in Wistar rats caused increase in PKCθ activity as a result to DAG accumulation (94). A study indicated that overexpression of dominant negative PKCθ in skeletal muscles leads to obesity and impairment of the IR/IRS-1/PI3K signaling cascade and its downstream effectors such as Akt which is implicated in insulin resistance (95). A serial muscle biopsies of lean, obese and obese-diabetic human subjects before and during lipid infusion showed that the total and cytosolic DAG accumulation was associated with PKCθ activation and impairment in insulin signaling (96). Similarly, a study by ltani et al. reported a three-fold increase in DAG accumulation that resulted in changes in PKCβII and PKCδ in lipid-induced insulin resistant human muscle (97). Furthermore, administration of lipid infusions in rats and humans stimulated activation of PKCθ and PKCδ leading to impairment of insulin-stimulated glucose uptake in skeletal muscle (98,99). Additionally, high levels of saturated free-fatty acid (palmitate) led to 5-fold increase in PKCζ ın L6 skeletal muscle cells, while the PKC inhibitor Ro 31.8220 attenuated the palmitate induced insulin resistance (100). An in-depth study on PKCδ in mice reported that muscle PKCδ increased with age and its deletion improved insulin sensitivity (101). The above studies indicate the potential involvement of the PKC family of signaling molecules in the development of type 2 diabetes.

1.3.5 IKK-NFkB Pathway and Insulin Resistance in Skeletal Muscle

The family of transcription factors NFkB are involved in the regulation of multitude of genes including the regulation of pro-inflammatory genes. The proteins of NFkB consist of five members including p50, p65, RelB and c-Rel. In order to initiate transcriptional modification in the cell, two protein members of NFkB are necessary to be dimerized and bind to DNA. The predominant activating dimer of NFkB in skeletal muscle is the p50-p65 heterodimer (63). Furthermore, NFkB is generally localized in the cytoplasm where it is associated with the inhibitory protein inhibitor of kappa B (IkB). Stimuli such as ROS, cytokines, hyperglycemia and FFA are found to activate IkB kinase (IKK), which is an upstream regulator of IkB. When, IKK becomes activated it leads to rapid IkB phosphorylation and dissociation from NFkB. This further leads to degradation of IkB by the proteasomes in the cytoplasm (63). The degradation of IkB allows NFkB to be liberated from its inhibitory activity, enters the nucleus and causes induction of transcription of genes.

Exposure of L6 myotubes to palmitate significantly reduced insulin-stimulated glucose uptake and PI3K/Akt signaling while stimulated IkB degradation and NFkB translocation to the nucleus (52). Furthermore, the IKK inhibitors acetylsalicylate and parthenolide, abolished the palmitate-induced reduction in insulin-stimulated glucose uptake. Additionally, the decrease in insulin-stimulated glucose uptake seen with palmitate was attenuated in the presence of SN50, an inhibitor of NFkB translocation (52). Taken together these data indicate that the FFA-induced insulin resistance is prevented by inhibition of nuclear translocation of NFkB in L6 muscle cells (52). Muscle samples of vastus lateralis collected from T2DM patients indicated that there was a 60%

decrease in the IkB protein, an indication of elevated IKK/NFkB activity, which was correlated with muscle insulin resistance assessed with hyperinsulinemic-euglycemic clamp (63). Moreover, when T2DM subjects were exposed to aerobic exercise for 8 weeks, the IkB protein levels and glucose uptake were increased by 50% and 37% respectively and the TNF-α levels were decreased by 40% (63). Increase in TNFα expression was linked to increase in IKK phosphorylation (63).

A study reported that administration of salicylate (aspirin) in T2DM patients significantly decreased the plasma glucose levels (102). Salicylates are also reported to inhibit IKK activity and translocation of NFkB (103,104,102), suggesting that IKK may be a key player involved in the development of insulin resistance. Additionally, inhibition of IkBβ by salicylates prevented fat-induced pancreatic beta cell dysfuntion both *in vitro* and in rodents (*in vivo*). Overall, these findings indicate that the NFkB signaling pathway may be involved in the development of insulin resistance.

1.3.6 mTOR and p70 S6K Pathway and Insulin Resistance in Skeletal Muscle

The mammalian target of rapamycin (mTOR) is a 289 kDa serine/threonine kinase that is activated by hormonal factors such as insulin and nutritional factors such as amino acids (105,106). mTOR plays a major role in cellular growth and maintaining nutritional homeostasis. However, mTOR is often implicated in tumors where its activity is frequently increased (107). mTOR consists of two different complexes: a rapamycin-sensitive complex which includes the regulatory-associated protein of mTOR known as raptor (TORC1) and rapamycin-resistant complex known as rictor (TORC2) (105,106). Akt and mTOR signaling comprises the tuberous sclerosis complex (TSC) consisting of TSC1, TSC2, and a member of Ras family Rheb-GTPase (105). Rheb possesses intrinsic

GTPase activity and has the ability to bind to both GDP and GTP. The activity of mTOR is increased when Rheb is bound to GTP (108). Following phosphorylation of Akt, TSC2 gets phosphorylated and inhibited which drives the intrinsic GTPase activity of Rheb towards the GTP-bound /(active) form (108). Contrarywise, mTOR activity is supressed when Rheb is bound to GDP (105,108).

Phosphorylation of mTOR may be on different serine residues in order for its activity to be increased. For instance, PI3K-Akt phosphorylation of mTOR is on the Ser448 residue leading to increased mTOR activity (107). In order for mTOR to be activated different subunits of TORC1 for instance proline-rich Akt substrate 40 (PRAS40) are required for complete activation (108). A study has shown that PRAS40 is also required for activation of mTOR via Akt (109). and it is also reliant on the interaction of PRAS40 with mTOR on its kinase domain (109). Phosphorylation of the Ser2448 was reported to be an Akt phosphorylation site because it is sensitive to PI3K inhibition which leads to a decrease in the Akt activity (107,110). Phosphorylation of the Ser2448 residue of mTOR is widely accepted as an indicator of activation (107,110).

One of the downstream effectors of mTOR is the serine/threonine kinase, mitogen activated p70 S6K at 70 kDa which regulates the translation of a class of mRNA transcripts containing an oligopyrimidine tract at the start of their transcriptional sequence (111). Several of the mechanisms involved in protein synthesis are encoded by this class of mRNA transcripts which are responsible for approximately 20% of the cellular mRNA (111). The above process is accomplished by activation/phosphorylation of p70 S6K and further phosphorylation of 40S ribosomal subunit protein S6 which leads to promotion in the mRNAs translation (111). The regulation of p70 S6K may be

dependent on mTOR activation. The TORC1 complex stimulates phosphorylation of p70 S6K, therefore phosphorylation of the Thr229 in the catalytic domain and Thr389 in the linker domain are crucial for the action of p70 S6K (111). Moreover, phosphorylation of Thr389 mostly correlates with increased p70 S6K activity *in vivo* (112).

A study has shown that mTOR and p70 S6K can be activated by increasing amino acid levels which leads to serine phosphorylation of IRS-1 which in turn leads to decrease in insulin action in 3T3-L1 adipocytes and L6 muscle cells (113). The activity of mTOR and p70S6K was also highly elevated in hepatic and skeletal muscle tissue of rats fed with high fat diet which indicates that both kinases may play in the development of insulin resistance *in vivo* (74). This effect was completely abolished when the mTOR inhibitor rapamycin was used. The inhibition of mTOR as a result to rapamycin stems from the ability of rapamycin to interfere with the FKBP-rapamycin binding pocket of TOR (107). Another study performed on insulin resistant 3T3-L1 adipocytes that were pretreated with rapamycin showed an increase in glucose uptake indicating that mTOR may be downregulating insulin signaling (114). Additionally, treatment with rapamycin reduced serine phosphorylation of IRS-1 while prolonging insulin-induced PI3K activity in mouse skeletal muscle cells (75). Another study found that the phosphorylation of mTOR was significantly increased in FFA palmitate treated hepatocytes (56).

In addition to mTOR, its downstream effector p70 S6K is found to be implicated in the impairment of normal insulin signaling in both skeletal and adipose tissue (115). *In vitro* studies have demonstrated that treatment with small interference RNA against p70 S6K markedly increased insulin-induced Akt phosphorylation and improved insulin sensitivity in MEF mouse embryonic fibroblast cells (116). Mice that underwent p70 S6K

gene deletion had lower Ser307 and Ser636/639 phosphorylation of IRS-1 and improved insulin sensitivity when fed with high fat diet in comparison to their controls (74). In addition, a study has found that p70 S6K-deficient mice are protected from obesity when treated with high fat diet (59). On the other hand, increased levels of p70 S6K has been associated with a reduced Akt activity in insulin-resistant obese rodents (59). Both mTOR and p70 S6K regulate glucose homeostasis by negative feedback mechanism. When glucose homeostasis is achieved, Ser307 and Ser636/639 phosphorylation of IRS-1 is activated in order to inhibit the insulin-induced glucose uptake and maintain homeostasis. However, chronic hyperstimulation of mTOR and p70 S6K may lead to insulin resistance in skeletal muscle, adipose tissue and liver.

1.3.7 Free Fatty Acids (FFA)-Induced Skeletal Muscle Insulin Resistance

Free Fatty acids (FFA) are non-esterified fatty acids (NEFA) that play a pivotal role in establishing insulin resistance and type 2 diabetes mellitus (64). Studies that used nuclear magnetic resonance (NMR) spectroscopy showed a strong association between an intramyocellular triglyceride accumulation with skeletal muscle insulin resistance (117,118). An explanation for this phenomenon may be obtained from the Randle hypothesis in which the free fatty acids compete with glucose for substrate oxidation (119). Philip Randle proposed the theory in which elevated FFA leads to increase of mitochondrial acetyl-CoA/CoA and NADH+/NAD+ ratios which ultimately lead to inhibition of the pyruvate dehydrogenase activity and increase in citrate levels which in turn hinders phosphofructokinase activity leading to decrease in glucose uptake (119).

Moreover, studies found that skeletal muscle exposure to elevated FFA attenuates downstream insulin-induced Akt phosphorylation. Additionally, Akt inhibition has also

been associated with elevated ceramide concentration which is released as a result to acyl-CoA metabolism (64,120). Studies showed that exposure of rodent myotubes to palmitate increases the accumulation of ceramide which leads to insulin resistance (121,122). Pharmacological inhibition of ceramide synthesis using myriocin or triacsin-C prevented insulin resistance and restored glycemic control in prediabetic obese rats (123). An increase in ceramides in turn can often lead to activation phosphatases including phosphatase 2A and an increase in PKCζ activity that leads to dephosphorylation and inhibition of Akt thereby diminishing the insulin-induced glucose uptake in skeletal muscle (124,125).

L6 skeletal muscle cells treated with 0.75mM for 16 hours of palmitate had markedly decreased GLUT4 translocation to the cell membrane associated with a decrease in glucose uptake (126). In addition, *in vivo* studies performed in Sprague-Dawley rats infused with intralipid, showed a reduction in insulin sensitivity and a two fold increase in Ser307 phosphorylation of IRS-1 in muscle (127). Therefore, an increase in intramuscular and circulating FFA in overweight and obese individual may explain the reason for the increased risk of insulin resistance and type 2 diabetes development (51). Intramyocellular lipids do not seem to cause insulin resistance because they are localized in discreet lipid droplets mostly as TGs however, accumulation of intramyocellular lipids are markers for other lipid intermediates including ceramides, fatty acyl-CoA or diacylglycerols which in turn may directly impact the insulin signaling pathway through activation of signaling cascades that will inhibit the insulin stimulated glucose uptake such as serine phosphorylation of IRS-1 through upstream kinases such as PKCs, mTOR, p70 S6K and IKK/NFkB (117,51,49,55,128,129).

1.4 AMP-activated Protein Kinase Pathway (AMPK)

AMPK is a 62 kDa serine/threonine kinase energy sensor that plays a crucial role in regulating energy balance within the cell. AMPK is a heterotrimer which is composed of catalytic α subunit and regulatory β and γ subunits (130). Homologues subunits of each AMPK have been found in every eukaryotic species including worms, fruit flies, yeast, fish and mammals (131). Different isoforms of AMPK subunits have been found in mammals including α1, α2, β1, β2, γ1, γ2 as well as γ3 (132).

The N-terminal section of the α subunit of AMPK contains the serine/threonine kinase catalytic domain and the Thr172 residue which is phosphorylated and required for the activation of AMPK. The C-terminal segment of the α catalytic subunit is essential for association of the β and γ subunits (133). Furthermore, the physiological function of both β and γ subunits of AMPK have not been extensively studied nevertheless, it has been found that β subunit acts as a scaffold to link the α and γ subunits together. Studies conducted in transgenic Hampshire pigs expressing the dominant Rendement Napole phenotype achieved by a single missense mutation (R225Q) of the γ3 subunit of AMPK resulted in 70% decrease in glycogen content in muscle and higher oxidative capacity (134). Glycogen synthesis was significantly decreased after exercise in mice that underwent gene knockout of the γ3 subunit (135). Additionally, well established activators of AMPK failed to increase muscle glucose uptake and to protect against HFD-induced accumulation of triglycerides in AMPK γ3 knock-out mice (135). These studies provide substantial evidence that the γ subunit is involved in glucose metabolism and fat oxidation.

AMPK is activated as a result to an elevation in AMP/ATP ratio. Reduced ATP levels lead to an increase in AMPK activation as a result of increased muscle activity which leads to phosphorylation and inhibition of acetyl-CoA carboxylase (ACC). This inhibition causes reduction of malonyl-CoA levels which is a well-known inhibitor of carnitine palmitoyltransferase 1 (CPT 1) (136). Loss of CPT1 reduction causes promotion of fatty acid oxidation in muscle mitochondria which in turn leads to replenishment of ATP (132).

AMPK may be activated and regulated by its upstream kinases including liver kinase B1, calcium/calmodulin-dependent protein kinase (CaMKK), transforming growth factor β (TGFβ) activated kinase (TAK1) as well as by sirtuin 1 (SIRT1) (131). Activation of AMPK by AICAR, antimycin A, and sodium azide was completely abolished in human fibroblasts lacking LKB1 expression (137,138). Additionally, AMPK activation by stimulation with small molecule PT1 is prevented by STO-609, an inhibitor of CaMKK, in L6 muscle cells (139). AICAR (5-amino 4-imidazolecarboximide riboside), muscle contraction, metformin and polyphenols such as resveratrol are established activators of AMPK. AICAR or metformin, had no effect on AMPK phosphorylation in mice embryos that underwent TAK1 knockout (140). Additionally, resveratrol-induced activation of AMPK was inhibited in the presence of splitomicin, an inhibitor of SIRT1 in hepatocytes (141).

AMPK activation has a noteworthy impact in skeletal muscle and its activation triggers stimulation of glucose uptake, GLUT4 translocation, FA oxidation and mitochondrial biogenesis while reducing the rates of protein synthesis and glycogen storage (142). In recent years, AMPK activators have been recognized as promising

pharmacological interventions for the prevention and treatment of T2DM (143–149). Many reports indicate that in skeletal muscle both AICAR and contraction increase glucose uptake and insulin sensitivity through activation of AMPK resulting in GLUT4 translocation to cell membrane (150–152). Additionally, wortmannin, an inhibitor of PI3K, did not have any effect on the AICAR- and contraction-stimulated glucose uptake indicating that the signaling mechanism is insulin-independent (150–152). Metformin, is a biguanide drug that is currently the first line of treatment for T2DM. Metformin activates AMPK indirectly through inhibiting complex 1 of the mitochondrial respiratory chain and promoting a switch to anaerobic glycolysis thus increasing the AMP/ATP ratio leading to AMPK activation (153). Metformin treatment induces AMPK activation leading to GLUT4 translocation and therefore increase the glucose uptake in L6 and C2C12 muscle cells (154,155), rodent muscle (155,156) and human muscle extracted from diabetic patients (155,157). Moreover, metformin delays the onset of T2DM and increases overall body insulin sensitivity by approximately 30% in T2DM subjects (155,158). Activation of AMPK, inhibition of hepatic glucose production and increased GLUT4 translocation to the plasma membrane in adipose tissue and skeletal muscle may in part be attributed to the mechanism of action of metformin in attenuating insulin resistance (155,158). Other compounds such as polyphenols are also found to activate AMPK. Studies have indicated that 5μg/ml of rosemary extract (RE), 2 μM carnosic acid (CA) and 5 μM rosmarinic acid (RA), major polyphenol found in RE, increased glucose uptake to levels comparable to insulin and metformin and activated AMPK in L6 muscle cells (160–162). In addition compound C (CC), an inhibitor of AMPK, significantly

inhibited the RE- and CA-stimulated glucose uptake indicating that activation of AMPK may be the mechanism in which these polyphenols increase glucose uptake (160,161).

Recent evidence showed that AMPK activation may inhibit the NFkB signaling pathway mainly by deacetylation of the p65 protein of the NFkB complex (163). The NFkB subunits are not a direct target of AMPK however the inhibition of NFkB signaling is shown to be mediated by other AMPK targets such as SIRT1, peroxisome proliferator-activated receptor-gamma coactivator-1 (PGC-1) and p53 (163). Chemical activation of AMPK by AICAR significantly inhibited NFkB activation and translocation to the nucleus in endothelial cells (164). Additionally, stimuli such as salicylate (aspirin) that activate AMPK inhibit IKK and therefore NFkB translocation to the nucleus (103,104,102). Taken together, the studies above indicate that AMPK plays a pivotal role in energy metabolism and glucose uptake in skeletal muscle and its activation may be critical in combating insulin resistance and glucose homeostasis.

1.5 Rosemary and its phenolic compounds

Rosemary (*Rosmarinus officinalis*) is a plant belonging to the labiate family (Lamiaceae). It is an aromatic evergreen shrub indigenous to the Mediterranean region and South America (165). The fresh and dried leaves are frequently used as a food preservative and in traditional Mediterranean cuisine as a flavoring agent. Historically rosemary has been used medicinally to treat renal colic, dysmenorrhea, to stimulate hair growth and relieve symptoms caused by respiratory disorders (165,166). Today, rosemary extracts (RE) are often used in aromatherapy, cosmetics, to treat anxiety-related conditions and increase alertness (166). RE contains different classes of polyphenols

including phenolic acids, flavonoids and phenolic terpenes (167–171) (Table 1). Phenolic acids include a) the hydroxycinnamic acids: rosmarinic acid, chlorogenic acid, coumaric acid, coumaroylqunic acid, ferulic acid, m-hydroxybenzoic acid and p-coumaric acid b) the hydroxybenzoic acids: caffeic acid, dicaffeoylquinic acid, gallic acid, protocatechuic acid, syringic acid, vanillic acid and c) the hydroxyphenylacetic acids: homovanillic acid and p-hydroxybenzoic acid. Flavonoids include a) the flavones: apigenin, apigenin-7-O-glucoside, cirsimartin, genkwanin, homoplantaginin, ladanein, linaroside, luteolin, nepitrin, pectolinarigenin, scutellarein, salvigenin, tectochrysin, 4'5,7,8-tetrahydroxyflavone b) the flavonols: kaempferol, kaempferol-3-O-rutinoside, quercetin, rutin, and c) flavanones: hesperetin, hesperidin and naringenin-C-hexoside. Phenolic terpenes found in rosemary include a) diterpenes such as carnosol, carnosic acid, epirosmanol, epiisorosmanol, isorosmanol, militirone, methyl carnosate, rosmadial, rosmanol, rosmaridiphenol, 7-α-methoxyroamanol, 7-β-methoxyroamanol and b) triterpenes: betulin, betulinic acid, oleanolic acid, urosolic acid, α-amyrin, β-amyrin and 23-hydroxybetulinic acid (168,170–181).

The polyphenols found in highest quantity in RE are carnosic acid (CA), carnosol (COH) and rosmarinic acid (RA) (171,182). The production of these polyphenols is influenced by growth conditions such as sunlight exposure, soil quality, and water availability (183). Furthermore, anatomical regions of this herbal plant have varying levels of total phenolic content whereby the leaves contain the highest concentration of polyphenols in comparison to stem, branch and flower regions (184). RE has been shown to have antioxidant, anti-inflammatory, anti-microbial, anti-tumorigenic, and anti-hyperglycemic properties (185,186). These biological effects are highly correlated with

the polyphenolic content and CA, COH and RA are suggested to be responsible (185,186).

1.5.1 Evidence of Anti-Diabetic Effects of Rosemary Extract: *In Vitro* Studies

In vitro studies have shown that RE has an insulin-like effect to inhibit the production of glucose by hepatocytes. RE was shown to significantly suppress gluconeogenesis in HepG2 hepatocytes (187) (Table 2). In another study, RE was shown to significantly increase hepatocyte glucose uptake in a dose-dependent manner (188). CA, a major polyphenolic constituent of RE, prevented palmitate-induced lipid accumulation in hepatocytes (189) indicating that CA may potentially block cellular lipid accumulation in the long term and help against insulin resistance and T2DM. RE's polyphenolic constituents may also provide protection against chemically-induced reactive oxygen species production and hepatocyte death. RA exhibited significant cytoprotective effects against mycotoxin-induced reactive oxygen species (ROS) production and induction of apoptosis by blocking effects on caspase-3 activation in hepatocytes (190).

Treatment of 3T3-L1 adipocytes with RE (50 µg/ml) increased intracellular lipid levels and glucose uptake relative to the control (191). These effects of RE are similar to the lipid storing and glucose uptake effects of insulin in adipose tissue suggesting a potential of using RE against insulin resistance. In addition, it was reported that only CA and COH from all the major RE constituents, inhibited the differentiation of 3T3-L1 preadipocytes into mature adipocytes (192). Another study indicated that treatment with RE (30 µg/ml) resulted in complete inhibition of 3T3-L1 differentiation and CA (0.3-20 µM) alone exhibit a similar effect (193). In addition to the effects of RE on hepatic glucose production and adipocyte glucose uptake, RE has plays a role in intestinal glucose

absorption as well as carbohydrate digestion. Digestive enzymes such as amylase and α-glucosidase play an important role in carbohydrate digestion and absorption by converting complex carbohydrates to simple sugars such as glucose and fructose. Intestinal α-glucosidase allow glucose to be absorbed by the small intestine thereby increasing blood glucose levels. Inhibitors of α-glucosidase (acarbose, miglitol, voglibose) are used in the management of hyperglycemia present in T2DM. RE was found to have a significant α-glucosidase inhibitory activity (194) which was the most potent among the other extracts of herbs and spices tested. Moreover, RE was demonstrated to significantly inhibit porcine pancreatic amylase activity (PPAM) *in vitro* (195). PPAM hydrolases dietary polysaccharides into less complex saccharides allowing further digestion. Additionally, RA, a major polyphenolic constituent of RE also significantly inhibited PPAM (196).

Other effects of RE that may contribute to regulation of glucose homeostasis may be due to its effects on lipid/fat metabolism. Lipids are stored in our cells particularly adipocytes in the form of triglycerides (TG). The breakdown of TG is controlled by enzymes called lipases. Excessive activation of hormone sensitive lipase leads to increases in plasma lipid levels such as free fatty acids (FFA) contributing to insulin resistance and T2DM. The effects of RE were assessed on hormone sensitive lipase (HSL) and pancreatic lipase (PL), a key enzyme involved in fat digestion and was shown to significantly inhibit both enzymes in a dose-dependent manner in rat epididymal adipocytes (197). Pure RA was shown to inhibit PL and HSL in a dose dependent manner. Moreover, the extract had greater inhibitory activity compared to purified compounds suggesting that the extract contains a variety of constituents that may contribute synergistically in the inhibition of these enzymes (197). Additionally, *in vitro* analysis indicated that CA rich RE inhibited

PL activity by 70% (198). These studies clearly indicate that RE and its constituents CA and RA have in antilipolytic activity *in vitro.*

Skeletal muscle tissue is important target of insulin and accounts for approximately 80% of insulin mediated glucose uptake in the postprandial state. As a consequence, it plays a predominant role in glucose homeostasis. Treatment of L6 myotubes with RE increased glucose uptake in a dose- and time-dependent manner (160). Maximum stimulation of glucose uptake was seen with 5 µg/ml of RE was comparable to the maximum stimulation of glucose uptake by insulin or metformin (Table 2) (160). In addition, treatment of L6 myotubes with CA (20 µg/ml for 6 hours) resulted in significant increase in glucose uptake (199). Additionally, treatment with of L6 myotubes with CA (5µM for 4 hours) increased glucose uptake to levels comparable to insulin and metformin (161). Additionally, treatment with RA (5 µM for 4 hours) significantly increased glucose uptake that was comparable to insulin and metformin (162). All of the above *in vitro* studies indicate that RE has the potential to affect key insulin target tissues (liver, fat, muscle) and directly induce anti-diabetic effects.

Table 2: Anti-diabetic effects of RE and its main polyphenolic constituents: *in vitro* studies

Study	Cell/Model	Treatment	Effects
Yun et al.(187)	HepG2 hepatocytes	RE 100 µg/ml	↓ gluconeogenesis.
Tu et al.(188)	HepG2 hepatocytes	RE 0.4, 2, 10, 50 µg/ml	↑ glucose uptake
Wang et al.(189)	HepG2 hepatocytes	CA 10-20 µM	↓palmitate-induced lipid accumulation
Cui et al.(200)	HepG2 hepatocytes	COH 20-40 µM	↓*de novo* formation of intracellular TG
Renzulli et al.(190)	HepG2 hepatocytes	RA 25-50 µM	↓apoptosis ↓ROS production
Babish et al.(191)	3T3-L1 adipocytes	RE 50 µM/ml	↑intracellular lipid ↑glucose uptake
Takahashi et al.(192)	3T3-L1 adipocytes	CA 3 µM, COH 3 µM	↓ differentiation ↑intracellular GSH
Gaya et al.(193)	3T3-L1 adipocytes	RE 10-30 µg/ml CA 0.3-20 Mm	↓ differentiation.
Koga et al.(194)	Rat intestinal α-glucosidase (AGc)	RE (IC50 683-711 µg/ml)	↓AGc
Ingrid et al.(195)	Porcine Pancreatic α-amylase (PPAM)	RE 10-100 µg/ml	↓ PPAM activity (60%)
McCue et al.(196)	Porcine pancreatic α-amylase (PPAM)	RA 3.2 µg/ml	↓ amylase activity by 85%
Bustanji et al.(197)	Rat epididymal adipocytes Porcine pancreatic lipase (PL); Hormone sensitive lipase (HSL)	RE 6.3-200 µg/ml & its constituent RA	↓ PL ↓ HSL
Ibbara et al.(198)	Human PL	RE 100 µg/ml rich in CA	↓PL by 70%
Naimi et al.(160)	L6 rat muscle cells	RE 5 µg/mL for 4 h	↑ glucose uptake
Lipina et al.(199)	L6 rat muscle cells	CA 20 µg/mL for 6 h	↑ glucose uptake
Naimi et al.(161)	L6 rat muscle cells	CA 5 µM for 4 h	↑ glucose uptake
Vlavcheski et al. (162)	L6 rat muscle cells	RA 5 µM for 4 h	↑ glucose uptake

1.5.2 Evidence of Anti-Diabetic Effects of Rosemary Extract: *In Vivo* Studies

Several studies have been carried out in diabetic animal models to investigate the anti-hyperglycemic effects of RE (Table 3). In streptozotocin-(STZ) induced diabetic rats, administration of an aqueous RE resulted in significant decrease in fasting plasma glucose (FPG) level (201). In another study, administration of 50% ethanol extract of rosemary in STZ rats significantly decreased plasma glucose levels due to inhibition of glucosidase enzyme activity (194). In a more recent study, daily administration of aqueous RE (200 mg/kg) for three weeks caused significant reductions in blood glucose levels of both normal and STZ-induced diabetic rats (202). Similar effects were seen on blood glucose levels in STZ-induced diabetic rats given aqueous RE (4g/kg/day) for 4 weeks (203). In addition, the extract significantly reduced plasma, FPG, TG, total cholesterol (TC) and low density lipoprotein (LDL) while increasing plasma high density lipoprotein (HDL) and erythrocytes levels. In agreement with the above studies, blood glucose levels as well as TC and TG levels were significantly reduced in STZ-induced diabetic rats given aqueous RE (200 mg/kg/day) 2 weeks before and 2 weeks after STZ injection (204,205). Furthermore, administration of aqueous extract of rosemary prior to streptozotocin injection in rats significantly protected against STZ-induced elevations in blood glucose levels which was correlated with a significant protection against pancreatic β-cell loss (206). Administration of dried rosemary leaves for approximately 6 weeks in STZ-induced diabetic and healthy Sprague Dawley rats decreased the FPG, glycated hemoglobin (HbA1c), TC and TG and LDL levels in STZ-induced rats without effecting the plasma glucose levels or the lipid profile in the control group (207).

In addition to the STZ-induced diabetic model, the alloxan-induced diabetes animal model is also used extensively. Alloxan causes diabetes by rapid depletion of pancreatic β-cells leading to inflammation and sustained hyperglycemia secondary to a reduction in insulin release into circulation. In alloxan-induced diabetic rabbits, ethanol RE (200 mg/kg) lead to a significant reduction in FPG (208). In contrast, another study indicated that intramuscular administration of volatile oil of RE leaves inhibited insulin release and increased blood glucose levels leading to hyperglycemia in normal and alloxan-induced diabetic rabbits (209). In another study, oral administration of powdered RE added as 20% of diet or 20% aqueous RE to alloxan induced diabetic rats significantly decreased the fasting plasma glucose levels compared to control and the treatment demonstrated to reduce alloxan-induced hepatocyte vacuolar degeneration, necrosis, small hemorrhages and dilatation of hepatic sinusoids indicating hepatoprotective effects (210). Moreover, administration of RA (100-200 mg/kg) to alloxan-induced rats for eight weeks significantly inhibited glomerular hypertrophy, glomerular number loss and glomerulosclerosis compared with diabetic control indicating RA's renoprotective properties (211). Administration of 250 and 500 mg/kg/day of RE mixed with water (70%) for 63 days in male rats did not affect serum blood glucose, TG, TC levels or body weight but testosterone levels, spermatogenesis, sperm density and motility were significantly decreased (212). In addition, alanine aminotransferase (ALT) and aspartate aminotransferase (AST), *e*nzymes released due to liver damage, were also decreased.

Oral administration of CA (approximately 17mg/kg/day) to obese leptin receptor deficient mice for five weeks resulted in significant protection against fat-induced fasting and non-fasting hyperglycemia, improved glucose tolerance as well as decreased serum

insulin levels (213). CA also significantly inhibited weight gain, decreased regional areas of visceral fat, and prevented against fat accumulation in white adipose tissue as well as liver. Moreover, animals supplemented with CA exhibited decreased serum levels of triglycerides, cholesterol, and ALT as well as significantly decreasing hepatic lipid storage (213).

Apart from animal models of genetic and chemically-induced obesity and T2DM, the effects of RE have been examined in dietary animal models of obesity and T2DM. Daily, dietary supplementation of RE (500 mg/kg) standardized to contain 20% CA for 16 weeks in mice that were started on a high-fat diet (HFD) as juveniles significantly protected against HFD-induced elevations in plasma glucose and TC levels compared with HFD control mice (198). Notably, fasting insulinemia remained low during the length of the study and no significant differences were observed between the groups. Correlating with the observed reductions in total cholesterol levels, HFD mice supplemented with RE displayed significant decreases in fat mass and one to twofold increase in total fecal lipid content compared to HFD-fed control mice (198). Additionally, another study indicated that administration CA (20 mg/kg) in 5-20 mg/kg olive oil loaded mice, significantly repressed the elevation of TG levels, prevented epididymal fat gain and inhibited pancreatic lipase activity (214). Administration of 200 mg/kg of RE for 50 days in mice fed high fat diet, resulted in reduced b.w and fat mass and increase of fecal lipid excretion, while hepatic triglyceride content was decreased (215). Similarly, daily administration of aqueous RE (100 mg/kg b.w) to high-cholesterol fed mice for 36 days resulted in significant decline in plasma TG, TC, LDL levels, while HDL levels were increased compared to control mice (216). Furthermore, administration of aqueous RE (70-140

mg/kg b.w) and non-esterified phenolic RE (7 to 14 mg/kg b.w) for four weeks resulting in significant reduction in TC and non-HDL levels compared to control (217). High-fructose fed (HFR) mice given daily dose of RA (100 mg/kg b.w) for 60 days decreased fasting plasma glucose levels, improved glucose tolerance and reduced plasma insulin and glycated HbA1c levels (218). In contrast, obese mice and their lean counterparts fed 0.5% ethanol extract of rosemary enriched with CA (40%) incorporated in their standard chow for 64 days did not show significant differences in their glucose levels compared to control rats, although circulating insulin levels were found to be significantly decreased only in the lean rats (219). Noteworthy, the plasma glucose levels in all animals were within normal physiological range with a non-significant, slight increase in obese counterparts. The study also demonstrated a significant inhibition of gastric lipase (GL) in the stomach and pancreatic lipase (PL) in small intestine of rats consuming the RE(219) Furthermore, there was a significant attenuation of circulating plasma TNF-α, IL-1β, leptin and elevation of adiponectin levels (Table 3) (220).

Table 3: Anti-diabetic effects of RE and its main polyphenolic constituents: *in vivo* studies

Reference	Animal Model	Dose	Glucose	Other Measures
Erenmemisoglu et al.(201)	STZ-induced diabetic Swiss albino mice	Ad libitum (10 g leaves of rosemary in 1 L boiling water) for 3 months	↓FPG in healthy & diabetic animals	↔ creatinine, urea, bilirubin, total albumin, alkaline phosphatase
Koga et al.(194)	STZ-induced diabetic male ddY mice	RE aqueous & ethanol 20 mg/kg/day	↓ plasma glucose levels	↓α-glucosidase (AGc)
Khalil et al.(202)	STZ-induced diabetic male albino rats	RE aqueous, 200 mg/kg/day for 3 weeks	↓ FPG	↑vitamin C
Al-jamal.(203)	STZ-induced diabetic male albino rats	RE aqueous 4g/kg/day for 4 weeks	↓ FPG (20%)	↓TC, TG, LDL ↑HDL
Alnahdi.(204)	STZ-induced diabetic male albino rats	RE aqueous, 200 mg/kg/day 2 weeks prior and 3 weeks after STZ	↓FPG (36.9%)	↓TC, TG, LDL ↑HDL ↑hemoglobin levels
Emam.(205)	STZ-induced diabetic male albino rats	RE aqueous, 200 mg/kg/day for 21 days	↓FPG	↓TC ↓TG ↑TAC
Ramadan et al.(206)	STZ-induced diabetic male albino rats	RE aqueous, 200 mg/kg/day 2 weeks prior and 3 weeks after STZ	↓FPG in both groups ↑serum insulin ↑C-peptide ↓β-cell loss	↑total albumin
Soliman.(207)	STZ-induced diabetic male Dawley rats	Dried rosemary leaves powder 5g/100g of diet	↓FPG (53.97%), ↓HbA1c (24.56 %)	↓TG (45.43%) ↓TC (39.31%) ↓LDL (33.89 %)
Bakirel et al.(208)	Alloxan-induced diabetic rabbits	RE ethanol, 200 mg/kg for 6 hours (acute); for 1 week (subacute)	↓FPG in healthy and diabetic rabbits ↑plasma insulin levels	↓MDA (33.3%) ↑SOD (24%) ↑CAT (35%)
Alhader et al.(209)	Alloxan–induced male diabetic rabbits	RE volatile, 25 mg/kg intramuscular injection for	↑serum glucose levels ↓ serum insulin	

		30, 60 and 120 min		
Kensara et al.(210)	Alloxan-induced Sprague-Dawley male albino rats	20% RE aqueous and 20% RE powdered food for 45 days	↓FPG	↓hepatocyte necrosis ↓small hemorrhages ↓hepatocyte degradation
Tavafi et al.(211)	Alloxan-induced Sprague-Dawley uninephrectomized rats	RA 100-200 mg/kg/day for 8 weeks		↓glomerulosclerosis ↓creatinine and urea ↓glomerular number ↓serum MDA,
Nusier et al.(212)	Male adult Sprague-Dawley rats	70% RE aqueous, 250 and 500 mg/kg/day for 63 days.	↔ serum glucose	↔ body weight TG, TC ↓alanine aminotransferase (ALT) ↓Aspartate Aminotransferase (AST) ↓spermatogenesis ↓testosterone ↓sperm motility
Wang et al.(213)	Male ob/ob mice	CA 17mg/kg/day for 5 weeks	↓FPG (18%) ↓OGTT glucose levels ↓serum insulin (47%)	↓TC (24%) ↓TG (60%) ↓plasma FFA (13%) ↓hepatic lipids ↓ALT (64%)
Ibarra et al.(198)	HFD-treated male C57BL/6J mice	RE aqueous, containing 20% CA 500 mg/kg/day for 16 weeks	↓FPG (72%) ↔ insulin	↓body weight ↑fecal total lipid content (1-2 fold) ↓fat mass ↓TC (68%) ↔ TG
Ninomiya et al.(214)	HFD-(olive oil) treated male ddY mice	CA 20 mg/kg for 14 days COH 200 mg/kg for 14 days		↓body weight (7%) ↑epididymal fat ↓pancreatic lipase (IC50 12 and 4.4 µg/ml for CA and COH respecively)
Harach et al.(215)	HFD-treated male C57BL/6J mice	RE 20 or 200 mg/kg/day for 50 days	↔ FPG, ↔ glucose tolerance ↔ insulin	↓body weight and fat mass (64% and 57%) ↓Hepatic TG (39 %) ↔ serum TG and TC ↑fecal lipid excretion
Al Sheyab et al.(216)	Diet-induced HC female BALB/c mice	RE aqueous, 100 mg/kg/day for 36 days		↓TC, TG, LDL ↑HD
Afonso et al.(217)	Diet-induced HC Wistar rats	RE aqueous, 70-140 mg/kg/day		↓TC (39.8%) ↓non-HDL (44.4%)

		RE non-esterified phenolic 7-14 mg/kg/day of for 4 weeks		
Vanithadevi and Anuradha(218)	Fructose-fed (FF) Swiss albino mice	RA 100 mg/kg/day for 60 days	↓FPG levels ↓HbA1c ↓OGTT glucose levels ↓plasma insulin levels	↑diaphragm glucose utilization
Vaquero et al.(219)	Female Zucker lean (fa/+) and obese (fa/fa) rats	RE ethanol, enriched with 40% CA for 64 days	↔ plasma glucose levels ↓insulin levels in lean animals	↓TC, TG, LDL ↑HDL ↓leptin, TNF-α, IL-1β (lean rats) ↓gastric lipase activity

1.5.3 Evidence of Anti-Hyperglycemic Effects of Rosemary: Human studies

In addition to numerous *in vitro* cellular studies and *in vivo* animal studies, RE has been recently investigated in humans. Healthy participants were randomly selected into 3 groups and treated with 2, 5 or 10g/day of dried rosemary leaf powder for 8 weeks (221) (Table 4). Blood samples were taken from participants before and after the study. FPG was decreased by 18.25, 15.74 and 11.2% in the 10, 5 and 2g/day group respectively. TC levels were significantly decreased by 34.48% in the 10g/day group and 17.97% and 11.48% in the 5g/day and 2g/day respectively. LDL cholesterol in this group was also significantly lowered by 32.28% in the 10g/day treated group and 28.46% and 15.58 % in the 5g/day and 2g/day respectively. Additionally, HDL cholesterol was increased by 22.91% in the 10g/day group and 15.21% and 4.54% in the 5g/day and 2g/day respectively. Furthermore, triglyceride levels were also decreased by 29.06% in the 10g/day group and 21.3% and 14.97% in the 5g/day and 2g/day treated group respectively. In addition to the improvement in the overall lipid profile rosemary powder

seems to exhibit high antioxidant prosperities by decreasing malonaldehyde (MDA) by 36.21%, 12.43% and 13.6% in the 10g/day, 5g/day and 2g/day treated groups respectively. Glutathione reductase (GR) was decreased by 15.36%, 6.73%, and 0.95% in the 10g/day, 5g/day and 2g/day treated groups respectively. Additionally, there have been a few studies indirectly examining the effects of rosemary supplements with non-conclusive results. An observational, prospective, monocenter study examined the effect of 21 days of oral supplementation of aqueous RE (containing 77.7 mg RE with 0.97 mg COH, 8.60 mg CA, and 10.30 mg RA) in twelve healthy young volunteers found a significant decrease in plasminogen activator-inhibitor-1 (PAI-1) levels suggesting that RE may have anti-inflammatory and anti-blood clotting activity *in vivo* (222). Another observational study demonstrated that administration of RE and oleanolic acid, (440 mg thrice a day for 4 weeks and additional 880 mg twice a day for 4 weeks) in patients with osteoarthritis, fibromyalgia, and rheumatoid arthritis, was protective against inflammatory rheumatic diseases particularly in those with initial serum c-reactive protein (CRP) levels >7.0 mg/L (223).

Table 4: Anti-diabetic and antioxidant properties of RE: Human studies

Reference	Study methodology	Treatment	Effect
Labban et al.(221)	48 healthy individuals	Dry rosemary powder 2, 5 or 10 g/day, for 8 weeks	↓FPG ↓TC ↓LDL, ↓TG, ↑HDL, ↓MDA, ↓GR, ↑vitamin C, ↑β-carotene)
Sinkovic et al.(222)	12 healthy, young volunteers	RE 77.7 mg COH 0.97 mg CA 8.6 mg RA 10.30 mg for 21 days	↓ PAI-1 levels
Lukaczer et al.(223)	72 patients with rheumatic disease including osteoarthritis (OA), rheumatoid arthritis (RA) and fibromyalgia (FM).	Meta050 compound (RE, oleanolic acid and reduced iso-alpha-acids) 440 mg/day for 4 weeks 3 times per day 880 mg/day for 4 weeks 2 times per day.	↓CRP ↓ arthritis pain scores ↔ fibromyalgia scores

1.6 Rationale

Skeletal muscle is quantitatively the most significant target tissue of insulin and therefore plays an important role in glucose homeostasis. Impairments in insulin signaling in skeletal muscle leads to insulin resistance and T2DM. Increased plasma FFAs such as palmitate have been linked to insulin resistance *in vitro* and *in vivo* (52). Elevated free fatty acids (FFAs) in the blood, as seen in obesity, impair insulin action in muscle leading to insulin resistance and Type 2 diabetes mellitus. Serine phosphorylation of the insulin receptor and insulin receptor substrates (IRS) reduces insulin-stimulated tyrosine phosphorylation and insulin action. Protein kinases including GSK3 (40), JNK (41, 42), PKC's (66), mTOR (45), p70 S6K (47) have been found to be implicated in

FFA-induced insulin resistance both *in vitro* and *in vivo*. Several studies that used L6 and C2C12 skeletal muscle cells have indicated that palmitate elevates ceramide production, increases phosphorylation of Ser307 and Ser636/639 of IRS-1 leading to impairment in the insulin signaling (52,100). The above mentioned protein kinases can lead to phosphorylation of Ser307 and Ser636/639 residues of the IRS-1 which in turns impairs the downstream insulin signaling cascade thus significantly reducing the insulin stimulated glucose uptake (51). Additionally, studies have found that obese individuals with an increased FFA plasma levels have shown a significant reduction in the insulin-induced glucose uptake (51,224).

The biological effects of the polyphenols ignited an interest from the scientific community to be used as nutraceuticals to counteract different diseases. Rosemary extract and rosemary polyphenols have been shown to increase glucose uptake in skeletal muscle cells (160,161) and prevented high fat diet-induced insulin resistance in mice (198,213). However, the effects of RE and RE polyphenols have never been examined in FFA-induced insulin resistance in L6 muscle cells. Therefore, the exact mechanism of RE action needs to be elucidated by further investigating the key signaling molecules that may exhibit antidiabetic properties. Understanding the mechanism is required in order to enhance the potential of RE to be used as a preventative/therapeutic treatment strategy for insulin resistance type 2 diabetes mellitus.

1.7 Hypothesis

In the current thesis we hypothesize that:

1) Rosemary extract and its polyphenols CA, RA and COH prevent the palmitate-induced skeletal muscle insulin resistance.

2) Rosemary extract ameliorates the palmitate-induced IRS-l Ser307 & Ser636/639 phosphorylation

3) Rosemary extract ameliorates the palmitate-induced decrease in insulin-stimulated Akt phosphorylation.

4) Rosemary extract attenuates the FFA-induced increase in JNK, mTOR and p70 S6K.

5) Rosemary extract increases AMPK activation and AMPK may play a role in the RE and RE polyphenol-mediated effects.

1.8 Significance:

Currently there is no cure for diabetes mellitus however the treatment strategy usually includes managing and alleviation of the underlying pathological processes with life style changes such as regular exercise and healthy diet together with pharmacological interventions. Oral medication for the treatment of T2DM include sulfonylureas and meglitinides that stimulate insulin release from the β-cells, α-glucosidase inhibitors that inhibit intestinal glucose absorption, biuanides and thiazolidinediones that increase peripheral glucose transport and inhibit the hepatic glucose output via gluconeogenesis. However, despite the different treatment strategies available there is lack of drug efficacy which is accompanied by many unwanted side-effects. For instance, metformin, a

biguanide drug that is prescribed as a first line of treatment for T2DM is highly associated with acidosis and gastrointestinal issues such as diarrhea, nausea, vomiting and cramps (225). Overall, there is a continued interest for more effective treatment with less side-effects despite the medications available for the management of T2DM. Around 50% of the affected individuals with T2DM are living in poverty stricken area in Asia and Africa. As a result, there is pressing need for a more effective and less expensive treatment. The study of novel agents that can exhibit an insulin-like effect, improve insulin sensitivity and efficacy of treatment with less adverse effects that will broaden the spectrum of preventative and treatment options for T2DM is highly desired. The use of plants for healing purposes forms the origin of modern medicine. Moreover, the use of phytotherapy has been on the rise in the developed world considering that many conventional drugs such as aspirin (from willow tree bark) and morphine (opium poppy) as well as metformin (French lilac) have been extracted from plants. Together with the limited studies performed in humans, all the available information up to now provide evidence of antidiabetic, antioxidant and anti-inflammatory activities of RE in streptozotocin-induced diabetic mice (226), rats (205,206,227), alloxan-induced diabetic rabbits (228), genetic (229), and dietary (227,230,231) animal models of obesity and insulin resistance. The promising findings from *in vitro* and *in vivo* models suggest that RE and its polyphenols may be used as an agent for the management of diabetes. Investigating the effects of RE and RE polyphenols *in vitro* is needed in order to delineate their effects in different cells and tissue types thereby providing more evidence about its mechanism of action. On the other hand, clinical trials conducted on humans may be required to elucidate their therapeutic potential against insulin resistance.

CHAPTER 2: METHODOLOGY

2.1 Materials

Fetal Bovine Serum (FBS), rosmarinic acid, dimethyl sulfoxide (DMSO), *o*-phenylenediamine dihydrochloride (OPD) and cytochalasin B, were purchased from Sigma Life Sciences (St. Louis, MO). Materials for cell culture were purchased from GIBCO Life Technologies (Burlington ON). Anti-c-myc antibodies and Peroxidase-conjugated Goat anti-rabbit IgG were purchased from Sigma Life Sciences and Jackson ImmunoResearch Labs, (West Grove, PA. St. Louis, MO. Mississauga, ON respectively). Phospho- and total AMPK, Akt and HRP-conjugated anti-rabbit antibodies were purchased from New England BioLabs (NEB) (Missisauga, ON). Insulin (Humulin R) was from Eli Lilly (Indianapolis, IN). Compound C and wortmannin were purchased from Calbiochem (Gibbstown, NJ, USA). Luminol Enhancer reagents, polyvinylidene difluoride (PVDF) membrane, reagents for electrophoresis and Bradford protein assay were purchased from BioRad (Hercules, CA). BioRad. [^{3}H]-2-deoxy-D-glucose was purchased from PerkinElmer (Boston, MA).

2.2 Cells

The L6 skeletal muscle cells are an immortalized myogenic cell line obtained from rat hindlimb. The cells undertake the process of proliferation when grown in α-minimum essential media (α-MEM) containing 10% fetal bovine serum (FBS) and undergo spontaneous differentiation into multinucleated myotubes by placing them into α-MEM containing 2% FBS. L6 skeletal cells can grow in monolayers which makes them accessible to biologically active compounds/chemicals rendering them a good model for

investigating their effects. Additionally, they express both insulin receptor and insulin-like growth factor receptor (IGF-1) along with facilitated glucose transporters (GLUTs) such as GLUT1, GLUT3 and GLUT4 (241). Throughout the differentiation stage from myoblasts to myotubes, the expression of the insulin receptor as well as GLUTs transporters increases which results in insulin responsiveness (232,233). After insulin treatment, all three GLUTs expressed in the cell undergoing translocation to the cell membrane however GLUT4 is the transporter that is greatly affected by the insulin action (242). In agreement with the changes in GLUTs expression observed between the myoblast and myotube stage, the transport of glucose is also different as the cell differentiates. The basal glucose transport is highest in myoblast whereas insulin-induced glucose uptake is detected only after cell alignment and further increases as the cells differentiate to a myotube phase (243).

Cells in culture has been extensively used in order to investigate different hormonal and metabolic processes. There are several advantages in regards to using cells in culture. For instance, the cells in culture are a homogeneous population with small intracellular spaces unlike intact tissue preparation in addition to tightly controlled external environment and with absence of external factors found *in vivo* that could possibly interfere with the actual effect of the treatment. Furthermore, *in vitro* models are well-recognized when examining numerous acute and chronic treatments. Specifically, in this study L6 muscle cells were chosen considering that the palmitate-induced insulin resistant model was previously established in our lab. Isolation of human skeletal muscle strips are only possible during surgical procedures thus their availability is quite limited. In addition, there is a great risk of damaging the membrane integrity after harvesting the

muscle tissue (234). In primary cell culture stimulation with physiological concentration of insulin was not demonstrated to be effective. Moreover, establishing primary culture can be difficult and arduous process. Primary cell culture is not generally used taking into consideration that it is extremely sensitive and requires additional nutrients which need to be specifically customized for each cell type thereby increasing the cost.

Other than the L6 muscle cells, C2C12 are also insulin responsive and contain GLUT1 and GLUT4 transporters (234). However, the insulin responsiveness and the GLUTs content is much lower in comparison to L6 and C2C12 are usually implicated in studies that utilize contraction as a form of stimulation (235,236).

Although L6 muscle cells exhibit similar characteristics to skeletal muscle it is important to note that they are not identical. For instance, the actin network of L6 myotubes does not form the contractile sarcomeres found in skeletal muscle and the fully differentiated cells do not replicate the physiological interactions between the cells as seen *in vivo.* Additionally, the insulin-stimulated glucose uptake in L6 is lower compared to skeletal muscle (2 fold increase vs 4-5 fold respectively) (237).

Despite these differences L6 muscle cells exhibit many similarities to skeletal muscle (as mentioned above). Therefore, they provide a good model for investigating the mechanism of insulin action and different compounds that may affect glucose uptake and metabolism.

2.3 Cell Culture Technique

L6 muscle cells were grown in a 250 cm^3 flasks containing α-MEM media (pH 7.4) supplemented with 10% FBS (v/v), 1% antibiotic-antimycotic cocktail solution (100

U/ml penicillin, 100 μg/ml streptomycin and 250 ng/ml amphotericin B) and 5mM glucose until 60-70% confluency was reached. The myoblasts were then trypsinized, counted with a hemocytometer and 100 000-120 000 cells/ml (cells/well) were seeded in 12 or 6 well tissue culture plates in α-MEM containing 10% FBS (v/v) and 1% antibiotic-antimycotic cocktail solution. The 12 well plate contained 1 ml of cells with media and was used for glucose uptake measurements and the 6 well plate contained 2 ml of cells with media and was used for western blotting analysis. After the cells reached 100% confluency the cells were exposed to a 2% FBS (v/v) and 1% antibiotic-antimycotic cocktail containing media solution to allow the myoblasts to differentiate into myotubes. Fresh media was introduced every 48 hours and the cells were maintained for 5-6 days until becoming fully confluent differentiated myotubes.

Serum deprivation for 18 hours was performed in all experiments. The rate of the basal glucose transport is decreased by serum deprivation (238) thus the cells are not at their maximum transport capacity prior to stimulation. As a result, the increase in glucose uptake in response to treatment is more detectable.

After the treatment was completed, the cells were rinsed with HBS followed by glucose transport assay or cell lysis for western blotting. Stock solutions of RE and its polyphenols such as CA, RA were made by dissolving the powder in sterile DMSO. The cells were never exposed to more than 0.1% DMSO. Therefore, in parallel to the treatment group, a vehicle-treated group (0.0051% of DMSO) was used as a control. Insulin stock solution was prepared in α-MEM containing 2% FBS (v/v). Palmitate solution was conjugated with fatty acid-free bovine serum albumin (BSA) (Sigma, St. Louis, MO)

2.4 Preparation of Palmitate Stock

500 mL of distilled water was placed to boil in a 1000 mL size beaker and a water bath was pre-warmed at 45 degrees Celsius. 41 mg of palmitic acid was weighed out and transferred into a scintillation vial. Cut out Styrofoam was used to allow the vial to float on top of the boiling water. In a separate 50 mL vial 1.94g of BSA was dissolved in 20 mL of distilled water to make up 9.7% BSA solution. The solution was then vortexed and placed into a 45-50 degrees Celsius water bath followed by placing the scintillation vial containing the palmitic acid into the boiling water. Once the palmitic acid vial is in the boiling water 15mL vial containing 0.1 N NaOH was added to the hot water until the NaOH solution started to bubble. Once the palmitic acid was melted, 1.6 mL of 0.1 N NaOH was transferred into palmitic acid vial and allowed to dissolve. The solution was then transferred to a pre-warmed up water bath and allowed to equilibrate. Once the solution is in the water bath 18.4 mL of the pre-warmed BSA was quickly added to the vial to give a final stock of 8mM of palmitate solution. The final molar ration of free palmitate vs BSA was 6:1.

2.5 Preparation of Rosemary Extract (RE)

Following previously established protocols by the National Cancer Institute of the US (223, 226 from Madina) whole dried Rosemary leaves (Rosmarinus officinalis L.) (Compliments, Sobey's Missisauga, ON, Canada) were grounded and passed through a mesh sieve. 5 grams of ground leaves were steeped for 16 hours in dichloromethane-methanol (1:1) (30 mL). Under a slight vacuum the filtrate was collected followed by methanol (30 mL) extraction for 30 min. The solvent was removed using rotary

evaporator. Aliquots of the extract dissolved in dimethyl sulfoxide (DMSO) were prepared (100 μg/ml) and were stored at -20˚C (226).

2.6 Cell Treatment

L6 myotubes were serum deprived for 18 hours in the absence and presence of 5 μg/ml RE, 2 μM CA, 5 μM RA and 25 μM COH for 2 hours followed by treatment with 0.2 mM of palmitate for 16 hours. Cells were exposed to 100 nM insulin for 0.5 hours. A vehicle-treated control (0.0051% of DMSO) was used in parallel with the treated groups.

2.7 Glucose Uptake Assay

The glucose uptake assay is a radiometric assay measuring the specific GLUT transporter-mediated glucose uptake using [3H]-2-deoxy-D-glucose, a non metabolizable glucose analog. After the incubation the cells were washed 3 times with HEPES-buffered saline solution (HBS) containing 20 mM HEPES, 5mM KCl, 2.5mM MgSO4, 1mM CaCl2 and 14mM NaCl, pH 7.4. Following the washing, 2-deoxy-D-glucose uptake measurements were performed by exposing the cells to 250μl of HBS containing 10μM [3H]-2-deoxy-D-glucose for precisely 10 minutes. Measurements of nonspecific uptake of 2-deoxyD-glucose were achieved by exposing the cells to 10μM cytochalasin B (GLUT inhibitor). The specific uptake was obtained by subtracting the nonspecific from the total uptake (in the absence of cytochalasin B). The glucose uptake was terminated by placing the cells on ice followed by washing the cells 3 times with 1 mL of ice cold 0.9% NaCl solution and finally lysed with a 1 mL of 0.05N NaOH solution. The cell lysates were placed into scintillation vials followed by addition of 10 mL of scintillation fluid. The experiments were always performed in triplicates and as many times as indicated in

each figure. Radioactivity was measured using a ScintiCount (PerkinElmer) Scintillation Counter. The results are shown as percentage of control for each individual experiment.

2.8 Preparation of Cell Lysates for Western Blotting

L6 muscle cells grown in 6-well plates until differentiated into myotubes. After treatment, the cells were rinsed 2 times with PBS and placed on ice. PBS was aspirated and followed by addition of 100µl of cell lysis buffer (20mM Tris (pH 7.5), l50 mM NaCI, 1 mM EDTA, 1mM EGTA, 1% Triton X-100, 2.5mM sodium pyrophosphate, 1 mM p-glycerolphosphate, 1 mM Na3V04, 1 µg/ml leupeptin, add 1 mM PMSF before use and chill on ice) to each well. The cell lysates were collected into 1.5 mL eppendorf tube, protein assay was performed along with addition of equal amount of sodium dodecyl sulfate (SDS) buffer (62.5 mM Tris-HCI (pH 6.8), 2% w/v SDS, 10% glycerol, 0.01 % bromophenol blue, add 0.05% p-mercaptoethanol before use). The lysates were then boiled for 5 minutes and stored in -20 °C.

2.9 Protein Assay

Protein assay dye was purchased from BioRad and used to determine protein concentration on cell lystes. BSA protein standards were used in order to create a standard protein curve including 0, 0.1, 0.2, 0.4, 0.6, 0.8, 0.9, 1.0 mg/ml. Measurements were performed in triplicates where 10µl of each protein standard and lysed sample were pipetted into separate wells of a 96 well plate following by addition of 200µl of protein assay dye in each well. The plate was incubated at room temperature for 5 minutes which was followed by absorbance measurements in a microplate reader at 595nm. The final

concentration of the protein samples was calculated using Microsoft Excel and was used to determine the loading the same amount of protein during western blot analysis.

2.10 Western Blot Analysis

After treatment, the cells were washed three times with HBS and lysed with lysis buffer containing 150mM NaCI, 20mM Tris (pH 7.5), 1mM EDTA, 1% Triton X-100, 1mM EGTA 2.5mM NA407P2, 1mM Na3V04 1Mm, β-glycerolphosphate, 1mM PMSF, 1μg/ml leupeptin. The cells were scraped off and solubilized in electrophoresis (running) buffer which was followed by separation by sodium dodecyl sulfate (SDS) polyacrylamide gel (10%) electrophoresis. Each sample loaded contained 15 μg/ml of protein. The samples were then transferred electrophoretically to PVDF membranes. The membranes were placed in 5% (w/v) nonfat dry milk in Tris-buffered saline blocking followed by overnight incubation with primary antibody at 4°C. The total and phosphorylated forms of the proteins were detected by immunoblotting on separate PVDF membranes. The primary antibody were detected by HRP-conjugated antirabbit secondary antibody (1:2000). LumiGLOW reagent purchased from New England Biolabs and Alpha Innotech FluorChem (quantitative imaging system for fluorescent and chemiluminescent blots (Johannesburg, S.A) were used to develop the blots. The densitometry of the bands, expressed in arbitrary units, was calculated using image J. The results are shown as percentage of control for each individual experiment.

2.11 Statistical Analysis

Statistical analysis was completed using GraphPad Prism software 5.3. The data from several experiments were pooled and presented as mean ± standard error (SE). The

means of all the groups were obtained and compared to the control group using one-way analysis of variance (ANOVA) which was followed by Tukey's post hoc test for multiple comparison.

CHAPTER 3: RESULTS

3.1 Rosemary extract restores the insulin-stimulated glucose uptake in palmitate treated muscle cells

The effects of the free-fatty acid palmitate on insulin-stimulated glucose uptake in L6 myotubes was examined. Acute insulin stimulation (100 nM, 30 min) of the myotubes significantly increased the [^{3}H]-2-deoxy-D-glucose uptake (201±1.21% of control, $P<0.001$, Figure 4). Exposure of the cells to palmitate (0.2 mM, 16 hours) resulted in significant reduction of insulin-stimulated glucose uptake (117±15.6% of control) which indicates insulin resistance. Exposure of the cells to RE (5 μg/ml) alone resulted in significant increase in [^{3}H]-2-deoxy-D-glucose uptake (208±15.6% of control, $P<0.001$). Most importantly in palmitate-treated cells, exposure to RE resulted in significant restoration of insulin stimulated glucose uptake (179±10.5% of control, $P<0.001$, Figure 4). These data clearly indicate that the negative effect imposed by palmitate treatment is significantly ameliorated in the presence of RE. In addition, treatment with palmitate alone did not have any effect on the basal glucose uptake in comparison to the control group (103±2.7% of control) (Figure 4).

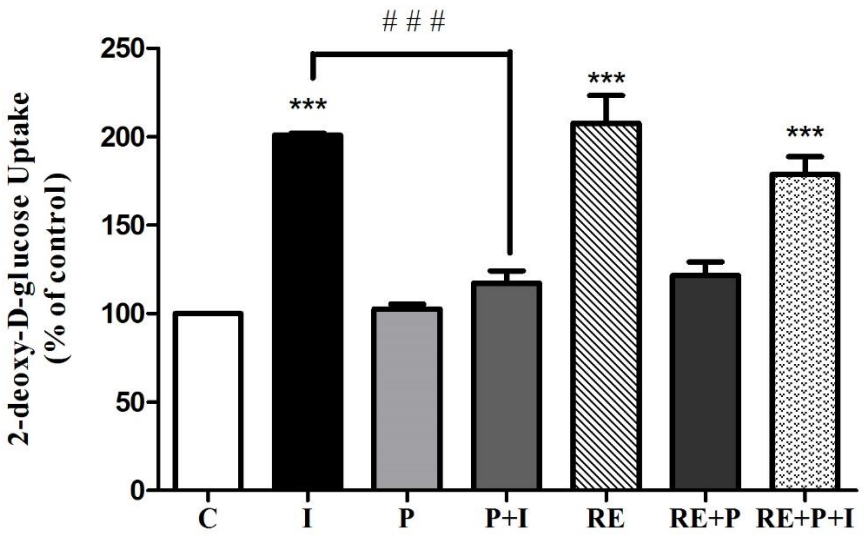

Figure 4: Rosemary extract restores insulin-stimulated glucose uptake in palmitate treated muscle cells. Fully differentiated myotubes were treated without (control, C) or with 5 μg/ml rosemary extract (RE) for 2 hours followed by treatment without or with 0.2 mM of palmitate (P) for 16 hours and stimulation without or with 100 nM insulin (I) for 30 min. [^{3}H]-2-deoxy-D-glucose uptake measurements were performed as indicated in the method section. The results are the mean of 4-7 independent experiments, each performed in triplicate and expressed as percent of control (*** P<0.001 vs. control, ### P<0.001 vs. insulin alone).

3.2 Rosemary extract prevents the palmitate-induced Ser307 and Ser636/639 phosphorylation of IRS-1.

After we established insulin resistance at the glucose uptake level, we investigated the effects of palmitate and RE downstream of the insulin receptor therefore the phosphorylation and expression of the IRS-1 was examined. Previous *in vitro* studies conducted in L6 muscle cells and rat muscle *in vivo* have indicated that increased phosphorylation levels of Ser307 and Ser636/639 of IRS-1 leads to impairment in the

insulin signaling leading to insulin resistance (64,94). We investigated the phosphorylation of the IRS-1 protein on Ser307 and Ser636/639 residues using specific antibodies. Exposure of L6 myotubes to 0.2 mM palmitate resulted in significant increase in Ser307 and Ser636/639 phosphorylation of IRS-1 (199.4±24.98%, 162±6.74% of control, $P<0.001$, $P<0.01$ respectively) (Figure 5). Treatment with 5 μg/ml RE did not have any effect on the basal Ser307 or Ser636/639 phosphorylation (118±11.24%, 105±3.51% of control respectively) but completely abolished the palmitate-induced increase in Ser307 and Ser636/639 phosphorylation of IRS-1 (108±16.91% of control and 107±7.32% of control). The total levels of IRS-1 were not impacted by the treatments (P: 103.3±8.63, RE: 98.82±13.21, RE+P: 108±9.33) (Figure 5). These data indicate that exposure to palmitate significantly increased serine phosphorylation of IRS-1 and treatment with RE completely abolished this effect.

A.

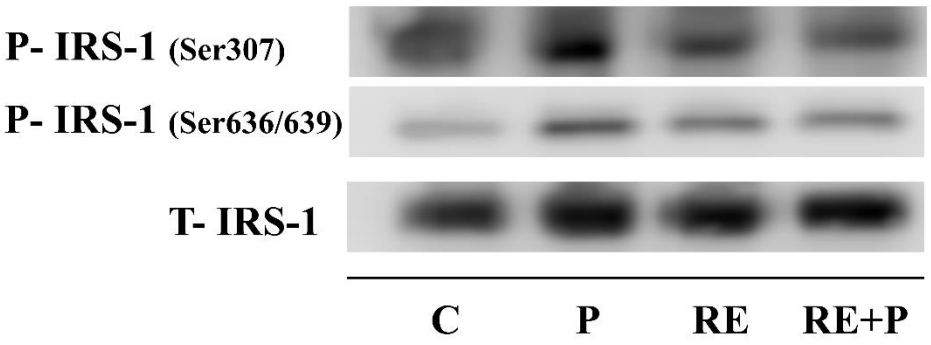
P- IRS-1 (Ser307)
P- IRS-1 (Ser636/639)
T- IRS-1
C
P
RE
RE+P

B.

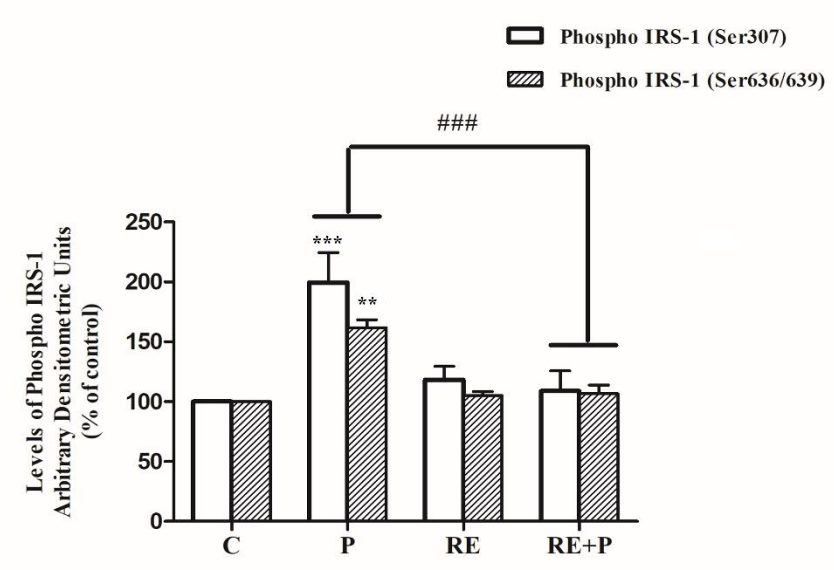
Phospho IRS-1 (Ser307)
Phospho IRS-1 (Ser636/639)
###
***
**
Levels of Phospho IRS-1
Arbitrary Densitometric Units
(% of control)
250
200
150
100
50
0
C
P
RE
RE+P

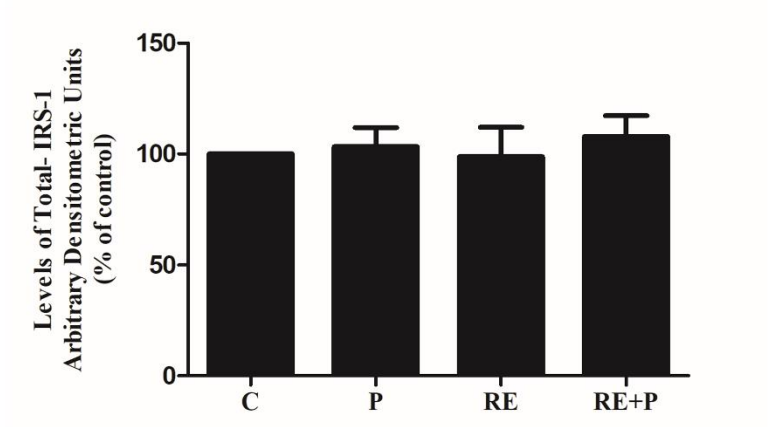
Levels of Total- IRS-1
Arbitrary Densitometric Units
(% of control)
150
100
50
0
C
P
RE
RE+P

Figure 5: Effects of palmitate and RE on IRS-l expression and Ser307, Ser636/639 phosphorylation. Fully differentiated myotubes were treated without (control, C) or with 5 μg/ml RE for 2 hours followed by treatment without or with 0.2 mM of palmitate (P) for 16 hours and stimulation without or with 100 nM insulin (I) for 15 min. After treatment, the cells were lysed and SDS-PAGE was performed, followed by immunoblotting with specific antibodies that recognize phosphorylated (Ser307, Ser636/639) or total IRS-1. A representative immunoblot is shown. The densitometry of the bands, expressed in arbitrary units, was calculated using image J. The values are the mean ± SE of three separate experiments (*** P<0.001, ** P<0.01 vs. control, ### P<0.001 vs. palmitate alone).

3.3 Rosemary extract restores the insulin-stimulated Akt phosphorylation in palmitate treated myotubes

Next we investigated the effect of palmitate on insulin stimulated Akt phosphorylation and expression in the absence or presence of RE. Treatment of L6 myotubes with insulin resulted in a significant increase in Akt Ser473 and Thr308 phosphorylation (I: 312±19.21 and 289±23.12% of control respectively, p<0.001) as established by our group and others (162,161,239,234). Treatment of the cells with palmitate significantly attenuated the insulin-stimulated Akt phosphorylation on Ser473 and Thr308 residues (P+I: 121.9±31.30 and 131±35.90% of control respectively, p<0.001) (Figure 6) which is in accordance with other studies (100). Palmitate and RE alone did not have any effect on the basal Ser473 or Thr308 Akt phosphorylation (P: 98.2±3.02, 95±6.20, RE: 103±4.10, 105±6.2%, RE+P: 109.1±9.06, 111±5.92% of control, respectively). However, in the presence of RE, the decline in the insulin-

stimulated Akt phosphorylation on Ser473 and Thr308 with palmitate was completely prevented (RE+P+I: 346.7±66 and 312±30.31% of control respectively, $P<0.001$ (Figure 6). The total levels of Akt were not significantly affected by any of the treatments (I: 108±8.4, P: 99 ± 5.9, P+I: 101±11.6, RE: 94±5.72, RE+P: 93.6±7.2, RE+P+I: 93±15.23% of control) (Figure 6).

A.

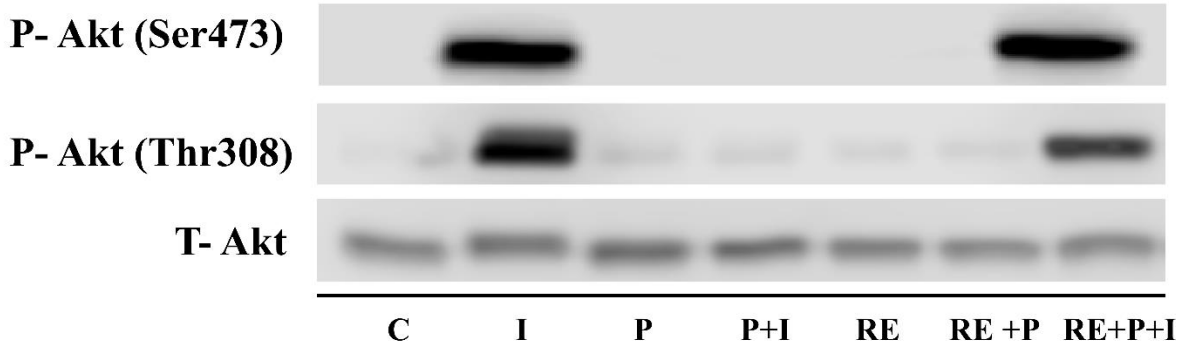
P- Akt (Ser473)
P- Akt (Thr308)
T- Akt
C
I
P
P+I
RE
RE +P
RE+P+I

B.

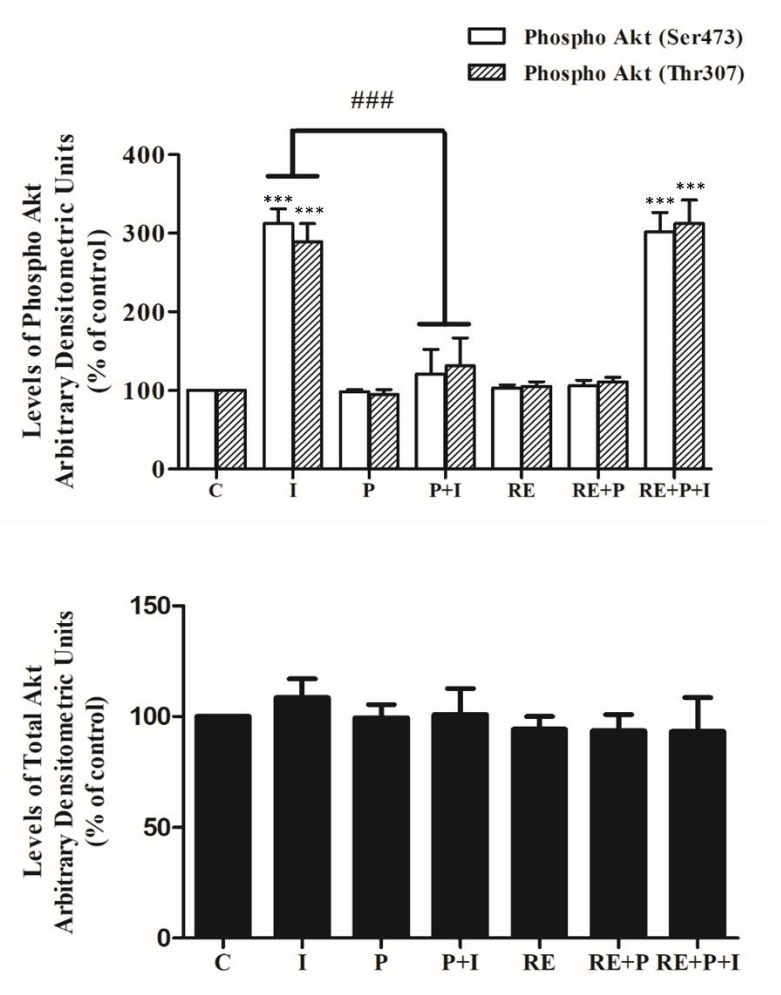
Phospho Akt (Ser473)
Phospho Akt (Thr307)
###
Levels of Phospho Akt
Arbitrary Densitometric Units
(% of control)
400
300
200
100
0
***
***
***
***
C
I
P
P+I
RE
RE+P
RE+P+I
Levels of Total Akt
Arbitrary Densitometric Units
(% of control)
150
100
50
0
C
I
P
P+I
RE
RE+P
RE+P+I

Figure 6: Effects of palmitate and RE on Akt expression and Ser473 and Thr308 phosphorylation. Fully differentiated myotubes were treated without (control, C) or with 5 μg/ml rosemary extract (RE) for 2 hours followed by treatment without or with 0.2 mM of palmitate (P) for 16 hours and stimulation without or with 100 nM insulin (I) for 15 min. After exposure to treatment, the cells were lysed and SDS-PAGE was performed, followed by immunoblotting with specific antibodies that recognize phosphorylated Ser473, Thr308 or total Akt. A representative immunoblot is shown. The densitometry of the bands, expressed in arbitrary units, was calculated using image J. The values are the mean ± SE of three separate experiments (*** $P<0.001$ vs. control, ### $P<0.001$ vs. insulin alone).

3.4 Rosemary extract prevents the palmitate-induced phosphorylation of JNK in L6 myotubes

Following the establishment that chronic exposure to palmitate increases the phosphorylation of Ser307 and Ser636/639 of IRS-1, we examined the signaling molecules that may be involved in the process. JNK is a serine/threonine kinase shown to increase serine phosphorylation of IRS-1 and involved in insulin resistance (83,87). We hypothesized that the levels of JNK phosphorylation and/or expression would be increased by palmitate. Indeed, exposure of the cells to palmitate (0.2 mM) significantly increased JNK phosphorylation (250±9.77% of control, $P<0.001$) and prior treatment with RE completely abolished the palmitate-induced phosphorylation of JNK (114±12.90% of control, $P<0.001$) (Figure 7). RE alone did not have any impact on the phosphorylation of JNK (98±7.44% of control). Moreover, the total levels of JNK were

not significantly changed by any treatment: P: 107 ±7.21, RE: 104±7.53 and RE+P: 105±8.76% of control (Figure 7).

A.

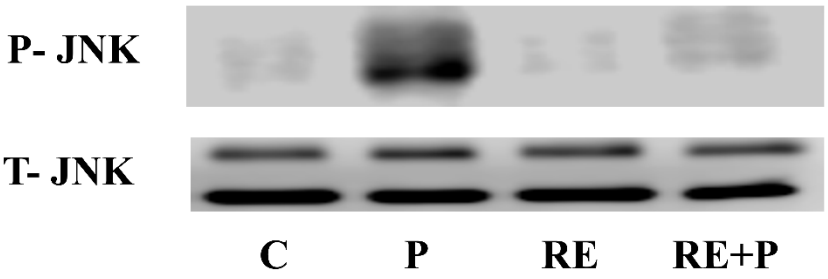
P- JNK
T- JNK
C
P
RE
RE+P

B.

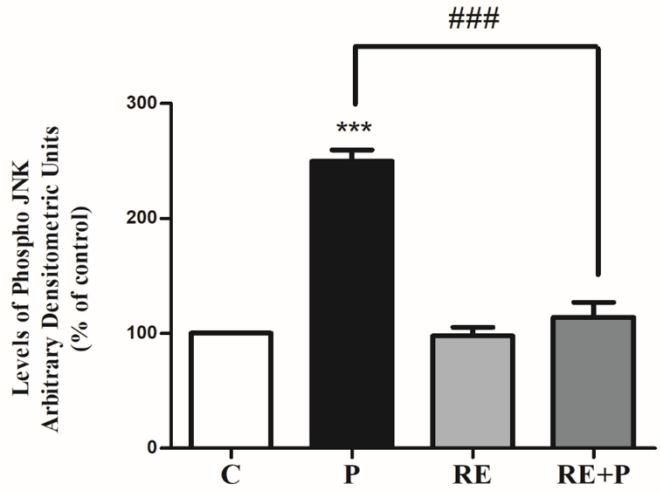
###
***
Levels of Phospho JNK
Arbitrary Densitometric Units
(% of control)
300
200
100
0
C
P
RE
RE+P

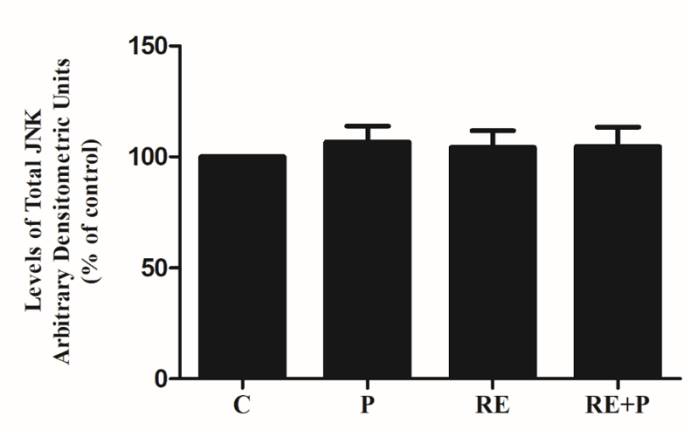
Levels of Total JNK
Arbitrary Densitometric Units
(% of control)
150
100
50
0
C
P
RE
RE+P

Figure 7: Effects of palmitate and RE on JNK expression and phosphorylation. Fully differentiated myotubes were treated without (control, C) or with 5 μg/ml RE followed by treatment without or with 0.2 mM of palmitate (P) for 16 hours. After exposure to treatment, the cells were lysed and SDS-PAGE was performed, followed by immunoblotting with specific antibodies that recognize phosphorylated Thr183/Tyr185 or total JNK. A representative immunoblot is shown. The densitometry of the bands, expressed in arbitrary units, was calculated using image J. The values are the mean ± SE of three separate experiments (*** P<0.001 vs. control, ### P<0.001 vs. palmitate alone).

3.5 Rosemary extract prevents the palmitate-induced phosphorylation of mTOR in L6 myotubes

Another kinase implicated in serine phosphorylation of IRS-1 is mTOR. Therefore, we examined the effects of palmitate on mTOR Exposure to palmitate 0.2 mM significantly increased mTOR phosphorylation (403±85.60% of control, P< 0.001) (Figure 8). RE completely abolished the palmitate-induced phosphorylation of mTOR (60±20.53% of control, P<0.001). RE alone did not have any impact on the phosphorylation of mTOR (104±13.71% of control). The total levels of mTOR were not significantly changed by the treatments: P: 104±3.01, RE: 93±2.44, and RE+P: 88±3.85% of control (Figure 8).

A.

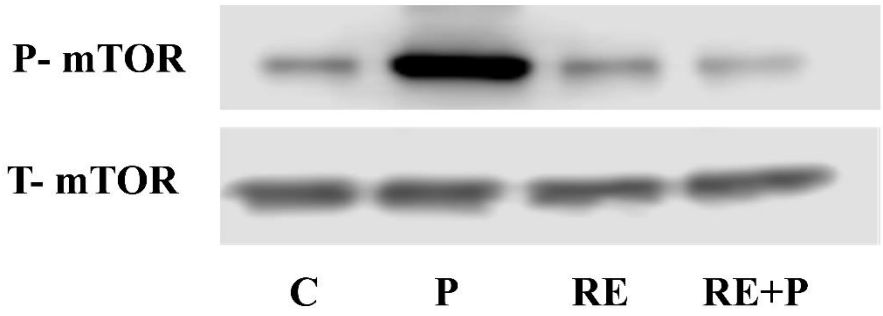
P- mTOR
T- mTOR
C
P
RE
RE+P

B.

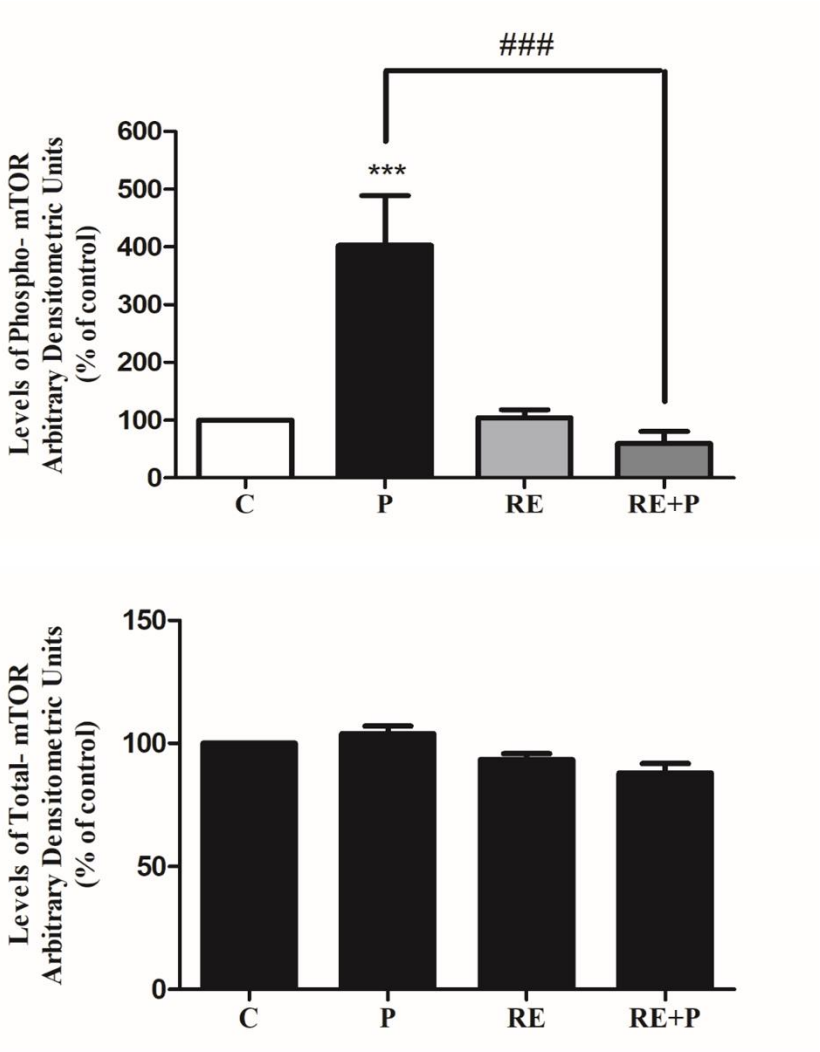
###
***
Levels of Phospho- mTOR Arbitrary Densitometric Units (% of control)
600
500
400
300
200
100
0
C
P
RE
RE+P
Levels of Total- mTOR Arbitrary Densitometric Units (% of control)
150
100
50
0
C
P
RE
RE+P

Figure 8: Effects of palmitate and RE on mTOR expression and phosphorylation. Fully differentiated myotubes were treated without (control, C) or with 5 μg/ml RE for 2 hours followed by treatment without or with 0.2 mM of palmitate (P) for 16 hours. After exposure to treatment, the cells were lysed and SDS-PAGE was performed, followed by immunoblotting with specific antibodies that recognize phosphorylated Ser2448 or total mTOR. A representative immunoblot is shown. The densitometry of the bands, expressed in arbitrary units, was calculated using image J. The values are the mean ± SE of three separate experiments (*** P<0.001 vs. control, ### P<0.001 vs. palmitate alone).

3.6 Rosemary extract prevents the palmitate-induced phosphorylation of p70 S6K in L6 myotubes

We further investigated the effect of palmitate on p70 6SK phosphorylation and expression a downstream effector of mTOR, implicated in serine phosphorylation of IRS-1 and insulin resistance. Myotubes exposed to 0.2 mM palmitate significantly increased p70 S6K phosphorylation levels (200±42.55% of control, P<0.001) (Figure 9). Treatment with RE prevented the palmitate-induced phosphorylation of p70 S6K (90±7.11% of control, p<0.001). RE alone did not have any effect on the phosphorylation of p70 6SK (82.12±6.04% of control). The total levels of p70 S6K were not affected by any of the treatments (P: 105±5.83, RE: 97 ± 2.21, and RE+P: 92.22 ± 4.23% of control (Figure 9).

A.

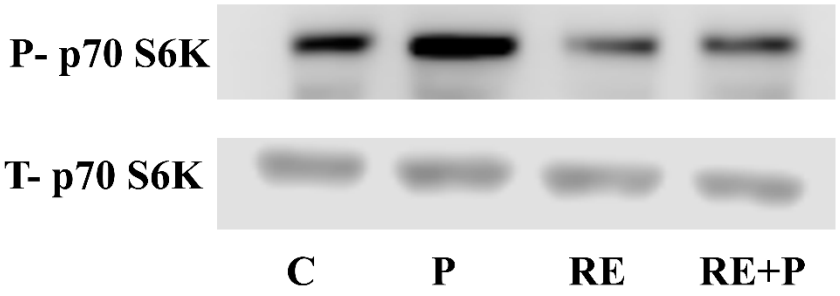
P- p70 S6K
T- p70 S6K
C
P
RE
RE+P

B.

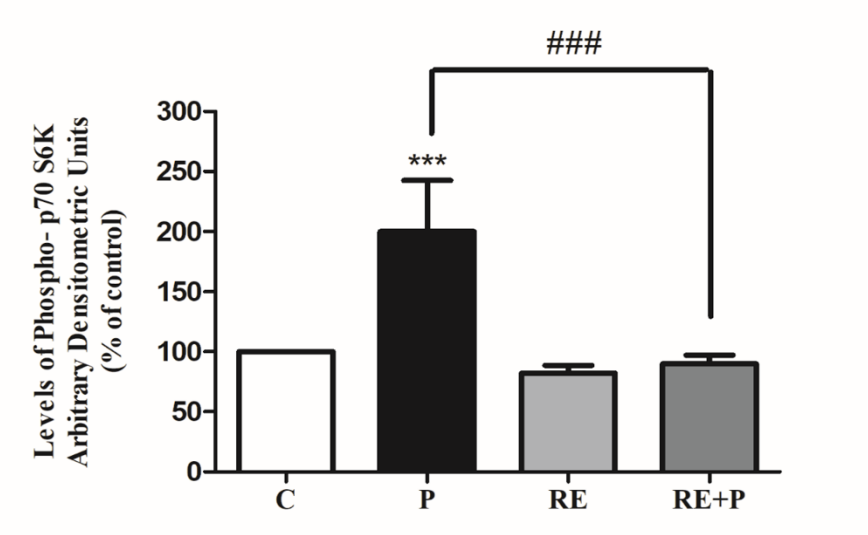
###
***
Levels of Phospho- p70 S6K Arbitrary Densitometric Units (% of control)
300
250
200
150
100
50
0
C
P
RE
RE+P

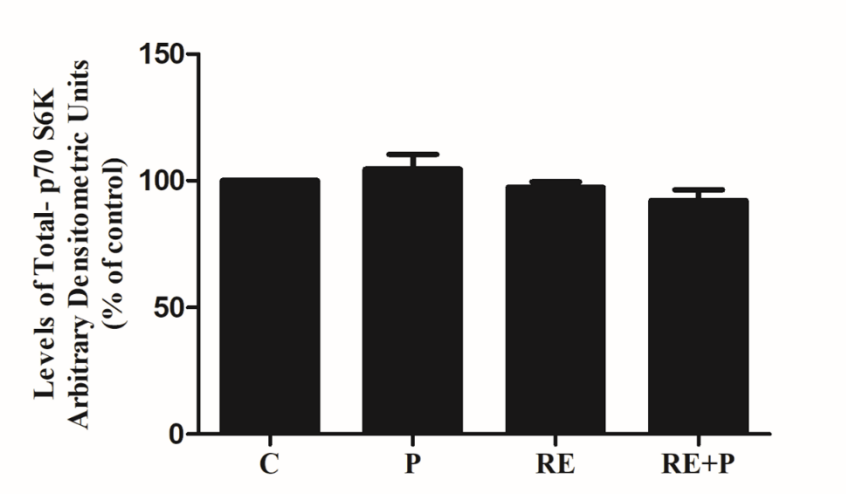
Levels of Total- p70 S6K Arbitrary Densitometric Units (% of control)
150
100
50
0
C
P
RE
RE+P

Figure 9: Effects of palmitate and RE on p70 S6K expression and phosphorylation. Fully differentiated myotubes were treated without (control, C) or with 5 μg/ml RE for 2 hours followed by treatment without or with 0.2 mM of palmitate (P) for 16 hours. After exposure to treatment, the cells were lysed and SDS-PAGE was performed, followed by immunoblotting with specific antibodies that recognize phosphorylated Thr389 or total p70 S6K. A representative immunoblot is shown. The densitometry of the bands, expressed in arbitrary units, was calculated using image J. The values are the mean ± SE of three separate experiments (*** P<0.001 vs. control, ### P<0.001 vs. palmitate alone).

3.7 Rosemary extract stimulates the phosphorylation of AMPK in the presence of palmitate

Previous studies by our group showed that rosemary extract and its polyphenols CA and RA increase glucose uptake and this effect may be mediated through AMPK (160–162). We investigated the chronic effect of RE on the phosphorylation of AMPK. Our results indicate that chronic treatment with RE with 5 μg/ml significantly increased phosphorylation of AMPK (295±26.94% of control, P<0.001) (Figure 10). Most importantly, RE increases phosphorylation of AMPK even in the presence of 0.2 mM of palmitate (270±22.54% of control, P<0.001). Treatment with palmitate alone did not have any have a significant effect on the phosphorylation of AMPK (150±14.32% of control). Furthermore, the total levels of AMPK were not affected by any of the treatments (P: 103±8.63, RE: 99±13.21, and RE+P: 108±9.33% of control) (Figure 10).

A.

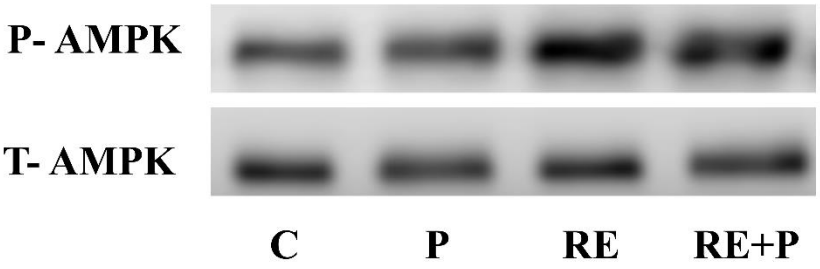
P- AMPK
T- AMPK
C
P
RE
RE+P

B.

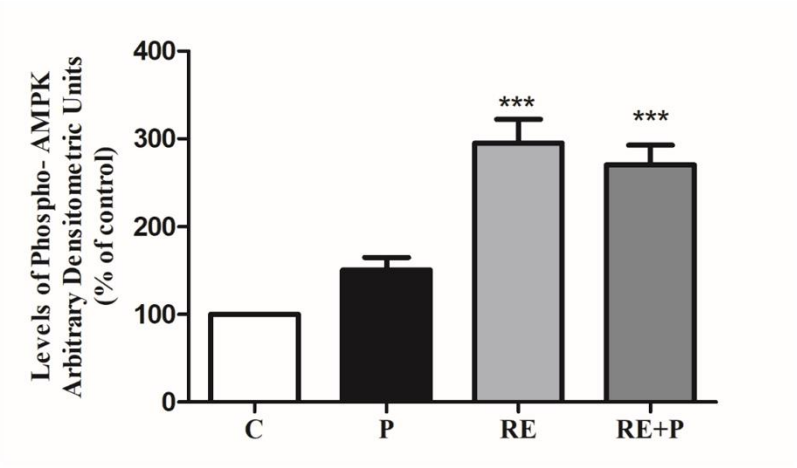
Levels of Phospho- AMPK
Arbitrary Densitometric Units
(% of control)
400
300
200
100
0
***
***
C
P
RE
RE+P

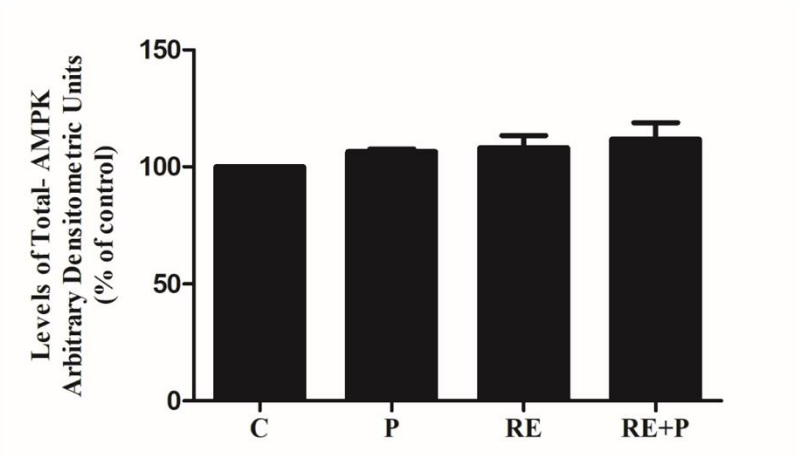
Levels of Total- AMPK
Arbitrary Densitometric Units
(% of control)
150
100
50
0
C
P
RE
RE+P

Figure 10: Effects of palmitate and RE on AMPK expression and phosphorylation. Fully differentiated myotubes were treated without (control, C) or with 5 μg/ml RE for 2 hours followed by treatment without or with 0.2 mM of palmitate (P) for 16 hours. After exposure to treatment, the cells were lysed and SDS-PAGE was performed, followed by immunoblotting with specific antibodies that recognize phosphorylated Thr172 or total AMPK. A representative immunoblot is shown. The densitometry of the bands, expressed in arbitrary units, was calculated using image J. The values are the mean ± SE of three separate experiments (*** P<0.001 vs. control).

3.8 Carnosic acid, a polyphenol in rosemary extract, restores the insulin-stimulated glucose uptake in palmitate treated muscle cells

The effects of carnosic acid on insulin-stimulated glucose uptake in palmitate treated L6 myotubes were examined. Stimulation with insulin (100 nM, 30 min) resulted in two-fold increase in [^{3}H]-2-deoxy-D-glucose uptake (203±2.3% of control, P<0.001) (Figure 11). Exposure to palmitate (0.2 mM) alone did not affect the basal glucose uptake (105±3.0 of control). The acute insulin response was significantly decreased in the palmitate-treated cells (118±4.9% of control) (Figure 11). Exposure to carnosic acid (CA) (2 μM) alone significantly increased glucose uptake (212±21.1% of control, P<0.001). Most importantly, the presence of CA significantly restored the insulin-stimulated glucose uptake (185±7.8% of control, P<0.001) in palmitate treated cells (Figure 11). These data indicate that the negative effects of palmitate were prevented in the presence of carnosic acid.

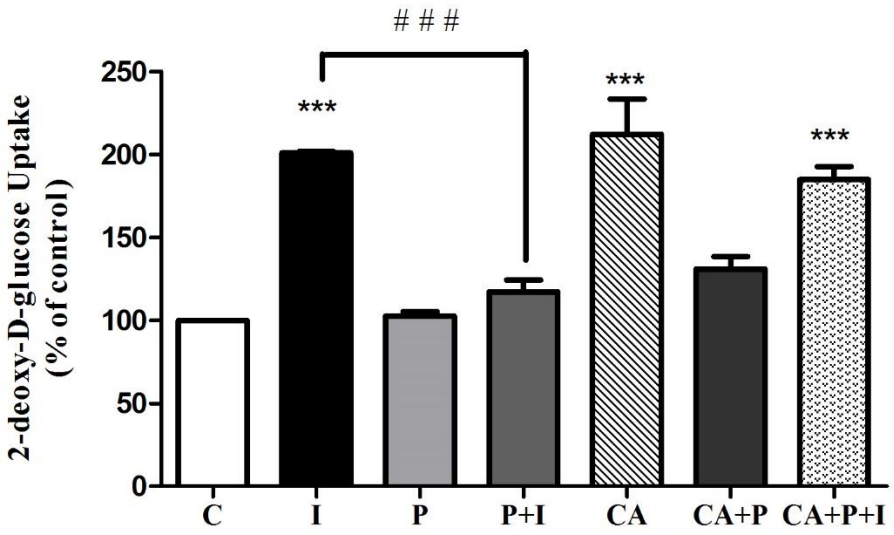

Figure 11: Carnosic acid, a polyphenol in rosemary extract, restores insulin-stimulated glucose uptake in palmitate treated muscle cells. Fully differentiated myotubes were treated without (control, C) or with 2 μM CA for 2 hours followed by treatment without or with 0.2 mM of palmitate (P) for 16 hours and stimulation without or with 100 nM insulin (I) for 30 min. [^{3}H]-2-deoxy-D-glucose uptake measurements were performed as indicated in the method section. The results are the mean of 4-7 independent experiments, each performed in triplicate and expressed as percent of control (***P<0.001 vs. control).

3.9 Rosmarinic acid, a polyphenol found in rosemary extract restores the insulin-stimulated glucose uptake in palmitate treated muscle cells

The effects of rosmarinic acid on insulin-stimulated glucose uptake in palmitate treated L6 myotubes were examined. Stimulation with insulin (100 nM, 30 min) resulted in two-fold increase in [^{3}H]-2-deoxy-D-glucose uptake (198±3.0% of control, P<0.001) (Figure 12). Exposure to palmitate (0.2 mM) alone did not affect the basal glucose uptake (103±2.0 of control). The acute insulin response was significantly decreased in the

palmitate-treated cells (116±5.0% of control). Exposure to rosmarinic acid (RA) (5 μM) alone significantly increased glucose uptake (177±6.8% of control, P<0.001). Most importantly, the presence of RA significantly restored the insulin-stimulated glucose uptake (181±14.5% of control, P<0.001) in palmitate treated cells (Figure 12). These data indicate that the negative effects of palmitate were abolished in the presence of rosmarinic acid.

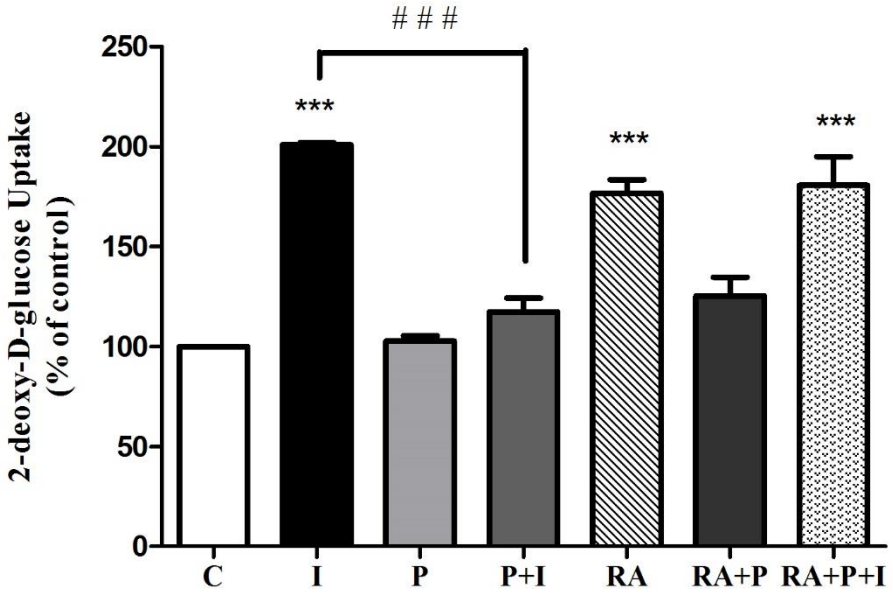

Figure 12: **Rosmarinic acid, a polyphenol in rosemary extract, restores insulin-stimulated glucose uptake in palmitate treated muscle cells.** Fully differentiated myotubes were treated without (control, C) or with 5 μM RA for 2 hours followed by treatment without or with 0.2 mM of palmitate (P) for 16 hours and stimulation without or with 100 nM insulin (I) for 30 min. [^{3}H]-2-deoxy-D-glucose uptake measurements were performed as indicated in the method section. The results are the mean of 4-7

independent experiments, each performed in triplicate and expressed as percent of control (***P<0.01).

3.10 Carnosol, a polyphenol found in rosemary extract restores the insulin-stimulated glucose uptake in palmitate treated muscle cells

The effects of carnosol (COH) on insulin-stimulated glucose uptake in palmitate treated L6 myotubes were examined. Stimulation with insulin (100 nM, 30 min) resulted in two-fold increase in the [^{3}H]-2-deoxy-D-glucose uptake (202±3.0% of control, P<0.001) (Figure 13). Exposure to palmitate (0.2 mM) alone did not affect the basal glucose uptake (103±2.0 of control). The acute insulin response was significantly decreased in the palmitate-treated cells (117±4.9% of control). Exposure to COH (25 μM) alone significantly increased glucose uptake (209±18.2% of control, P<0.001). Most importantly, the presence of COH significantly restored the insulin-stimulated glucose uptake (208±23.0% of control, P<0.001) in palmitate treated cells (Figure 13). These data indicate that the negative effects of palmitate were abolished in the presence of carnosol.

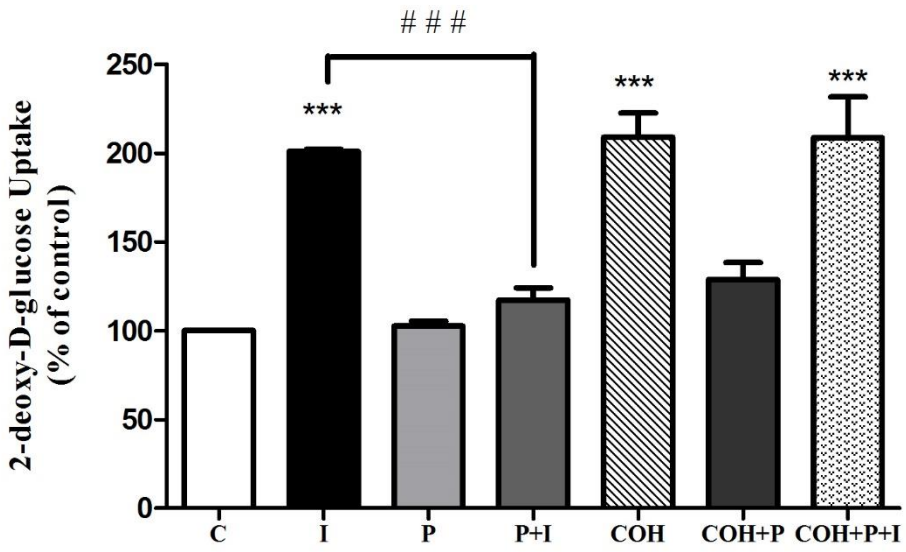

Figure 13: **Carnosol, a polyphenol in rosemary extract, restores insulin-stimulated glucose uptake in palmitate treated muscle cells.** Fully differentiated myotubes were treated without (control, C) or with 25 μM COH for 2 hours followed by treatment without or with 0.2 mM of palmitate (P) for 16 hours and stimulation without or with 100 nM insulin (I) for 30 min. [^{3}H]-2-deoxy-D-glucose uptake measurements were performed as indicated in the method section. The results are the mean of 4-7 independent experiments, each performed in triplicate and expressed as percent of control (***P<0.001).

CHAPTER 4: DISCUSSION

4.1 Rosemary extract ameliorates palmitate-induced insulin resistance

Obesity and elevated FFAs are highly correlated with insulin resistance and are major risk factors for the development of type 2 diabetes mellitus (51). Therefore, the development of therapeutic agents to combat FFA-induced insulin resistance would be beneficial. Previous studies have shown that the FFA palmitate induces insulin resistance in skeletal muscle cells (52,240,126,127). Exposure of L6 myotubes to 0.2 mM palmitate significantly decreased the insulin-stimulated glucose uptake. Similarly, studies have shown that exposure of L6 to 0.2 mM for 18 hours decreased the insulin-stimulated glucose uptake indicating insulin resistance (52,240). The palmitate concentration used in the present study was 0.2 mM and our data are in agreement with other studies where similar palmitate concentrations induced insulin resistance (52,126) (Figure 4, 11-13).

Most importantly, in the presence of rosemary extract (RE), carnosic acid (CA), rosmarinic acid (RA) and carnosol (COH) the palmitate-induced insulin resistance was

prevented and the insulin-stimulated glucose uptake was restored to levels comparable to the response seen with insulin alone (Figure 4, 11-13).

Considering the fact that 80% of postprandial glucose uptake is attributed to skeletal muscle, new, more affordable interventions that may improve glucose transport in this tissue is highly desirable. Recent studies have shown that rosemary extract (RE) and rosemary extract polyphenols, increase glucose uptake *in vitro* (160–162,188,199). The effect of RE and its polyphenols were previously examined in healthy muscle cells (160–162). However, their effect on palmitate-induced insulin resistant L6 muscle cells were never investigated. Our study is the first to show that RE and RE polyphenols prevented palmitate-induced insulin resistance in L6 muscle cells.

4.2 Investigating the Mechanism of Action of RE and its Polyphenols in Insulin Resistant Myotubes

In the present study we found that exposure of L6 cells to 0.2 mM palmitate for 16 hours increased Ser307 and Ser636/639 phosphorylation of IRS-1 (Figure 5). These data are in agreement with other studies (61,59,55,74,241). Exposure of L6 muscle cells to 0.75 mM palmitate for 16 hours resulted in significant increase of Ser307 and Ser636/639 phosphorylation on IRS-1 (126). Similarly, exposure of L6 to 0.5 mM palmitate for 16 hours significantly increased Ser307 of IRS-1 (241). Exposure of C2C12 myotubes to 0.75 mM palmitate for 16 hours also increased Ser307 phosphorylation of IRS-1 (242). Apart from these *in vitro* studies, *in vivo* animal studies have shown increased serine phosphorylation of IRS-1 by elevated fatty acids that correlate with insulin resistance. Administration of high-fat/high-carbohydrate diet *ad libitum* in mice resulted in increase of Ser307 phosphorylation of IRS-1 in muscle tissue (61). Additionally, administration of HFD for 16 weeks in mice resulted in increase in

Ser636/639 phosphorylation of IRS-1 in muscle and adipose tissue (74). Similarly, in mice fed with high fat diet for 10 weeks the phosphorylation of Ser307 and Ser636/639 was markedly increased in muscle and adipose tissue (59). These serine residues on IRS-1 have been associated with a reduced function of insulin stimulated IRS-1 and more specifically by a decreased association between IRS-1 and PI3K, downstream activation of the insulin signaling cascade and glucose uptake (55). The serine residues are located towards the end of the phosphotyrosine binding domain of IRS-1 and moderate the interaction of IRS-1 with the insulin receptor (55,69). The association of the insulin receptor and IRS-1 is significantly lowered once IRS-1 becomes phosphorylated on its serine residues. Exposure to RE completely restored the insulin-stimulated glucose uptake in palmitate-induced insulin resistant muscle cells. These findings are the first to show that exposure of the cells to RE and its polyphenols are associated with a prevention of the palmitate-induced insulin resistance and restoration of the insulin response in L6 muscle cells. These data are in agreement with other studies where metformin, the first line of treatment for T2DM, decreased the palmitate-induced Ser307 phosphorylation of IRS-1 in L6 muscle cells (154).

Furthermore, our data showed that exposure of the cells to 0.2 mM palmitate for 16 hours significantly attenuated the insulin-stimulated phosphorylation of Akt (Figure 6). Our data is in agreement with other studies (100,243–247). Exposure of 3T3-L1 adipocytes to 0.75 mM palmitate for 16 hours significantly attenuated the insulin-stimulated phosphorylation of Akt (243). Exposure of L6 myotubes to 0.75 mM palmitate resulted in abolishment of insulin-stimulated phosphorylation of Akt (100). Similarly, exposure of C2C12 cells to 0.5 mM palmitate for 16 hours resulted in a

significant decrease in insulin-stimulated phosphorylation of Akt (245). The above mentioned *in vitro* studies are also in agreement with *in vivo* studies. Namely, administration of high fat diet in C57BL/6 mice for 8 weeks significantly decreased the insulin-stimulated phosphorylation of Akt in liver tissue (246). Similarly, administration of high fat diet in mice significantly attenuated the insulin-induced phosphorylation of Akt in isolated soleus muscle (247). Exposure of the cells to RE restored the palmitate-induced attenuation of the insulin response (Figure 6). These findings are the first to show that treatment with RE is associated with a complete restoration of the insulin action in palmitate-induced insulin resistance L6 muscle cells. These data are in agreement with other studies where treatment with metformin abolished the palmitate-induced attenuation of Akt in L6 muscle cells (244).

Exposure of L6 muscle cells to 0.2 mM for 16 hours palmitate significantly increased the phosphorylation of JNK (Figure 7). Our data is in agreement with the previous studies (83,87,248,249,249,250). Treatment of L6 muscle cells with 0.75 mM palmitate significantly increased the phosphorylation of JNK (248). Similarly, in C2C12 muscle cells, treatment with 0.5 mM palmitate for 12, 24 and 36 hours significantly increased the phosphorylation of JNK (250). Additionally, in primary human myotubes, treatment with 0.4 mM palmitate for 12 hours significantly increased the phosphorylation of JNK. Exposure of 3T3-L1 adipocytes to 0.5 mM palmitate for 12 hours significantly increased the phosphorylation of JNK (249). In rats fed with high lipid containing western diet for 10-30 days the phosphorylation of JNK was significantly increased in hepatic, adipose and muscle tissue (83). Additionally, in C57BL/6J mice lipid infusion significantly increased the phosphorylation of JNK in muscle tissue (251). Furthermore,

in Swiss mice fed with fat-rich diet for 8 weeks, the phosphorylation of JNK was markedly increased (252). On the other hand, in mice that underwent targeted mutation of the JNK locus in order to abolish JNK expression, high fat diet-induced insulin resistance was completely prevented (87). All these findings are in agreement with our study and indicate that JNK phosphorylation by FFA is associated with insulin resistance. More importantly, exposure of the cells to RE significantly attenuated the palmitate-induced phosphorylation of JNK (Figure 7). These findings are the first to show that exposure of the cells to RE are associated with a decrease in the palmitate-induced phosphorylation of JNK in L6 muscle cells. Moreover, these data are also in agreement with other studies where quercetin, a polyphenol from the flavonoid group, significantly attenuated the palmitate-induced phosphorylation of JNK in L6 muscle cells and in muscles obtained from an ob/ob mice (248).

Furthermore, exposure of L6 cells to 0.2mM palmitate significantly increased the phosphorylation of mTOR and its downstream effector p70 6SK (Figure 8 and 9). Our data is in agreement with previous studies (253–256,249). Exposure of L6 myotubes to 0.4 mM palmitate for 4 hours increased the phosphorylation of mTOR and its downstream effector p70S6K (253). Similarly, exposure of C2C12 myotubes to 0.75 mM palmitate for 18 hours significantly increased the phosphorylation of mTOR and p70 S6K (254). Exposure of 3T3-L1 adipocytes to 0.5 mM palmitate for 12 hours significantly increased the phosphorylation of mTOR and its downstream effector p70 S6K (249). Chronic consumption of high fat diet in Sprague-Dawley rats for 8 weeks resulted in a significant increase in phosphorylation of mTOR in skeletal muscle (253). Similarly, in C57BL/6 mice administration of high fat diet for 8 weeks resulted in a significant

increase in mTOR and p70 S6K phosphorylation in skeletal muscle (255). The studies above are in agreement with our study indicating increased mTOR and p70 S6K phosphorylation by FFA that is associated with insulin resistance. More importantly, exposure of the cells to RE significantly attenuated the palmitate-induced phosphorylation of mTOR and p70 S6K (Figure 8 and 9). These findings are the first to show that RE is associated with a decrease in palmitate-induced phosphorylation of mTOR and p70 S6K in L6 muscle cells. Furthermore, these data are in agreement with other studies where treatment with metformin reversed the palmitate-induced increase in mTOR and p70 S6K in C2C12 muscle cells (256).

Furthermore, we investigated the total and phosphorylated levels of AMPK. Previously, we found that treatment of L6 myotubes with RE, CA and RA significantly increased the phosphorylation of AMPK (160–162). In the present study, we found that 0.2 mM palmitate for 16 hours did not significantly increase the levels of AMPK (Figure 10). These findings are in agreement with previous studies (256,257). Therefore, we proceeded to examine the effects of RE in the presence of palmitate in muscle cells. Exposure of the cells to RE significantly increased the phosphorylation of AMPK even in the presence of palmitate (Figure 10). These effects of RE are similar to the effects of metformin. Metformin significantly increased the phosphorylation of AMPK in the presence of palmitate in C2C12 and L6 muscle cells (244,256). Another study in L6 found that metformin ameliorates palmitate-induced insulin resistance through AMPK activation and suppression of sterol regulatory element-binding protein-1c (SREBP-1c), a transcription factor involved in fatty acids synthesis (244). AMPK is a known inhibitor of SREBP (258) therefore RE as an activator of AMPK may also supress the promoter

activity of SREBP and ameliorate FFA-induced insulin resistance. Furthermore, studies have indicated that activation of AMPK significantly lowers the activity of mTOR and its downstream effector p70 S6K (259,260). AMPK may directly affect mTOR by phosphorylation of the TSC2 and raptor leading to inhibition in its kinase activity (110,261). This process is attained by the increase in TSC activity via AMPK phosphorylation which in turn drives the intrinsic GTPase activity of Rheb towards the GDP-bound form (110,261). Considering that treatment with RE causes phosphorylation of AMPK, this may be the mechanism by which RE attenuates the palmitate-induced phosphorylation of mTOR and p70 S6K in muscle cells. The AMPK pathway has been viewed as an appealing target for the treatment/prevention of insulin resistance and T2DM. The role that AMPK plays in mediating the effects of RE and RE polyphenols may need further investigations such as using inhibitor of AMPK (Compound C) or siRNA techniques. If indeed AMPK plays a major role in the positive effects observed in RE and RE polyphenols treated palmitate-induced insulin resistant cells then inhibition of AMPK would diminish the effects of the polyphenols, returning the L6 myotubes to their initial insulin resistant state.

It should be noted that exposure to RE alone resulted in 2-fold increase in AMPK phosphorylation compared to control.

Given that AMPK activation can occur by an increase in the AMP: ATP ratio as well as activation of its upstream kinases LKB1 and CaMKK it is important to elucidate whether these upstream kinases are the mechanisms by which the bioactive compounds of RE activate AMPK. Currently, there are no studies that investigated the effects of RE and its polyphenols on the mechanism of AMPK activation. RE and RE polyphenols may

allosterically moderate the activity of AMPK, increase the activity of its upstream kinases including LKB1 and CaMKK (262,263) or lead to an increase in the AMP: ATP ratios as a result to inhibition of the mitochondrial complex 1. Studies have demonstrated that metformin significantly inhibits the mitochondrial complex 1 (153,157,264) thereby activating AMPK. A recent study has indicated that in the absence of fructose 1,6 biphosphate (FBP), a glycolytic intermediate, the interaction between aldolase and the vacuolar-ATPase on the lysosomal surface is altered which leads to creation of AXIN-based AMPK-activation complex that causes activation of AMPK (265). If the process of glycolysis is inhibited by RE, the production of FBP will be decreased which would lead to activation of AMPK. On the other hand, if RE indeed inhibits glycolysis and possibly acting as a calorie restrictor thereby increasing the AMP: ATP ratios the levels of phosphorylated AMPK will also be increased.

To our surprise, exposure of the cells to RE and palmitate did not have a significant effect on the glucose uptake indicating that in the presence of palmitate not only the acute insulin response was abolished but also the effect of RE is attenuated (Figure 4). It should be noted that RE in the presence of palmitate, resulted in a significant increase in AMPK phosphorylation and our data indicate that this increase was enough to abolish palmitate-induced phosphorylation of mTOR and p70 S6K leading to decrease in serine phosphorylation of IRS-1 but not sufficient to increase the glucose uptake in the cells (Figure 10, RE+P increased AMPK phosphorylation, Figure 4: RE+P no significant increase in glucose uptake). We have investigated previously the effects of RE, CA and RA on glucose transporters in GLUT4 and GLUT1 overexpressing cells and found no effect on glucose transporter translocation (160–162) and we had proposed that

RE, RA and CA may increase glucose uptake by affecting GLUT3 translocation or by affecting glucose transporter activity. The lack of a significant increase in glucose uptake by RE in the presence of palmitate (Figure 4: RE+P) indicates that palmitate may affect a signaling step downstream of AMPK such as TBC1D1 that prevents the increase in glucose transporter activity/glucose uptake.

A limited number of studies have also examined the antidiabetic effects of RE and its polyphenols *in vivo*. In high fat diet-induced diabetic mice, administration of RE significantly decreased the fasting plasma glucose levels (72%), decreased total cholesterol (68%), total fat fecal excretion (1-2 fold) and body weight thereby improving the lipid profile of the mice (230). Another study found that RE enriched with CA significantly ameliorated the high fat diet induced obesity and metabolic syndrome in mice (266). Administration of RE enriched with CA in obese rats resulted in significant attenuation of TNFα and interleukin 1β indicating anti-inflammatory effects of RE (267). Moreover, several other studies showed that dietary supplementation of RE enriched with CA resulted in body weight and epidydimal fat reduction (214), as well as suppression of hepatic steatosis (268). Additionally, in high fat diet-induced diabetic rats administration of RA dose-dependently ameliorated hyperglycemia and insulin resistance in addition to increasing GLUT4 translocation to the plasma membrane in muscle (227). Moreover, a recent study conducted in humans that were administered dried rosemary leaves powder have shown significant improvement in the blood lipid profile, antioxidant levels and decrease in fasting plasma glucose levels (221). These studies demonstrate that RE and its polyphenols exhibit antihyperglycemic and antidiabetic properties *in vivo* and are in agreement with our

findings. However, there are currently no studies that elucidate the mechanism involved in the effects of RE and its polyphenols. The present study is the first to show increased serine phosphorylation of IRS-1, and increased phosphorylation of mTOR, p70S6K and JNK by palmitate and an effect of RE treatment to inhibit them and restore insulin-stimulated Akt phosphorylation and insulin stimulated glucose uptake.

It is already established that high oxidative stress is associated with the development of diabetes (269). Numerous physiological and biochemical processes in the human body produce reactive oxygen species (ROS) such as superoxide, and hydrogen peroxide as byproducts. Overproduction of such free radicals causes oxidative damage to biomolecules (membrane lipids, nucleic acids, and proteins) resulting in cellular damage and leading to many chronic diseases including diabetes (269) while the intake of natural antioxidants has been associated with reduced disease risk radical scavenging molecules, such as phenolic compounds, nitrogen compounds, vitamins, terpenoids, and some other endogenous metabolites, that have been found to be rich in antioxidant activity (183,269). Palmitate is a widely known inducer of ROS generation in different tissues including muscle (270). Exposure to 0.75 mM palmitate for 24 hours palmitate significantly increased the production of ROS in L6 muscle cells (271). Treatment with 0.4 palmitate for 6 hours significantly increased the production of ROS in rat's hepatocytes. In primary human hepatocytes exposure to 0.4 mM palmitate for 12 hours also increased the production of ROS (272). The findings above are also in agreement with *in vivo* where administration of high fat diet in Wistar rats for 8 weeks significantly increased the ROS production (273). Many studies have shown that RE and RE polyphenols attenuate the production of ROS and decrease oxidative stress by exhibiting strong antioxidant

activities *in vitro* and *in vivo* in liver, adipose and skeletal muscle (228,192,205). Considering that oxidative stress and the production of ROS is highly linked to insulin resistance and T2DM (274), RE may indirectly affect glucose uptake by attenuating the oxidative stress and signaling pathways that may negatively impact the glucose uptake and induce pathological states such as insulin resistance and T2DM. Additionally, oxidative stress and production of ROS can significantly increase the phosphorylation of JNK(275–278). Given that RE and its polyphenols exhibit strong antioxidant properties (228,192,205) that can delay or prevent the oxidation of different substrates, it may prevent the phosphorylation of JNK that is induced by exposure of the cells to palmitate, a known generator of ROS. Therefore, the antioxidant effects of RE may be the mechanism by which RE attenuates the palmitate-induced phosphorylation of JNK.

Based on the current evidence from *in vivo* studies the RE dosage used *in vivo* ranges from 50-200 mg/kg b.w however, how this translates to human is not addressed, especially the issue of bioavailability, metabolites and absorption. On that note, only limited number of studies investigated the bioavailability of CA and RA *in vivo*. This information is relevant to our study since RE and its polyphenols show significant bioavailability *in vivo* that can also be detected in different tissues. Oral administration of RE enriched with CA 80-120 mg (29-49 mg CA) in rats resulted in presence of bioactive concentrations of CA and carnosol in plasma (2-30 μM) and tissues such as the liver (1-15 μg/g) and small and large intestines (up to several hundred μg/g) (279). Intragastric administration of 90 mg/kg of CA in rats resulted in slow absorption with maximum time of absorption (Tmax) of 125.6 min and bioavailability of 65% with maximum plasma concentration (Cmax) of 42 mg/L (220)**.** Moreover, CA had shorter half-life with

intravenous administration (68 min) in comparison to intragastric administration (961 min) (220)**.** Another study found that intragastric administration of 65 mg/kg CA in rats had bioavailability of 40%, Tmax of 137 min and Cmax of 35 mg/L (280). Additionally, CA was mostly found in a free form in plasma and undergoes fecal excretion rather than urinary in animals (280). As per the European Food Safety Authority (EFSA) regulations, the predicted maximal exposure to CA (used as a food additive) is a roughly 0.2 mg/kg b.w/day (281)**.** Considering the average body weight, 65 % bioavailability and total plasma volume the plasma Cmax of CA is calculated to be approximately 3 nM (282)**.** Thus, the doses reported by Vaquero et al. in rats which is the equivalent to human doses of 50-100 mg of RE or 20-40 mg of CA/kg b.w/day may only be achieved through additional consumption of supplements that are enriched with these compounds (220). These values are within the range of the limits specified by the EFSA considering that no adverse effects were observed in rats that were fed for 90 days (281)**.**

Oral administration of 50 mg/kg b.w of RA in rats reaches maximum plasma concentration of 4.63 μM after 30 min and may be found free, conjugated or in methylated form of RA (283)**.** The RA metabolites include ferulic, caffeic and m-coumaric acid and it is typically excreted through the urinary tract (283). Another study showed that the Cmax of RA in plasma reached 1.36 μM (0.5 mg/L) after 10 min in rats that were administered 0.1 mmol/kg (36 mg/kg/b.w) (284)**.** Another study conducted in healthy men being administered a single intake of perilla extract that contained 200 mg of RA showed Cmax of 0.87-1.43 μM 30 min post-intake (283). However, the relative potency of the RA metabolites have not been investigated and remain to be determined. Overall the above mentioned studies indicate that administration of RE or RE

polyphenols *in vivo* results in detectable polyphenol levels in plasma (1-105 μM (285,286) range in some studies) and tissues and strongly suggest that our *in vitro* findings have in *vivo* relevance.

The exact mechanism by which CA and RA or other RE polyphenols enter the cells is not yet established or directly examined. Nevertheless, assumptions can be made considering the chemical properties of these polyphenols. CA is a lipid-soluble molecule (169) and it is possible that CA can penetrate through the cell membrane through simple diffusion and therefore accumulate in the cytosol. On the other hand, RA is a water-soluble molecule thus it may require a protein channel or a protein carrier in order to enter the cell (287). Studies have indicated that RA is not affected by the enzymes secreted in the digestive system including lipase and amylase nor it is hydrolyzed in the intestines. However, it can be degraded into metabolites by the gut microflora before absorption such as hydroxylated phenylphropionic and m-coumeric acid (238,284)**.** The metabolic derivatives of RA were shown to be absorbed and transported through the tissues by the monocarboxylic acid transporter (MCT) (238,284). Moreover, in human intestinal Caco-2 cells RA via paracellular diffusion (284)**.** Additionally, previous data indicates that RE and its polyphenols have low toxicity and noteworthy bioavailability therefore it would be feasible to study the antihyperglycemic effects of these compounds *in vivo*.

4.3 Summary/Conclusion

The prevalence of T2DM is constantly increasing and according to the International Diabetes association it is expected to affect 420 million people worldwide by the year 2040. Additionally, insulin resistance and T2DM are highly correlated with

the development of other pathological states including metabolic syndrome, cardiovascular diseases and cancer (185). As a result, new treatment strategies to aid in the prevention and management of T2DM may be beneficial for our society. As previously indicated, increased levels of FFA and obesity are reported to mediate insulin resistance in muscle cells (45,118). More recently, RE and its polyphenols have been reported to exhibit antidiabetic properties in insulin target tissues *in vitro* and *in vivo*. The present study has shown that palmitate can induce insulin resistance in L6 rat skeletal muscle cells. Exposure of the cells to palmitate significantly decreased the insulin-stimulated glucose uptake, Akt phosphorylation and increased the phosphorylation of Serine307 and Ser636/639 residues on IRS-1. Additionally, palmitate considerably increased the phosphorylation of JNK, mTOR and its downstream effector p70 6SK. Most importantly RE and RE polyphenols restored insulin-stimulated glucose uptake, insulin-stimulated Akt phosphorylation, increased AMPK phosphorylation and abolished the palmitate-induced JNK, mTOR and p70 S6K phosphorylation

4.4 Future Directions and Limitations

Further studies need to be conducted in order to more accurately investigate the mechanism of action of RE. With that being said, utilizing siRNA against major signaling molecules that are correlated with insulin resistance and were investigated above such as AMPK, JNK, mTOR and p70 S6K. It is expected that siRNA against the kinases that are associated with insulin resistance would be the same as RE and its polyphenols, to ameliorate the negative effects of palmitate in L6 myotubes Additionally, elucidating the mechanism by which AMPK is activated by RE and its polyphenols by ATP assays, mitochondrial function and biogenesis should further clarify the mechanism by which RE

and its polyphenols affect AMPK. The present study exploited a well-established model of palmitate-induced insulin resistance in L6 myotubes *in vitro* (51,100). The methodology of this study was focused on investigating the levels of phosphorylation and expression of different proteins involved in the insulin signaling including IRS-1, Akt, mTOR, p70 S6K, and JNK as well as AMPK. These investigations were conducted using immunoblotting. Additionally, the levels of tyrosine phosphorylation/expression of IRS-1 should be examined. We hypothesize that in the presence of palmitate, the levels of tyrosine phosphorylation of IRS-1 is significantly decreased. As mentioned in the introduction, PKC and GSK3 have been implicated as strong mediators involved in the development of insulin resistance in skeletal muscle cells. The effect of RE and its polyphenols on PKC and GSK3 could also be examined. Additionally, the IKK/NFkB and immune response pathway has been markedly implicated in FFA-induced insulin resistance (288,289). RE and its polyphenols may have the ability to attenuate IKK/NFkB activity therefore future research could examine the effects of these polyphenols on the IKK/NFkB signaling pathway. Furthermore, *in vivo* studies need to be conducted in the future. For this purpose rat/mouse animal model of obesity such as HFD-induced insulin resistance model may be used in order to further examine the physiological effects and the mechanism of action of RE and its polyphenols. In addition, primary tissue culture of hepatic, adipose and muscle tissue could be extracted from these *in vivo* models in order to add further understanding to this particular research.

REFERENCE:

1. Kahn CR. Insulin Action, Diabetogenes, and the Cause of Type II Diabetes. Diabetes. 1994 Aug 1;43(8):1066–85.

2. Bliss M. The Discovery of Insulin: The Twenty-fifth Anniversary Edition. University of Toronto Press; 2000. 336 p.

3. Tripathy D, Chavez AO. Defects in Insulin Secretion and Action in the Pathogenesis of Type 2 Diabetes Mellitus. Curr Diab Rep. 2010;(3):184.

4. White B, Porterfield S. Endocrine and Reproductive Physiology: Mosby Physiology Monograph Series. Elsevier Health Sciences; 2012. 352 p.

5. Saltiel AR. New perspectives into the molecular pathogenesis and treatment of type 2 diabetes. Cell. 2001 Feb 23;104(4):517–29.

6. Manning BD, Cantley LC. AKT/PKB signaling: navigating downstream. Cell. 2007 Jun 29;129(7):1261–74.

7. Whiteman EL, Cho H, Birnbaum MJ. Role of Akt/protein kinase B in metabolism. Trends Endocrinol Metab. 2002 Dec 1;13(10):444–51.

8. Barthel A, Schmoll D, Unterman TG. FoxO proteins in insulin action and metabolism. Trends Endocrinol Metab. 2005 May 1;16(4):183–9.

9. Kramer HF, Witczak CA, Fujii N, Jessen N, Taylor EB, Arnolds DE, et al. Distinct signals regulate AS160 phosphorylation in response to insulin, AICAR, and contraction in mouse skeletal muscle. Diabetes. 2006 Jul;55(7):2067–76.

10. Sakamoto K, Holman GD. Emerging role for AS160/TBC1D4 and TBC1D1 in the regulation of GLUT4 traffic. Am J Physiol Endocrinol Metab. 2008 Jul;295(1):E29-37.

11. Brady MJ, Nairn AC, Saltiel AR. The regulation of glycogen synthase by protein phosphatase 1 in 3T3-L1 adipocytes. Evidence for a potential role for DARPP-32 in insulin action. J Biol Chem. 1997 Nov 21;272(47):29698–703.

12. Van Obberghen E, Baron V, Delahaye L, Emanuelli B, Filippa N, Giorgetti-Peraldi S, et al. Surfing the insulin signaling web. Eur J Clin Invest. 2001 Nov;31(11):966–77.

13. Lee J, Pilch PF. The insulin receptor: structure, function, and signaling. Am J Physiol. 1994 Feb;266(2 Pt 1):C319-334.

14. Ellis L, Clauser E, Morgan DO, Edery M, Roth RA, Rutter WJ. Replacement of insulin receptor tyrosine residues 1162 and 1163 compromises insulin-stimulated kinase activity and uptake of 2-deoxyglucose. Cell. 1986 Jun 6;45(5):721–32.

15. Myers MG, Sun XJ, White MF. The IRS-1 signaling system. Trends Biochem Sci. 1994 Jul 1;19(7):289–93.

16. Hribal ML, Federici M, Porzio O, Lauro D, Borboni P, Accili D, et al. The Gly→Arg972 Amino Acid Polymorphism in Insulin Receptor Substrate-1 Affects Glucose Metabolism in Skeletal Muscle Cells. J Clin Endocrinol Metab. 2000 May 1;85(5):2004–13.

17. Kido Y, Burks DJ, Withers D, Bruning JC, Kahn CR, White MF, et al. Tissue-specific insulin resistance in mice with mutations in the insulin receptor, IRS-1, and IRS-2. J Clin Invest. 2000 Jan;105(2):199–205.

18. Withers DJ, Gutierrez JS, Towery H, Burks DJ, Ren JM, Previs S, et al. Disruption of IRS-2 causes type 2 diabetes in mice. Nature. 1998 Feb 26;391(6670):900–4.

19. Vollenweider P, Ménard B, Nicod P. Insulin resistance, defective insulin receptor substrate 2-associated phosphatidylinositol-3' kinase activation, and impaired atypical protein kinase C (zeta/lambda) activation in myotubes from obese patients with impaired glucose tolerance. Diabetes. 2002 Apr;51(4):1052–9.

20. Karlsson HKR, Zierath JR. Insulin signaling and glucose transport in insulin resistant human skeletal muscle. Cell Biochem Biophys. 2007;48(2–3):103–13.

21. Goodyear LJ, Giorgino F, Sherman LA, Carey J, Smith RJ, Dohm GL. Insulin receptor phosphorylation, insulin receptor substrate-1 phosphorylation, and phosphatidylinositol 3-kinase activity are decreased in intact skeletal muscle strips from obese subjects. J Clin Invest. 1995 May;95(5):2195–204.

22. Björnholm M, Kawano Y, Lehtihet M, Zierath JR. Insulin receptor substrate-1 phosphorylation and phosphatidylinositol 3-kinase activity in skeletal muscle from NIDDM subjects after in vivo insulin stimulation. Diabetes. 1997 Mar;46(3):524–7.

23. Pratipanawatr W, Pratipanawatr T, Cusi K, Berria R, Adams JM, Jenkinson CP, et al. Skeletal muscle insulin resistance in normoglycemic subjects with a strong family history of type 2 diabetes is associated with decreased insulin-stimulated insulin receptor substrate-1 tyrosine phosphorylation. Diabetes. 2001 Nov;50(11):2572–8.

24. Cheatham B, Vlahos CJ, Cheatham L, Wang L, Blenis J, Kahn CR. Phosphatidylinositol 3-kinase activation is required for insulin stimulation of pp70 S6 kinase, DNA synthesis, and glucose transporter translocation. Mol Cell Biol. 1994 Jul;14(7):4902–11.

25. Okada T, Kawano Y, Sakakibara T, Hazeki O, Ui M. Essential role of phosphatidylinositol 3-kinase in insulin-induced glucose transport and antilipolysis in rat adipocytes. Studies with a selective inhibitor wortmannin. J Biol Chem. 1994 Feb 4;269(5):3568–73.

26. Kahn SE. The importance of the beta-cell in the pathogenesis of type 2 diabetes mellitus. Am J Med. 2000 Apr 17;108 Suppl 6a:2S–8S.

27. Katagiri H, Asano T, Ishihara H, Inukai K, Shibasaki Y, Kikuchi M, et al. Overexpression of catalytic subunit p110alpha of phosphatidylinositol 3-kinase increases glucose transport activity with translocation of glucose transporters in 3T3-L1 adipocytes. J Biol Chem. 1996 Jul 19;271(29):16987–90.

28. Brachmann SM, Ueki K, Engelman JA, Kahn RC, Cantley LC. Phosphoinositide 3-kinase catalytic subunit deletion and regulatory subunit deletion have opposite effects on insulin sensitivity in mice. Mol Cell Biol. 2005 Mar;25(5):1596–607.

29. Luo J, Sobkiw CL, Hirshman MF, Logsdon MN, Li TQ, Goodyear LJ, et al. Loss of class IA PI3K signaling in muscle leads to impaired muscle growth, insulin response, and hyperlipidemia. Cell Metab. 2006 May;3(5):355–66.

30. Bouzakri K, Roques M, Gual P, Espinosa S, Guebre-Egziabher F, Riou J-P, et al. Reduced activation of phosphatidylinositol-3 kinase and increased serine 636 phosphorylation of insulin receptor substrate-1 in primary culture of skeletal muscle cells from patients with type 2 diabetes. Diabetes. 2003 Jun;52(6):1319–25.

31. Kohn AD, Summers SA, Birnbaum MJ, Roth RA. Expression of a constitutively active Akt Ser/Thr kinase in 3T3-L1 adipocytes stimulates glucose uptake and glucose transporter 4 translocation. J Biol Chem. 1996 Dec 6;271(49):31372–8.

32. Katome T, Obata T, Matsushima R, Masuyama N, Cantley LC, Gotoh Y, et al. Use of RNA interference-mediated gene silencing and adenoviral overexpression to elucidate the roles of AKT/protein kinase B isoforms in insulin actions. J Biol Chem. 2003 Jul 25;278(30):28312–23.

33. Bae SS, Cho H, Mu J, Birnbaum MJ. Isoform-specific regulation of insulin-dependent glucose uptake by Akt/protein kinase B. J Biol Chem. 2003 Dec 5;278(49):49530–6.

34. Wang Q, Somwar R, Bilan PJ, Liu Z, Jin J, Woodgett JR, et al. Protein kinase B/Akt participates in GLUT4 translocation by insulin in L6 myoblasts. Mol Cell Biol. 1999 Jun;19(6):4008–18.

35. Lencioni C, Lupi R, Del Prato S. Beta-cell failure in type 2 diabetes mellitus. Curr Diab Rep. 2008 Jun;8(3):179–84.

36. Cho H, Mu J, Kim JK, Thorvaldsen JL, Chu Q, Crenshaw EB, et al. Insulin resistance and a diabetes mellitus-like syndrome in mice lacking the protein kinase Akt2 (PKB beta). Science. 2001 Jun 1;292(5522):1728–31.

37. Garofalo RS, Orena SJ, Rafidi K, Torchia AJ, Stock JL, Hildebrandt AL, et al. Severe diabetes, age-dependent loss of adipose tissue, and mild growth deficiency in mice lacking Akt2/PKB beta. J Clin Invest. 2003 Jul;112(2):197–208.

38. Rondinone CM, Carvalho E, Wesslau C, Smith UP. Impaired glucose transport and protein kinase B activation by insulin, but not okadaic acid, in adipocytes from subjects with Type II diabetes mellitus. Diabetologia. 1999 Jul;42(7):819–25.

39. Kane S, Sano H, Liu SCH, Asara JM, Lane WS, Garner CC, et al. A method to identify serine kinase substrates. Akt phosphorylates a novel adipocyte protein with a Rab GTPase-activating protein (GAP) domain. J Biol Chem. 2002 Jun 21;277(25):22115–8.

40. Sano H, Kane S, Sano E, Mîinea CP, Asara JM, Lane WS, et al. Insulin-stimulated phosphorylation of a Rab GTPase-activating protein regulates GLUT4 translocation. J Biol Chem. 2003 Apr 25;278(17):14599–602.

41. Thong FSL, Bilan PJ, Klip A. The Rab GTPase-activating protein AS160 integrates Akt, protein kinase C, and AMP-activated protein kinase signals regulating GLUT4 traffic. Diabetes. 2007 Feb;56(2):414–23.

42. Bruss MD, Arias EB, Lienhard GE, Cartee GD. Increased phosphorylation of Akt substrate of 160 kDa (AS160) in rat skeletal muscle in response to insulin or contractile activity. Diabetes. 2005 Jan;54(1):41–50.

43. Iwase H, Kobayashi M, Nakajima M, Takatori T. The ratio of insulin to C-peptide can be used to make a forensic diagnosis of exogenous insulin overdosage. Forensic Sci Int. 2001 Jan 1;115(1):123–7.

44. Shulman GI, Rothman DL, Jue T, Stein P, DeFronzo RA, Shulman RG. Quantitation of muscle glycogen synthesis in normal subjects and subjects with non-insulin-dependent diabetes by 13C nuclear magnetic resonance spectroscopy. N Engl J Med. 1990 Jan 25;322(4):223–8.

45. Bogardus C, Lillioja S, Stone K, Mott D. Correlation between muscle glycogen synthase activity and in vivo insulin action in man. J Clin Invest. 1984 Apr;73(4):1185–90.

46. Kahn BB, Flier JS. Obesity and insulin resistance. J Clin Invest. 2000 Aug 15;106(4):473–81.

47. Leahy JL. Pathogenesis of Type 2 Diabetes Mellitus. Arch Med Res. 2005 May 1;36(3):197–209.

48. Pendergrass M, Bertoldo A, Bonadonna R, Nucci G, Mandarino L, Cobelli C, et al. Muscle glucose transport and phosphorylation in type 2 diabetic, obese nondiabetic, and genetically predisposed individuals. Am J Physiol Endocrinol Metab. 2007 Jan;292(1):E92-100.

49. DeFronzo RA. Dysfunctional fat cells, lipotoxicity and type 2 diabetes. Int J Clin Pract Suppl. 2004 Oct;(143):9–21.

50. Petersen KF, Shulman GI. Etiology of insulin resistance. Am J Med. 2006 May;119(5 Suppl 1):S10-16.

51. Hulver MW, Dohm GL. The molecular mechanism linking muscle fat accumulation to insulin resistance. Proc Nutr Soc. 2004 May;63(2):375–80.

52. Sinha S, Perdomo G, Brown NF, O'Doherty RM. Fatty acid-induced insulin resistance in L6 myotubes is prevented by inhibition of activation and nuclear localization of nuclear factor kappa B. J Biol Chem. 2004 Oct 1;279(40):41294–301.

53. Kanety H, Feinstein R, Papa MZ, Hemi R, Karasik A. Tumor necrosis factor alpha-induced phosphorylation of insulin receptor substrate-1 (IRS-1). Possible mechanism for suppression of insulin-stimulated tyrosine phosphorylation of IRS-1. J Biol Chem. 1995 Oct 6;270(40):23780–4.

54. Ueno M, Carvalheira JBC, Tambascia RC, Bezerra RMN, Amaral ME, Carneiro EM, et al. Regulation of insulin signalling by hyperinsulinaemia: role of IRS-1/2 serine phosphorylation and the mTOR/p70 S6K pathway. Diabetologia. 2005 Mar;48(3):506–18.

55. Gual P, Le Marchand-Brustel Y, Tanti J-F. Positive and negative regulation of insulin signaling through IRS-1 phosphorylation. Biochimie. 2005 Jan;87(1):99–109.

56. Mordier S, Iynedjian PB. Activation of mammalian target of rapamycin complex 1 and insulin resistance induced by palmitate in hepatocytes. Biochem Biophys Res Commun. 2007 Oct 12;362(1):206–11.

57. Carlson CJ, White MF, Rondinone CM. Mammalian target of rapamycin regulates IRS-1 serine 307 phosphorylation. Biochem Biophys Res Commun. 2004 Apr 2;316(2):533–9.

58. Manning BD. Balancing Akt with S6K: implications for both metabolic diseases and tumorigenesis. J Cell Biol. 2004 Nov 8;167(3):399–403.

59. Um SH, Frigerio F, Watanabe M, Picard F, Joaquin M, Sticker M, et al. Absence of S6K1 protects against age- and diet-induced obesity while enhancing insulin sensitivity. Nature. 2004 Sep 9;431(7005):200–5.

60. Lee J, Kim M-S. The role of GSK3 in glucose homeostasis and the development of insulin resistance. Diabetes Res Clin Pract. 2007 Sep;77 Suppl 1:S49-57.

61. Hirosumi J, Tuncman G, Chang L, Görgün CZ, Uysal KT, Maeda K, et al. A central role for JNK in obesity and insulin resistance. Nature. 2002 Nov 21;420(6913):333–6.

62. Li Y, Soos TJ, Li X, Wu J, Degennaro M, Sun X, et al. Protein kinase C Theta inhibits insulin signaling by phosphorylating IRS1 at Ser(1101). J Biol Chem. 2004 Oct 29;279(44):45304–7.

63. Sriwijitkamol A, Christ-Roberts C, Berria R, Eagan P, Pratipanawatr T, DeFronzo RA, et al. Reduced skeletal muscle inhibitor of kappaB beta content is associated with insulin resistance in subjects with type 2 diabetes: reversal by exercise training. Diabetes. 2006 Mar;55(3):760–7.

64. Le Marchand-Brustel Y, Gual P, Grémeaux T, Gonzalez T, Barrès R, Tanti J-F. Fatty acid-induced insulin resistance: role of insulin receptor substrate 1 serine phosphorylation in the retroregulation of insulin signalling. Biochem Soc Trans. 2003 Dec;31(Pt 6):1152–6.

65. Tanti JF, Grémeaux T, van Obberghen E, Le Marchand-Brustel Y. Serine/threonine phosphorylation of insulin receptor substrate 1 modulates insulin receptor signaling. J Biol Chem. 1994 Feb 25;269(8):6051–7.

66. Draznin B. Molecular mechanisms of insulin resistance: serine phosphorylation of insulin receptor substrate-1 and increased expression of p85alpha: the two sides of a coin. Diabetes. 2006 Aug;55(8):2392–7.

67. Ruiz-Alcaraz AJ, Liu H-K, Cuthbertson DJ, McManus EJ, Akhtar S, Lipina C, et al. A novel regulation of IRS1 (insulin receptor substrate-1) expression following short term insulin administration. Biochem J. 2005 Dec 1;392(Pt 2):345–52.

68. Reynoso R, Salgado LM, Calderón V. High levels of palmitic acid lead to insulin resistance due to changes in the level of phosphorylation of the insulin receptor and insulin receptor substrate-1. Mol Cell Biochem. 2003 Apr;246(1–2):155–62.

69. Aguirre V, Uchida T, Yenush L, Davis R, White MF. The c-Jun NH(2)-terminal kinase promotes insulin resistance during association with insulin receptor substrate-1 and phosphorylation of Ser(307). J Biol Chem. 2000 Mar 24;275(12):9047–54.

70. Aguirre V, Werner ED, Giraud J, Lee YH, Shoelson SE, White MF. Phosphorylation of Ser307 in Insulin Receptor Substrate-1 Blocks Interactions with the Insulin Receptor and Inhibits Insulin Action. J Biol Chem. 2002 Jan 11;277(2):1531–7.

71. Capurso C, Capurso A. From excess adiposity to insulin resistance: The role of free fatty acids. Vascul Pharmacol. 2012 Sep 1;57(2):91–7.

72. Kim JK, Fillmore JJ, Sunshine MJ, Albrecht B, Higashimori T, Kim D-W, et al. PKC-θ knockout mice are protected from fat-induced insulin resistance. J Clin Invest. 2004 Sep 15;114(6):823–7.

73. Bard-Chapeau EA, Hevener AL, Long S, Zhang EE, Olefsky JM, Feng G-S. Deletion of Gab1 in the liver leads to enhanced glucose tolerance and improved hepatic insulin action. Nat Med. 2005 May;11(5):567–71.

74. Le Bacquer O, Petroulakis E, Paglialunga S, Poulin F, Richard D, Cianflone K, et al. Elevated sensitivity to diet-induced obesity and insulin resistance in mice lacking 4E-BP1 and 4E-BP2. J Clin Invest. 2007 Feb;117(2):387–96.

75. Tremblay F, Brûlé S, Hee Um S, Li Y, Masuda K, Roden M, et al. Identification of IRS-1 Ser-1101 as a target of S6K1 in nutrient- and obesity-induced insulin resistance. Proc Natl Acad Sci U S A. 2007 Aug 28;104(35):14056–61.

76. Taniguchi CM, Emanuelli B, Kahn CR. Critical nodes in signalling pathways: insights into insulin action. Nat Rev Mol Cell Biol. 2006 Feb;7(2):85–96.

77. Ciaraldi TP, Nikoulina SE, Bandukwala RA, Carter L, Henry RR. Role of glycogen synthase kinase-3 alpha in insulin action in cultured human skeletal muscle cells. Endocrinology. 2007 Sep;148(9):4393–9.

78. Woodgett JR, Cohen P. Multisite phosphorylation of glycogen synthase. Molecular basis for the substrate specificity of glycogen synthase kinase-3 and casein kinase-II (glycogen synthase kinase-5). Biochim Biophys Acta. 1984 Aug 14;788(3):339–47.

79. Nikoulina SE, Ciaraldi TP, Mudaliar S, Mohideen P, Carter L, Henry RR. Potential role of glycogen synthase kinase-3 in skeletal muscle insulin resistance of type 2 diabetes. Diabetes. 2000 Feb;49(2):263–71.

80. Summers SA, Kao AW, Kohn AD, Backus GS, Roth RA, Pessin JE, et al. The role of glycogen synthase kinase 3beta in insulin-stimulated glucose metabolism. J Biol Chem. 1999 Jun 18;274(25):17934–40.

81. Liberman Z, Eldar-Finkelman H. Serine 332 phosphorylation of insulin receptor substrate-1 by glycogen synthase kinase-3 attenuates insulin signaling. J Biol Chem. 2005 Feb 11;280(6):4422–8.

82. Stuart CA, Howell MEA, Cartwright BM, McCurry MP, Lee ML, Ramsey MW, et al. Insulin resistance and muscle insulin receptor substrate-1 serine hyperphosphorylation. Physiol Rep [Internet]. 2014 Dec 3;2(12). Available from: http://www.ncbi.nlm.nih.gov/pmc/articles/PMC4332214/

83. Prada P, Zecchin H, Gasparetti A, Torsoni M, Ueno M, Hirata A, et al. Western diet modulates insulin signaling, c-jun N-terminal kinase activity, and insulin receptor substrate-1(ser307) phosphorylation in a tissue-specific fashion. ENDOCRINOLOGY. 2005 Mar;146(3):1576–87.

84. Tuncman G, Hirosumi J, Solinas G, Chang L, Karin M, Hotamisligil GS. Functional in vivo interactions between JNK1 and JNK2 isoforms in obesity and insulin resistance. Proc Natl Acad Sci U S A. 2006 Jul 11;103(28):10741–6.

85. Ichijo H. From receptors to stress-activated MAP kinases. Oncogene. 1999 Nov 1;18(45):6087–93.

86. Jaeschke A, Czech MP, Davis RJ. An essential role of the JIP1 scaffold protein for JNK activation in adipose tissue. Genes Dev. 2004 Aug 15;18(16):1976–80.

87. Solinas G, Naugler W, Galimi F, Myung-Shik Lee, Karin M. Saturated fatty acids inhibit induction of insulin gene transcription by JNK-mediated phosphorylation of insulin-receptor substrates. Proc Natl Acad Sci U S A. 2006 Jan 1;103(44):16454–9.

88. Díaz-Delfín J, Morales M, Caelles C. Hypoglycemic action of thiazolidinediones/peroxisome proliferator-activated receptor gamma by inhibition of the c-Jun NH2-terminal kinase pathway. Diabetes. 2007 Jul;56(7):1865–71.

89. Zhang Z, Li X, Lv W, Yang Y, Gao H, Yang J, et al. Ginsenoside Re reduces insulin resistance through inhibition of c-Jun NH2-terminal kinase and nuclear factor-kappaB. Mol Endocrinol Baltim Md. 2008 Jan;22(1):186–95.

90. Newton AC. Protein kinase C: structure, function, and regulation. J Biol Chem. 1995 Dec 1;270(48):28495–8.

91. Rosse C, Linch M, Kermorgant S, Cameron AJM, Boeckeler K, Parker PJ. PKC and the control of localized signal dynamics. Nat Rev Mol Cell Biol. 2010 Feb;11(2):103–12.

92. Dey D, Basu D, Roy SS, Bandyopadhyay A, Bhattacharya S. Involvement of novel PKC isoforms in FFA induced defects in insulin signaling. Mol Cell Endocrinol. 2006 Feb 26;246(1–2):60–4.

93. Griffin ME, Marcucci MJ, Cline GW, Bell K, Barucci N, Lee D, et al. Free fatty acid-induced insulin resistance is associated with activation of protein kinase C theta and alterations in the insulin signaling cascade. Diabetes. 1999 Jun 1;48(6):1270–4.

94. Yu C, Chen Y, Cline GW, Zhang D, Zong H, Wang Y, et al. Mechanism by which fatty acids inhibit insulin activation of insulin receptor substrate-1 (IRS-1)-associated phosphatidylinositol 3-kinase activity in muscle. J Biol Chem. 2002 Dec 27;277(52):50230–6.

95. Serra C, Federici M, Buongiorno A, Senni MI, Morelli S, Segratella E, et al. Transgenic mice with dominant negative PKC-theta in skeletal muscle: a new model of insulin resistance and obesity. J Cell Physiol. 2003 Jul;196(1):89–97.

96. Szendroedi J, Yoshimura T, Phielix E, Koliaki C, Marcucci M, Zhang D, et al. Role of diacylglycerol activation of PKCθ in lipid-induced muscle insulin resistance in humans. Proc Natl Acad Sci U S A. 2014 Jul 1;111(26):9597–602.

97. Itani SI, Ruderman NB, Schmieder F, Boden G. Lipid-induced insulin resistance in human muscle is associated with changes in diacylglycerol, protein kinase C, and IkappaB-alpha. Diabetes. 2002 Jul;51(7):2005–11.

98. Shulman GI. Cellular mechanisms of insulin resistance in humans. Am J Cardiol. 1999 Jul 8;84(1A):3J–10J.

99. Boden G. Interaction between free fatty acids and glucose metabolism. Curr Opin Clin Nutr Metab Care. 2002 Sep;5(5):545–9.

100. Powell DJ, Turban S, Gray A, Hajduch E, Hundal HS. Intracellular ceramide synthesis and protein kinase Czeta activation play an essential role in palmitate-induced insulin resistance in rat L6 skeletal muscle cells. Biochem J. 2004 Sep 1;382(Pt 2):619–29.

101. Li M, Vienberg SG, Bezy O, O'Neill BT, Kahn CR. Role of PKCδ in Insulin Sensitivity and Skeletal Muscle Metabolism. Diabetes. 2015 Dec;64(12):4023–32.

102. Menzaghi C, Plengvidhya N, Ma X, Warram JH, Shoelson SE, Doria A. Genetic variability in insulin action inhibitor Ikkbeta (IKBKB) does not play a major role in the development of type 2 diabetes. J Clin Endocrinol Metab. 2002 Apr;87(4):1894–7.

103. Yin M-J, Yamamoto Y, Gaynor RB. The anti-inflammatory agents aspirin and salicylate inhibit the activity of IκB kinase-β. Nature. 1998 Nov 5;396(6706):77–80.

104. Yuan M, Konstantopoulos N, Lee J, Hansen L, Li ZW, Karin M, et al. Reversal of obesity- and diet-induced insulin resistance with salicylates or targeted disruption of Ikkbeta. Science. 2001 Aug 31;293(5535):1673–7.

105. Yang X, Yang C, Farberman A, Rideout TC, de Lange CFM, France J, et al. The mammalian target of rapamycin-signaling pathway in regulating metabolism and growth. J Anim Sci. 2008 Apr;86(14 Suppl):E36-50.

106. Loewith R, Hall MN. Target of Rapamycin (TOR) in Nutrient Signaling and Growth Control. Genetics. 2011 Dec;189(4):1177–201.

107. Navé BT, Ouwens M, Withers DJ, Alessi DR, Shepherd PR. Mammalian target of rapamycin is a direct target for protein kinase B: identification of a convergence point for opposing effects of insulin and amino-acid deficiency on protein translation. Biochem J. 1999 Dec 1;344 Pt 2:427–31.

108. Kimball SR. The role of nutrition in stimulating muscle protein accretion at the molecular level. Biochem Soc Trans. 2007 Nov;35(Pt 5):1298–301.

109. Vander Haar E, Lee S-I, Bandhakavi S, Griffin TJ, Kim D-H. Insulin signalling to mTOR mediated by the Akt/PKB substrate PRAS40. Nat Cell Biol. 2007 Mar;9(3):316–23.

110. Cheng SWY, Fryer LGD, Carling D, Shepherd PR. Thr2446 is a novel mammalian target of rapamycin (mTOR) phosphorylation site regulated by nutrient status. J Biol Chem. 2004 Apr 16;279(16):15719–22.

111. Pullen N, Thomas G. The modular phosphorylation and activation of p70s6k. FEBS Lett. 1997 Jun 23;410(1):78–82.

112. Weng QP, Kozlowski M, Belham C, Zhang A, Comb MJ, Avruch J. Regulation of the p70 S6 kinase by phosphorylation in vivo. Analysis using site-specific anti-phosphopeptide antibodies. J Biol Chem. 1998 Jun 26;273(26):16621–9.

113. Tremblay F, Gagnon A, Veilleux A, Sorisky A, Marette A. Activation of the mammalian target of rapamycin pathway acutely inhibits insulin signaling to Akt and glucose transport in 3T3-L1 and human adipocytes. Endocrinology. 2005 Mar;146(3):1328–37.

114. Berg CE, Lavan BE, Rondinone CM. Rapamycin partially prevents insulin resistance induced by chronic insulin treatment. Biochem Biophys Res Commun. 2002 May 10;293(3):1021–7.

115. Takano A, Usui I, Haruta T, Kawahara J, Uno T, Iwata M, et al. Mammalian target of rapamycin pathway regulates insulin signaling via subcellular redistribution of insulin receptor substrate 1 and integrates nutritional signals and metabolic signals of insulin. Mol Cell Biol. 2001 Aug;21(15):5050–62.

116. Harrington LS, Findlay GM, Gray A, Tolkacheva T, Wigfield S, Rebholz H, et al. The TSC1-2 tumor suppressor controls insulin-PI3K signaling via regulation of IRS proteins. J Cell Biol. 2004 Jul 19;166(2):213–23.

117. Krssak M, Falk Petersen K, Dresner A, DiPietro L, Vogel SM, Rothman DL, et al. Intramyocellular lipid concentrations are correlated with insulin sensitivity in humans: a 1H NMR spectroscopy study. Diabetologia. 1999 Jan;42(1):113–6.

118. Perseghin G, Scifo P, De Cobelli F, Pagliato E, Battezzati A, Arcelloni C, et al. Intramyocellular triglyceride content is a determinant of in vivo insulin resistance in humans: a 1H-13C nuclear magnetic resonance spectroscopy assessment in offspring of type 2 diabetic parents. Diabetes. 1999 Aug;48(8):1600–6.

119. Randle PJ. Regulatory interactions between lipids and carbohydrates: the glucose fatty acid cycle after 35 years. Diabetes Metab Rev. 1998 Dec;14(4):263–83.

120. Bird SR, Hawley JA. Update on the effects of physical activity on insulin sensitivity in humans. BMJ Open Sport — Exerc Med [Internet]. 2017 Mar 1;2(1). Available from: http://www.ncbi.nlm.nih.gov/pmc/articles/PMC5569266/

121. Holland WL, Brozinick JT, Wang L-P, Hawkins ED, Sargent KM, Liu Y, et al. Inhibition of ceramide synthesis ameliorates glucocorticoid-, saturated-fat-, and obesity-induced insulin resistance. Cell Metab. 2007 Mar;5(3):167–79.

122. Chavez JA, Siddique MM, Wang ST, Ching J, Shayman JA, Summers SA. Ceramides and glucosylceramides are independent antagonists of insulin signaling. J Biol Chem. 2014 Jan 10;289(2):723–34.

123. Shimabukuro M, Higa M, Zhou YT, Wang MY, Newgard CB, Unger RH. Lipoapoptosis in beta-cells of obese prediabetic fa/fa rats. Role of serine palmitoyltransferase overexpression. J Biol Chem. 1998 Dec 4;273(49):32487–90.

124. Stratford S, Hoehn KL, Liu F, Summers SA. Regulation of insulin action by ceramide: dual mechanisms linking ceramide accumulation to the inhibition of Akt/protein kinase B. J Biol Chem. 2004 Aug 27;279(35):36608–15.

125. Chaurasia B, Summers SA. Ceramides – Lipotoxic Inducers of Metabolic Disorders. Trends Endocrinol Metab. 2015 Oct 1;26(10):538–50.

126. Dimopoulos N, Watson M, Sakamoto K, Hundal HS. Differential effects of palmitate and palmitoleate on insulin action and glucose utilization in rat L6 skeletal muscle cells. Biochem J. 2006 Nov 1;399(3):473–81.

127. Lang CH. Elevated plasma free fatty acids decrease basal protein synthesis, but not the anabolic effect of leucine, in skeletal muscle. Am J Physiol Endocrinol Metab. 2006 Sep;291(3):E666-674.

128. Savage DB, Petersen KF, Shulman GI. Disordered Lipid Metabolism and the Pathogenesis of Insulin Resistance. Physiol Rev. 2007 Apr;87(2):507–20.

129. Kitessa SM, Abeywardena MY. Lipid-Induced Insulin Resistance in Skeletal Muscle: The Chase for the Culprit Goes from Total Intramuscular Fat to Lipid Intermediates, and Finally to Species of Lipid Intermediates. Nutrients [Internet]. 2016 Jul 29;8(8). Available from: http://www.ncbi.nlm.nih.gov/pmc/articles/PMC4997379/

130. Xiao B, Heath R, Saiu P, Leiper FC, Leone P, Jing C, et al. Structural basis for AMP binding to mammalian AMP-activated protein kinase. Nature. 2007 Sep 27;449(7161):496–500.

131. Carling D. The AMP-activated protein kinase cascade--a unifying system for energy control. Trends Biochem Sci. 2004 Jan;29(1):18–24.

132. Kahn BB, Alquier T, Carling D, Hardie DG. AMP-activated protein kinase: ancient energy gauge provides clues to modern understanding of metabolism. Cell Metab. 2005 Jan;1(1):15–25.

133. Woods A, Cheung PC, Smith FC, Davison MD, Scott J, Beri RK, et al. Characterization of AMP-activated protein kinase beta and gamma subunits. Assembly of the heterotrimeric complex in vitro. J Biol Chem. 1996 Apr 26;271(17):10282–90.

134. Nilsson EC, Long YC, Martinsson S, Glund S, Garcia-Roves P, Svensson LT, et al. Opposite transcriptional regulation in skeletal muscle of AMP-activated protein kinase gamma3 R225Q transgenic versus knock-out mice. J Biol Chem. 2006 Mar 17;281(11):7244–52.

135. Barnes BR, Marklund S, Steiler TL, Walter M, Göran Hjälm, Amarger V, et al. The 5′-AMP-activated Protein Kinase γ3 Isoform Has a Key Role in Carbohydrate and Lipid Metabolism in Glycolytic Skeletal Muscle. J Biol Chem. 2004 Sep 10;279(37):38441–7.

136. Coughlan KA, Valentine RJ, Ruderman NB, Saha AK. AMPK activation: a therapeutic target for type 2 diabetes? Diabetes Metab Syndr Obes Targets Ther. 2014 Jun 24;7:241–53.

137. Wang W, Yang X, López de Silanes I, Carling D, Gorospe M. Increased AMP:ATP ratio and AMP-activated protein kinase activity during cellular senescence linked to reduced HuR function. J Biol Chem. 2003 Jul 18;278(29):27016–23.

138. Mitchelhill KI, Michell BJ, House CM, Stapleton D, Dyck J, Gamble J, et al. Posttranslational modifications of the 5'-AMP-activated protein kinase beta1 subunit. J Biol Chem. 1997 Sep 26;272(39):24475–9.

139. Pang T, Zhang Z-S, Gu M, Qiu B-Y, Yu L-F, Cao P-R, et al. Small molecule antagonizes autoinhibition and activates AMP-activated protein kinase in cells. J Biol Chem. 2008 Jun 6;283(23):16051–60.

140. Xie M, Zhang D, Dyck JRB, Li Y, Zhang H, Morishima M, et al. A pivotal role for endogenous TGF-beta-activated kinase-1 in the LKB1/AMP-activated protein kinase energy-sensor pathway. Proc Natl Acad Sci U S A. 2006 Nov 14;103(46):17378–83.

141. Hou X, Xu S, Maitland-Toolan KA, Sato K, Jiang B, Ido Y, et al. SIRT1 regulates hepatocyte lipid metabolism through activating AMP-activated protein kinase. J Biol Chem. 2008 Jul 18;283(29):20015–26.

142. Saeedi R, Parsons HL, Wambolt RB, Paulson K, Sharma V, Dyck JRB, et al. Metabolic actions of metformin in the heart can occur by AMPK-independent mechanisms. Am J Physiol Heart Circ Physiol. 2008 Jun;294(6):H2497-2506.

143. Towler MC, Hardie DG. AMP-activated protein kinase in metabolic control and insulin signaling. Circ Res. 2007 Feb 16;100(3):328–41.

144. Hardie DG. AMP-activated protein kinase: an energy sensor that regulates all aspects of cell function. Genes Dev. 2011 Sep 15;25(18):1895–908.

145. Hardie DG, Ross FA, Hawley SA. AMPK: a nutrient and energy sensor that maintains energy homeostasis. Nat Rev Mol Cell Biol. 2012 Mar 22;13(4):251–62.

146. Gasparrini M, Giampieri F, M. Alvarez Suarez J, Mazzoni L, Y. Forbes Hernandez T, L. Quiles J, et al. AMPK as a New Attractive Therapeutic Target for Disease Prevention: The Role of Dietary Compounds AMPK and Disease Prevention. Curr Drug Targets. 2016 Jun 1;17(8):865–89.

147. Kang SWS, Haydar G, Taniane C, Farrell G, Arias IM, Lippincott-Schwartz J, et al. AMPK Activation Prevents and Reverses Drug-Induced Mitochondrial and Hepatocyte Injury by Promoting Mitochondrial Fusion and Function. PloS One. 2016;11(10):e0165638.

148. Forbes-Hernández TY, Giampieri F, Gasparrini M, Afrin S, Mazzoni L, Cordero MD, et al. Lipid Accumulation in HepG2 Cells Is Attenuated by Strawberry Extract through AMPK Activation. Nutrients. 2017 Jun 16;9(6).

149. Zhou B, Leng Y, Lei S-Q, Xia Z-Y. AMPK activation restores ischemic post‐conditioning cardioprotection in STZ‐induced type 1 diabetic rats: Role of autophagy. Mol Med Rep. 2017 Sep;16(3):3648–56.

150. Hayashi T, Hirshman MF, Kurth EJ, Winder WW, Goodyear LJ. Evidence for 5′AMP-Activated Protein Kinase Mediation of the Effect of Muscle Contraction on Glucose Transport. Diabetes. 1998 Aug 1;47(8):1369–73.

151. Friedrichsen M, Mortensen B, Pehmøller C, Birk JB, Wojtaszewski JFP. Exercise-induced AMPK activity in skeletal muscle: Role in glucose uptake and insulin sensitivity. Mol Cell Endocrinol. 2013 Feb 25;366(2):204–14.

152. Richter EA, Hargreaves M. Exercise, GLUT4, and Skeletal Muscle Glucose Uptake. Physiol Rev. 2013 Jul 1;93(3):993–1017.

153. Owen MR, Doran E, Halestrap AP. Evidence that metformin exerts its anti-diabetic effects through inhibition of complex 1 of the mitochondrial respiratory chain. Biochem J. 2000 Jun 15;348(Pt 3):607–14.

154. Bogachus LD, Turcotte LP. Genetic downregulation of AMPK-α isoforms uncovers the mechanism by which metformin decreases FA uptake and oxidation in skeletal muscle cells. Am J Physiol - Cell Physiol. 2010 Dec 1;299(6):C1549–61.

155. Rena G, Hardie DG, Pearson ER. The mechanisms of action of metformin. Diabetologia. 2017 Aug 3;

156. Suwa M, Egashira T, Nakano H, Sasaki H, Kumagai S. Metformin increases the PGC-1α protein and oxidative enzyme activities possibly via AMPK

phosphorylation in skeletal muscle in vivo. J Appl Physiol. 2006 Dec 1;101(6):1685–92.

157. Musi N, Hirshman MF, Nygren J, Svanfeldt M, Bavenholm P, Rooyackers O, et al. Metformin Increases AMP-Activated Protein Kinase Activity in Skeletal Muscle of Subjects With Type 2 Diabetes. Diabetes. 2002 Jul 1;51(7):2074–81.

158. Stumvoll M, Nurjhan N, Perriello G, Dailey G, Gerich JE. Metabolic effects of metformin in non-insulin-dependent diabetes mellitus. N Engl J Med. 1995 Aug 31;333(9):550–4.

159. Jørgensen SB, Viollet B, Andreelli F, Frøsig C, Birk JB, Schjerling P, et al. Knockout of the alpha2 but not alpha1 5'-AMP-activated protein kinase isoform abolishes 5-aminoimidazole-4-carboxamide-1-beta-4-ribofuranosidebut not contraction-induced glucose uptake in skeletal muscle. J Biol Chem. 2004 Jan 9;279(2):1070–9.

160. Naimi M, Tsakiridis T, Stamatatos TC, Alexandropoulos DI, Tsiani E. Increased skeletal muscle glucose uptake by rosemary extract through AMPK activation. Appl Physiol Nutr Metab Physiol Appliquée Nutr Métabolisme. 2015 Apr;40(4):407–13.

161. Naimi M, Vlavcheski F, Murphy B, Hudlicky T, Tsiani E. Carnosic acid as a component of rosemary extract stimulates skeletal muscle cell glucose uptake via AMPK activation. Clin Exp Pharmacol Physiol. 2016 Sep 22;

162. Vlavcheski F, Naimi M, Murphy B, Hudlicky T, Tsiani E. Rosmarinic Acid, a Rosemary Extract Polyphenol, Increases Skeletal Muscle Cell Glucose Uptake and Activates AMPK. Mol Basel Switz. 2017 Oct 7;22(10).

163. Salminen A, Hyttinen JMT, Kaarniranta K. AMP-activated protein kinase inhibits NF-κB signaling and inflammation: impact on healthspan and lifespan. J Mol Med Berl Ger. 2011 Jul;89(7):667–76.

164. Cacicedo JM, Yagihashi N, Keaney JF, Ruderman NB, Ido Y. AMPK inhibits fatty acid-induced increases in NF-kappaB transactivation in cultured human umbilical vein endothelial cells. Biochem Biophys Res Commun. 2004 Nov 26;324(4):1204–9.

165. Karin Schwarz. Phenolic Diterpenes from Rosemary and Sage. In: Functional Foods [Internet]. CRC Press; 2002 [cited 2016 Feb 22]. (Functional Foods and Nutraceuticals). Available from: http://www.crcnetbase.com/doi/abs/10.1201/9781420012873.ch6

166. Ulbricht C, Abrams TR, Brigham A, Ceurvels J, Clubb J, Curtiss W, et al. An evidence-based systematic review of rosemary (Rosmarinus officinalis) by the natural standard research collaboration. J Diet Suppl. 2010 Jan 1;7(4):351–413.

167. al-Sereiti MR, Abu-Amer KM, Sen P. Pharmacology of rosemary (Rosmarinus officinalis Linn.) and its therapeutic potentials. Indian J Exp Biol. 1999 Feb;37(2):124–30.

168. Ho C-T, Wang M, Wei G-J, Huang T-C, Huang M-T. Chemistry and antioxidative factors in rosemary and sage. Biofactors. 2000 Dec;13(1–4):161.

169. Zhang Y, Smuts JP, Dodbiba E, Rangarajan R, Lang JC, Armstrong DW. Degradation study of carnosic acid, carnosol, rosmarinic acid, and rosemary extract (Rosmarinus officinalis L.) assessed using HPLC. J Agric Food Chem. 2012 Sep 12;60(36):9305–14.

170. Hossain MB, Rai DK, Brunton NP, Martin-Diana AB, Barry-Ryan C. Characterization of phenolic composition in Lamiaceae spices by LC-ESI-MS/MS. J Agric Food Chem. 2010 Oct 13;58(19):10576–81.

171. Vallverdú-Queralt A, Regueiro J, Martínez-Huélamo M, Rinaldi Alvarenga JF, Leal LN, Lamuela-Raventos RM. A comprehensive study on the phenolic profile of widely used culinary herbs and spices: rosemary, thyme, oregano, cinnamon, cumin and bay. Food Chem. 2014 Jul 1;154:299–307.

172. Papageorgiou V, Gardeli C, Mallouchos A, Papaioannou M, Komaitis M. Variation of the chemical profile and antioxidant behavior of Rosmarinus officinalis L. and Salvia fruticosa Miller grown in Greece. J Agric Food Chem. 2008 Aug 27;56(16):7254–64.

173. Ibañez E, Kubátová A, Señoráns FJ, Cavero S, Reglero G, Hawthorne SB. Subcritical Water Extraction of Antioxidant Compounds from Rosemary Plants. J Agric Food Chem. 2003 Jan 1;51(2):375–82.

174. Mulinacci N, Innocenti M, Bellumori M, Giaccherini C, Martini V, Michelozzi M. Storage method, drying processes and extraction procedures strongly affect the phenolic fraction of rosemary leaves: an HPLC/DAD/MS study. Talanta. 2011 Jul 15;85(1):167–76.

175. Bai N, He K, Roller M, Lai C-S, Shao X, Pan M-H, et al. Flavonoids and Phenolic Compounds from Rosmarinus officinalis. J Agric Food Chem. 2010 May 12;58(9):5363–7.

176. Borrás Linares I, Arráez-Román D, Herrero M, Ibáñez E, Segura-Carretero A, Fernández-Gutiérrez A. Comparison of different extraction procedures for the comprehensive characterization of bioactive phenolic compounds in Rosmarinus officinalis by reversed-phase high-performance liquid chromatography with diode array detection coupled to electrospray time-of-flight mass spectrometry. J Chromatogr A. 2011 Oct 21;1218(42):7682–90.

177. Almela L, Sánchez-Muñoz B, Fernández-López JA, Roca MJ, Rabe V. Liquid chromatograpic-mass spectrometric analysis of phenolics and free radical

scavenging activity of rosemary extract from different raw material. J Chromatogr A. 2006 Jul 7;1120(1–2):221–9.

178. Herrero M, Plaza M, Cifuentes A, Ibáñez E. Green processes for the extraction of bioactives from Rosemary: Chemical and functional characterization via ultra-performance liquid chromatography-tandem mass spectrometry and in-vitro assays. J Chromatogr A. 2010 Apr 16;1217(16):2512–20.

179. Razboršek MI, Vončina DB, Doleček V, Vončina E. Determination of major phenolic acids, phenolic diterpenes and triterpenes in rosemary (Rosmarinus officinalis L.) by gas chromatography and mass spectrometry. Acta Chim Slov. 2007 Jan 1;54(1):60–7.

180. Liu J. Oleanolic acid and ursolic acid: Research perspectives. J Ethnopharmacol. 2005 Aug 22;100(1–2):92–4.

181. Vicente G, García-Risco MR, Fornari T, Reglero G. Isolation of carnosic acid from rosemary extracts using semi-preparative supercritical fluid chromatography. J Chromatogr A. 2013 Apr 19;1286:208–15.

182. Genena AK, Hense H, Smania Junior A, Machado de Souza S. Rosemary (Rosmarinus officinalis) – a study of the composition, antioxidant and antimicrobial activities of extracts obtained with supercritical carbon dioxide. Cienc E Tecnol Aliment. 2008 Jan 1;28(2):463–9.

183. Bent S. Herbal medicine in the United States: review of efficacy, safety, and regulation: grand rounds at University of California, San Francisco Medical Center. J Gen Intern Med. 2008 Jun;23(6):854–9.

184. Moreno S, Scheyer T, Romano CS, Vojnov AA. Antioxidant and antimicrobial activities of rosemary extracts linked to their polyphenol composition. Free Radic Res. 2006 Feb;40(2):223–31.

185. Naimi M, Vlavcheski F, Shamshoum H, Tsiani E. Rosemary Extract as a Potential Anti-Hyperglycemic Agent: Current Evidence and Future Perspectives. Nutrients. 2017 Sep 1;9(9).

186. Moore J, Yousef M, Tsiani E. Anticancer Effects of Rosemary (Rosmarinus officinalis L.) Extract and Rosemary Extract Polyphenols. Nutrients. 2016 Nov 17;8(11).

187. Yun YS, Noda S, Shigemori G, Kuriyama R, Takahashi S, Umemura M, et al. Phenolic Diterpenes from Rosemary Suppress cAMP Responsiveness of Gluconeogenic Gene Promoters. Phytother Res. 2013;(6):906.

188. Tu Z, Moss-Pierce T, Ford P, Jiang T. Rosemary (Rosmarinus officinalis L.) Extract Regulates Glucose and Lipid Metabolism by Activating AMPK and PPAR Pathways in HepG2 Cells. J Agric FOOD Chem. 2013 Mar 20;61(11):2803–10.

189. Wang T. Carnosic acid (CA) prevents lipid accumulation in hepatocytes through the EGFR/MAPK pathway. J Gastroenterol. 2012 Jul 1;47(7):805–13.

190. Renzulli C, Galvano F, Pierdomenico L, Speroni E, Guerra M. Effects of rosmarinic acid against aflatoxin B-1 and ochratoxin-A-induced cell damage in a human hepatoma cell line (Hep G2). J Appl Toxicol. 2004 Aug;24(4):289–96.

191. Babish JG, Pacioretty LM, Bland JS, Minich DM, Hu J, Tripp ML. Antidiabetic screening of commercial botanical products in 3T3-L1 adipocytes and db/db mice. J Med Food. 2010 Jun;13(3):535–547 13p.

192. Takahashi T, Tabuchi T, Tamaki Y, Kosaka K, Takikawa Y, Satoh T. Carnosic acid and carnosol inhibit adipocyte differentiation in mouse 3T3-L1 cells through induction of phase2 enzymes and activation of glutathione metabolism. Biochem Biophys Res Commun. 2009;(3):549.

193. Gaya M, Repetto V, Toneatto J, Anesini C, Piwien-Pilipuk G, Moreno S. Antiadipogenic effect of carnosic acid, a natural compound present in Rosmarinus officinalis, is exerted through the C/EBPs and PPARγ pathways at the onset of the differentiation program. Biochim Biophys Acta -- Gen Subj. 2013 Jan 1;1830(6):3796–806.

194. Koga K, Shibata H, Yoshino K, Nomoto K. Effects of 50% Ethanol Extract from Rosemary (Rosmarinus officinalis) on α-Glucosidase Inhibitory Activity and the Elevation of Plasma Glucose Level in Rats, and Its Active Compound. J Food Sci. 2006 Sep 1;71(7):S507–12.

195. Ingrid F, Matthias F. M. Traditionally used plants in diabetes therapy: phytotherapeutics as inhibitors of alpha-amylase activity / Plantas tradicionalmente utilizadas na terapia da diabetes: fitomedicamentos como inibidores da atividade alfa-amilase. Rev Bras Farmacogn. 2006;(1):1.

196. McCue PP, Shetty K. Inhibitory effects of rosmarinic acid extracts on porcine pancreatic amylase in vitro. Asia Pac J Clin Nutr. 2004;13(1):101–6.

197. Yasser Bustanji AI. Inhibition of hormone sensitive lipase and pancreatic lipase by Rosmarinus officinalis extract and selected phenolic constituents. J Med Plants Res. 2010;4(21):2235–42.

198. Ibarra A, Cases J, Roller M, Chiralt-Boix A, Coussaert A, Ripoll C. Carnosic acid-rich rosemary (Rosmarinus officinalis L.) leaf extract limits weight gain and improves cholesterol levels and glycaemia in mice on a high-fat diet. Br J Nutr. 2011 Oct;106(8):1182–9.

199. Lipina C, Hundal HS. Carnosic acid stimulates glucose uptake in skeletal muscle cells via a PME-1/PP2A/PKB signalling axis. Cell Signal. 2014 Nov 1;26:2343–9.

200. Long Cui, Mun Ock Kim, Jee Hee Seo, Il Soon Kim, Nam Ye Kim, Sun Hwa Lee, et al. Abietane diterpenoids of Rosmarinus officinalis and their diacylglycerol acyltransferase-inhibitory activity. Food Chem. 2012 Jan 1;132(4):1775–80.

201. Erenmemisoglu A, Saraymen R, Ustun S. Effect of a Rosmarinus officinalis leave extract on plasma glucose levels in normoglycaemic and diabetic mice. Pharm. 1997 Aug;52(8):645–6.

202. Khalil O, Ramadan K, Danial E, Alnahdi H, Ayaz N. Antidiabetic activity of Rosmarinus officinalis and its relationship with the antioxidant property. Afr J Pharm Pharmacol. 2012 Apr;6(14):1031–6.

203. Al-Jamal A-R, Alqadi T. Effects of Rosemary (Rosmarinus officinalis) on Lipid Profile of Diabetic Rats. Jordan J Biol Sci. 2011 Dec;4(4):199–203.

204. Alnahdi H S. Effect of Rosmarinus Officinalis Extract on some Cardiac Enzymes of Streptozotocin-induced Diabetic Rats. J Health Sci. 2012;2(4):33–7.

205. Emam M. Comparative evaluation of antidiabetic activity of Rosmarinus officinalis L. and Chamomile recutita in streptozotocin induced diabetic rats. Agric Biol J N Am. 2012 Jun;3(6):247–52.

206. Ramadan KS, Khalil OA, Danial EN, Alnahdi HS, Ayaz NO. Hypoglycemic and hepatoprotective activity of Rosmarinus officinalis extract in diabetic rats. J Physiol Biochem. 2013 Dec;69(4):779–83.

207. Soliman GZA. Effect of Rosmarinus Officinalis on Lipid Profile of Streptozotocin-induced Diabetic Rats. Egypt J Hosp Med. 2013 Oct;53:809–15.

208. Bakırel T, Bakırel U, Keleş OÜ, Ülgen SG, Yardibi H. In vivo assessment of antidiabetic and antioxidant activities of rosemary (Rosmarinus officinalis) in alloxan-diabetic rabbits. J Ethnopharmacol. 2008 Feb 28;116(1):64–73.

209. Alhader A, Hasan Z, Aqel M. Hyperglycemic and Insulin Release Inhibitory Effects of Rosmarinus-Officinalis. J Ethnopharmacol. 1994 Jul 22;43(3):217–21.

210. Kensara O, ElSawy N, Altaf F, Header E. Hypoglycemic and Hepato-protective Effects of Rosmarinus officinalis in Experimental Diabetic Rats. UQU Med J. 2010;Vol. 1(2):98–113.

211. Tavafi M, Ahmadvand H, Khalatbari A, Tamjidipoor A. Rosmarinic Acid Ameliorates Diabetic Nephropathy in Uninephrectomized Diabetic Rats. Iran J Basic Med Sci. 2011 Jun 5;14(3):275–83.

212. Nusier MK, Bataineh HN, Daradkah HM. Adverse effects of rosemary (Rosmarinus officinalis L.) on reproductive function in adult male rats. Exp Biol Med Maywood NJ. 2007 Jun;232(6):809–13.

213. Wang T, Takikawa Y, Satoh T, Yoshioka Y, Kosaka K, Tatemichi Y, et al. Carnosic acid prevents obesity and hepatic steatosis in ob/ob mice. Hepatol Res. 2011 Jan;41(1):87–92.

214. Ninomiya K, Matsuda H, Shimoda H, Norihisa N, Kasajima N, Yoshino T, et al. Carnosic acid, a new class of lipid absorption inhibitor from sage. Bioorg Med Chem Lett. 2004 Apr 19;14(8):1943–6.

215. Harach T, Aprikian O, Monnard I, Moulin J, Membrez M, Beolor J-C, et al. Rosemary (Rosmarinus officinalis L.) leaf extract limits weight gain and liver steatosis in mice fed a high-fat diet. Planta Med. 2010;(6):566.

216. Al Sheyab FM, Abuharfeil N, Salloum L, Bani Hani R, Awad DS. The Effect of Rosemary (Rosmarinus officinalis. L) Plant Extracts on the Immune Response and Lipid Profile in Mice. J Biol Life Sci [Internet]. 2011 Nov 30 [cited 2016 Feb 22];3(1). Available from: http://www.macrothink.org/journal/index.php/jbls/article/view/906

217. Afonso MS, Silva AM de O, Carvalho EBT, Rivelli DP, Barros SBM, Rogero MM, et al. Phenolic compounds from rosemary (Rosmarinus officinalis L.) attenuate oxidative stress and reduce blood cholesterol concentrations in diet-induced hypercholesterolemic rats. Nutr Metab. 2013 Jan 1;10(Feb.):9.

218. Vanithadevi B, Anuradha V BalasCarani Venkataraman. Effect of rosmarinic acid on insulin sensitivity, glyoxalase system and oxidative events in liver of fructose-fed mice. Int J Diabetes Metab. 2008;(16):35–44.

219. Romo Vaquero M, Yáñez-Gascón M-J, García Villalba R, Larrosa M, Fromentin E, Ibarra A, et al. Inhibition of Gastric Lipase as a Mechanism for Body Weight and Plasma Lipids Reduction in Zucker Rats Fed a Rosemary Extract Rich in Carnosic Acid. PLoS ONE. 2012 Jun 22;7(6):e39773.

220. Romo Vaquero M, García Villalba R, Larrosa M, Yáñez-Gascón MJ, Fromentin E, Flanagan J, et al. Bioavailability of the major bioactive diterpenoids in a rosemary extract: metabolic profile in the intestine, liver, plasma, and brain of Zucker rats. Mol Nutr Food Res. 2013 Oct;57(10):1834–46.

221. Labban L, Mustafa UE-S, Ibrahim YM. The Effects of Rosemary (Rosmarinus officinalis) Leaves Powder on Glucose Level, Lipid Profile and Lipid Perodoxation. Int J Clin Med. 2014;05(06):297–304.

222. Sinkovic A, Suran D, Lokar L, Fliser E, Skerget M, Novak Z, et al. Rosemary extracts improve flow-mediated dilatation of the brachial artery and plasma PAI-1 activity in healthy young volunteers. Phytother Res PTR. 2011 Mar;25(3):402–7.

223. Lukaczer D, Darland G, Tripp M, Liska D, Lerman RH, Schiltz B, et al. A pilot trial evaluating Meta050, a proprietary combination of reduced iso-alpha acids, rosemary

extract and oleanolic acid in patients with arthritis and fibromyalgia. Phytother Res PTR. 2005 Oct;19(10):864–9.

224. Wilding JPH. The importance of free fatty acids in the development of Type 2 diabetes. Diabet Med J Br Diabet Assoc. 2007 Sep;24(9):934–45.

225. DeFronzo R. Metformin-associated lactic acidosis: Current perspectives on causes and risk. 65(2):20–9.

226. Erenmemisoglu A. Effect of a Rosmarinus officinalis leave extract on plasma glucose levels in normoglycaemic and diabetic mice. Pharmazie. 1997 Aug;52(8):645–6.

227. Runtuwene J, Cheng K-C, Asakawa A, Amitani H, Amitani M, Morinaga A, et al. Rosmarinic acid ameliorates hyperglycemia and insulin sensitivity in diabetic rats, potentially by modulating the expression of PEPCK and GLUT4. Drug Des Devel Ther. 2016 Jul 7;10:2193–202.

228. Bakirel T, Bakirel U, Keles OU, Ulgen SG, Yardibi H. In vivo assessment of antidiabetic and antioxidant activities of rosemary (Rosmarinus officinalis) in alloxan-diabetic rabbits. J Ethnopharmacol. 2008 Feb 28;116(1):64–73.

229. Romo Vaquero M, Yáñez-Gascón M-J, García Villalba R, Larrosa M, Fromentin E, Ibarra A, et al. Inhibition of Gastric Lipase as a Mechanism for Body Weight and Plasma Lipids Reduction in Zucker Rats Fed a Rosemary Extract Rich in Carnosic Acid. PLoS ONE [Internet]. 2012 Jun 22 [cited 2016 Feb 22];7(6). Available from: http://www.ncbi.nlm.nih.gov/pmc/articles/PMC3382157/

230. Ibarra A, Cases J, Roller M, Chiralt-Boix A, Coussaert A, Ripoll C. Carnosic acid-rich rosemary (Rosmarinus officinalis L.) leaf extract limits weight gain and improves cholesterol levels and glycaemia in mice on a high-fat diet. Br J Nutr. 2011 Oct;106(8):1182–9.

231. Afonso MS, de O Silva AM, Carvalho EB, Rivelli DP, Barros SB, Rogero MM, et al. Phenolic compounds from Rosemary (Rosmarinus officinalis L.) attenuate oxidative stress and reduce blood cholesterol concentrations in diet-induced hypercholesterolemic rats. Nutr Metab. 2013;10(1):19.

232. Klip A, Li G, Walker D. Insulin binding to differentiating muscle cells in culture. Can J Biochem Cell Biol. 1983 Jul 1;61(7):644–9.

233. Beguinot F, Kahn CR, Moses AC, Smith RJ. The development of insulin receptors and responsiveness is an early marker of differentiation in the muscle cell line L6. Endocrinology. 1986 Jan;118(1):446–55.

234. Klip A, Pâquet MR. Glucose transport and glucose transporters in muscle and their metabolic regulation. Diabetes Care. 1990 Mar;13(3):228–43.

235. McMahon DK, Anderson PA, Nassar R, Bunting JB, Saba Z, Oakeley AE, et al. C2C12 cells: biophysical, biochemical, and immunocytochemical properties. Am J Physiol. 1994 Jun;266(6 Pt 1):C1795-1802.

236. Manabe Y, Miyatake S, Takagi M, Nakamura M, Okeda A, Nakano T, et al. Characterization of an Acute Muscle Contraction Model Using Cultured C2C12 Myotubes. PLoS ONE [Internet]. 2012 Dec 31;7(12). Available from: http://www.ncbi.nlm.nih.gov/pmc/articles/PMC3534077/

237. Goodyear LJ, King PA, Hirshman MF, Thompson CM, Horton ED, Horton ES. Contractile activity increases plasma membrane glucose transporters in absence of insulin. Am J Physiol. 1990 Apr;258(4 Pt 1):E667-672.

238. Mitsumoto Y, Burdett E, Grant A, Klip A. Differential expression of the GLUT1 and GLUT4 glucose transporters during differentiation of L6 muscle cells. Biochem Biophys Res Commun. 1991 Mar 15;175(2):652–9.

239. Klip A, Marette A. Acute and chronic signals controlling glucose transport in skeletal muscle. J Cell Biochem. 1992 Jan;48(1):51–60.

240. Perdomo G, Commerford SR, Richard A-MT, Adams SH, Corkey BE, O'Doherty RM, et al. Increased beta-oxidation in muscle cells enhances insulin-stimulated glucose metabolism and protects against fatty acid-induced insulin resistance despite intramyocellular lipid accumulation. J Biol Chem. 2004 Jun 25;279(26):27177–86.

241. Jaiswal N, Gunaganti N, Maurya CK, Narender T, Tamrakar AK. Free fatty acid induced impairment of insulin signaling is prevented by the diastereomeric mixture of calophyllic acid and isocalophyllic acid in skeletal muscle cells. Eur J Pharmacol. 2015 Jan 5;746(Supplement C):70–7.

242. Deng Y-T, Chang T-W, Lee M-S, Lin J-K. Suppression of Free Fatty Acid-Induced Insulin Resistance by Phytopolyphenols in C2C12 Mouse Skeletal Muscle Cells. J Agric Food Chem. 2012 Feb 1;60(4):1059–66.

243. Mazibuko SE, Joubert E, Johnson R, Louw J, Opoku AR, Muller CJF. Aspalathin improves glucose and lipid metabolism in 3T3-L1 adipocytes exposed to palmitate. Mol Nutr Food Res. 2015 Nov 1;59(11):2199–208.

244. Wu W, Tang S, Shi J, Yin W, Cao S, Bu R, et al. Metformin attenuates palmitic acid-induced insulin resistance in L6 cells through the AMP-activated protein kinase/sterol regulatory element-binding protein-1c pathway. Int J Mol Med. 2015 Jun;35(6):1734–40.

245. Capel F, Cheraiti N, Acquaviva C, Hénique C, Bertrand-Michel J, Vianey-Saban C, et al. Oleate dose-dependently regulates palmitate metabolism and insulin signaling in C2C12 myotubes. Biochim Biophys Acta BBA - Mol Cell Biol Lipids. 2016 Dec;1861(12, Part A):2000–10.

246. Luan Y, Zhang F, Cheng Y, Liu J, Huang R, Yan M, et al. Hemin Improves Insulin Sensitivity and Lipid Metabolism in Cultured Hepatocytes and Mice Fed a High-Fat Diet. Nutrients [Internet]. 2017 Jul 26;9(8). Available from: https://www.ncbi.nlm.nih.gov/pmc/articles/PMC5579599/

247. Jung TW, Kim H-C, Abd El-Aty AM, Jeong JH. Protectin DX ameliorates palmitate- or high-fat diet-induced insulin resistance and inflammation through an AMPK-PPARα-dependent pathway in mice. Sci Rep [Internet]. 2017 May 3;7. Available from: https://www.ncbi.nlm.nih.gov/pmc/articles/PMC5431091/

248. Anhê GF, Okamoto MM, Kinote A, Sollon C, Lellis-Santos C, Anhê FF, et al. Quercetin decreases inflammatory response and increases insulin action in skeletal muscle of ob/ob mice and in L6 myotubes. Eur J Pharmacol. 2012 Aug 15;689(1–3):285–93.

249. Yin J, Gu L, Wang Y, Fan N, Ma Y, Peng Y. Rapamycin Improves Palmitate-Induced ER Stress/NFκB Pathways Associated with Stimulating Autophagy in Adipocytes. Mediators Inflamm [Internet]. 2015;2015. Available from: https://www.ncbi.nlm.nih.gov/pmc/articles/PMC4310475/

250. Sadeghi A, Seyyed Ebrahimi SS, Golestani A, Meshkani R. Resveratrol Ameliorates Palmitate-Induced Inflammation in Skeletal Muscle Cells by Attenuating Oxidative Stress and JNK/NF-κB Pathway in a SIRT1-Independent Mechanism. J Cell Biochem. 2017 Sep 1;118(9):2654–63.

251. Kim BS, Cha H-N, Kim Y-W, Kim J-Y, Dan J-M, Park S-Y. Inhibition of lipid infusion-induced skeletal muscle insulin resistance by cotreatment with tempol and glutathione in mice. J Pharmacol Sci. 2009 Jul;110(3):370–80.

252. Araújo EP, Souza D, T C, Ueno M, Cintra DE, Bertolo MB, et al. Infliximab Restores Glucose Homeostasis in an Animal Model of Diet-Induced Obesity and Diabetes. Endocrinology. 2007 Dec 1;148(12):5991–7.

253. Rivas DA, Yaspelkis BB, Hawley JA, Lessard SJ. Lipid-induced mTOR activation in rat skeletal muscle reversed by exercise and 5'-aminoimidazole-4-carboxamide-1-beta-D-ribofuranoside. J Endocrinol. 2009 Sep;202(3):441–51.

254. Wang X, Yu W, Nawaz A, Guan F, Sun S, Wang C. Palmitate Induced Insulin Resistance by PKCtheta-Dependent Activation of mTOR/S6K Pathway in C2C12 Myotubes. Exp Clin Endocrinol Diabetes. 2010 Oct;118(09):657–61.

255. Woo JH, Shin KO, Lee YH, Jang KS, Bae JY, Roh HT. Effects of treadmill exercise on skeletal muscle mTOR signaling pathway in high-fat diet-induced obese mice. J Phys Ther Sci. 2016 Apr;28(4):1260–5.

256. Kwon B, Querfurth HW. Palmitate activates mTOR/p70S6K through AMPK inhibition and hypophosphorylation of raptor in skeletal muscle cells: Reversal by oleate is similar to metformin. Biochimie. 2015 Nov;118:141–50.

257. Liu X, Yuan H, Niu Y, Niu W, Fu L. The role of AMPK/mTOR/S6K1 signaling axis in mediating the physiological process of exercise-induced insulin sensitization in skeletal muscle of C57BL/6 mice. Biochim Biophys Acta. 2012 Nov;1822(11):1716–26.

258. Liu S, Jing F, Yu C, Gao L, Qin Y, Zhao J. AICAR-Induced Activation of AMPK Inhibits TSH/SREBP-2/HMGCR Pathway in Liver. PLoS ONE [Internet]. 2015 May 1;10(5). Available from: https://www.ncbi.nlm.nih.gov/pmc/articles/PMC4416759/

259. Cantó C, Auwerx J. AMP-activated protein kinase and its downstream transcriptional pathways. Cell Mol Life Sci CMLS. 2010 Oct;67(20):3407–23.

260. Mihaylova MM, Shaw RJ. The AMP-activated protein kinase (AMPK) signaling pathway coordinates cell growth, autophagy, & metabolism. Nat Cell Biol. 2011 Sep 2;13(9):1016–23.

261. Shaw RJ. LKB1 and AMPK control of mTOR signalling and growth. Acta Physiol Oxf Engl. 2009 May;196(1):65–80.

262. Woods A, Johnstone SR, Dickerson K, Leiper FC, Fryer LGD, Neumann D, et al. LKB1 Is the Upstream Kinase in the AMP-Activated Protein Kinase Cascade. Curr Biol. 2003 Nov 11;13(22):2004–8.

263. Sakamoto K, McCarthy A, Smith D, Green KA, Hardie DG, Ashworth A, et al. Deficiency of LKB1 in skeletal muscle prevents AMPK activation and glucose uptake during contraction. EMBO J. 2005 May 18;24(10):1810–20.

264. Turner N, Li J-Y, Gosby A, To SWC, Cheng Z, Miyoshi H, et al. Berberine and Its More Biologically Available Derivative, Dihydroberberine, Inhibit Mitochondrial Respiratory Complex I: A Mechanism for the Action of Berberine to Activate AMP-Activated Protein Kinase and Improve Insulin Action. Diabetes. 2008 May 1;57(5):1414–8.

265. Zhang C-S, Hawley SA, Zong Y, Li M, Wang Z, Gray A, et al. Fructose-1,6-bisphosphate and aldolase mediate glucose sensing by AMPK. Nature. 2017 Aug 3;548(7665):112–6.

266. Zhao Y, Sedighi R, Wang P, Chen H, Zhu Y, Sang S. Carnosic acid as a major bioactive component in rosemary extract ameliorates high-fat-diet-induced obesity and metabolic syndrome in mice. J Agric Food Chem. 2015 May 20;63(19):4843–52.

267. Romo-Vaquero M, Larrosa M, Yáñez-Gascón MJ, Issaly N, Flanagan J, Roller M, et al. A rosemary extract enriched in carnosic acid improves circulating adipocytokines and modulates key metabolic sensors in lean Zucker rats: Critical and contrasting differences in the obese genotype. Mol Nutr Food Res. 2014 May;58(5):942–53.

268. Park M-Y, Mun ST. Dietary carnosic acid suppresses hepatic steatosis formation via regulation of hepatic fatty acid metabolism in high-fat diet-fed mice. Nutr Res Pract. 2013 Aug;7(4):294–301.

269. Kaneto H, Katakami N, Matsuhisa M, Matsuoka T. Role of reactive oxygen species in the progression of type 2 diabetes and atherosclerosis. Mediators Inflamm. 2010;2010:453892.

270. Ly LD, Xu S, Choi S-K, Ha C-M, Thoudam T, Cha S-K, et al. Oxidative stress and calcium dysregulation by palmitate in type 2 diabetes. Exp Mol Med. 2017 Feb;49(2):e291.

271. Yuzefovych L, Wilson G, Rachek L. Different effects of oleate vs. palmitate on mitochondrial function, apoptosis, and insulin signaling in L6 skeletal muscle cells: role of oxidative stress. Am J Physiol - Endocrinol Metab. 2010 Dec;299(6):E1096–105.

272. Mäkinen S, Nguyen YH, Skrobuk P, Koistinen HA. Palmitate and oleate exert differential effects on insulin signalling and glucose uptake in human skeletal muscle cells. Endocr Connect. 2017 Jun 5;6(5):331–9.

273. Pinho RA, Sepa-Kishi DM, Bikopoulos G, Wu MV, Uthayakumar A, Mohasses A, et al. High-fat diet induces skeletal muscle oxidative stress in a fiber type-dependent manner in rats. Free Radic Biol Med. 2017 Sep;110:381–9.

274. Wellen KE, Hotamisligil GS. Inflammation, stress, and diabetes. J Clin Invest. 2005 May;115(5):1111–9.

275. Zhou J, Deo BK, Hosoya K, Terasaki T, Obrosova IG, Brosius FC, et al. Increased JNK phosphorylation and oxidative stress in response to increased glucose flux through increased GLUT1 expression in rat retinal endothelial cells. Invest Ophthalmol Vis Sci. 2005 Sep;46(9):3403–10.

276. Schwabe RF, Brenner DA. Mechanisms of Liver Injury. I. TNF-α-induced liver injury: role of IKK, JNK, and ROS pathways. Am J Physiol - Gastrointest Liver Physiol. 2006 Apr 1;290(4):G583–9.

277. Braga M, Hikim APS, Datta S, Ferrini MG, Brown D, Kovacheva EL, et al. Involvement of oxidative stress and caspase 2-mediated intrinsic pathway signaling in age-related increase in muscle cell apoptosis in mice. Apoptosis. 2008 Jun 1;13(6):822–32.

278. Jing E, Emanuelli B, Hirschey MD, Boucher J, Lee KY, Lombard D, et al. Sirtuin-3 (Sirt3) regulates skeletal muscle metabolism and insulin signaling via altered mitochondrial oxidation and reactive oxygen species production. Proc Natl Acad Sci. 2011 Aug 30;108(35):14608–13.

279. Baba S, Osakabe N, Natsume M, Terao J. Orally administered rosmarinic acid is present as the conjugated and/or methylated forms in plasma, and is degraded and metabolized to conjugated forms of caffeic acid, ferulic acid and m-coumaric acid. Life Sci. 2004 May 28;75(2):165–78.

280. Aguilar F. Use of rosemary extracts as a food additive: Scientific opinion of the panel on food additives, flavourings, processing aids, and materials in contact with food. Eur Food Saf Auth J. 2008;721:1–29.

281. Konishi Y, Hitomi Y, Yoshida M, Yoshioka E. Pharmacokinetic study of caffeic and rosmarinic acids in rats after oral administration. J Agric Food Chem. 2005 Jun 15;53(12):4740–6.

282. Dickmann LJ, VandenBrink BM, Lin YS. In vitro hepatotoxicity and cytochrome P450 induction and inhibition characteristics of carnosic acid, a dietary supplement with antiadipogenic properties. Drug Metab Dispos Biol Fate Chem. 2012 Jul;40(7):1263–7.

283. Bel-Rhlid R, Crespy V, Pagé-Zoerkler N, Nagy K, Raab T, Hansen C-E. Hydrolysis of rosmarinic acid from rosemary extract with esterases and Lactobacillus johnsonii in vitro and in a gastrointestinal model. J Agric Food Chem. 2009 Sep 9;57(17):7700–5.

284. Konishi Y, Kobayashi S. Transepithelial transport of rosmarinic acid in intestinal Caco-2 cell monolayers. Biosci Biotechnol Biochem. 2005 Mar;69(3):583–91.

285. Karthikkumar V, Sivagami G, Viswanathan P, Nalini N. Rosmarinic acid inhibits DMH-induced cell proliferation in experimental rats. J Basic Clin Physiol Pharmacol. 2015 Mar;26(2):185–200.

286. Yan M, Li G, Petiwala SM, Householter E, Johnson JJ. Standardized rosemary (Rosmarinus officinalis) extract induces Nrf2/sestrin-2 pathway in colon cancer cells. J Funct Foods. 2015 Mar 1;13(Supplement C):137–47.

287. Baba S, Osakabe N, Natsume M, Yasuda A, Muto Y, Hiyoshi K, et al. Absorption, metabolism, degradation and urinary excretion of rosmarinic acid after intake of Perilla frutescens extract in humans. Eur J Nutr. 2005 Feb;44(1):1–9.

288. Tsukumo DML, Carvalho-Filho MA, Carvalheira JBC, Prada PO, Hirabara SM, Schenka AA, et al. Loss-of-function mutation in Toll-like receptor 4 prevents diet-induced obesity and insulin resistance. Diabetes. 2007;56(8):1986–98.

289. Ivovic A, Oprescu AI, Koulajian K, Mori Y, Eversley JA, Zhang L, et al. IKKβ inhibition prevents fat-induced beta cell dysfunction in vitro and in vivo in rodents. Diabetologia. 2017 Oct;60(10):2021–32.

Appendix:

Buffers and Solutions:

A list for the preparation of each buffer and solution used to perform the experiments in the methods and results section will be presented below.

Glucose Uptake Assay: HBS Washing Buffer: 140mM NaCI, 5mM KCI, 20mM HEPES, 2.5mM $MgSO_4$, 1mM $CaCl_2$, dilute with DD water and fill to 800mL, adjust pH to 7.4 and then fill to l L. Total Radioactive Buffer: HBS buffer, dilute 1:1000 hot 2-[^{3}H] deoxy-D-glucose, and 1:1000 cold 2-[^{3}H] deoxy-D-glucose in HBS.

Non-specific radioactive buffer: Use total radioactive buffer, add 1:1000 cytochalasin B. 0.9% NaC1: Add 0.9g NaCI per 100ml DD water. 0.05N NaOH: Add 1ml 5N NaOH to 99ml DD water.

Fatty Acid (FA) Palmitate Solutions: Palmitic acid (41mg) was dissolved in bubbling O.IN NaOH (1.6mL) and diluted in prewarmed (45-50°C) 9.7% (WN) BSA solution (18.4mL).

Cell Lysis:

PBS Washing Buffer: 137mM NaCI, 2.7mM KCI, l.5mM KH_2PO_4, 8.lmM Na_2HPO_4, 0.68mM $CaCl_2$, 0.49mM $MgCl_2$, add water to lL and adjust pH to 7.4. SDS Sample Buffer: 62.5mM Tris-HCI (PH 6.8), 2% w/v SDS, 10% glycerol, 0.01 % bromophenol blue, add 0.05% p-mercaptoethanol before use.

Cell Lysis Buffer: 20mM Tris (PH 7.5), lS0mMNaCI, 1mM EDTA, 1mM EGTA, 1% Triton X-100, 2.5mM sodium pyrophosphate, 1mM p-glycerolphosphate, 1mM Na_3VO_4, 1 J.lg/mlleupeptin, add 1 mM PMSF before use and chill on ice.

Western Blotting:

l.5M Tris-HCI (pH 8.8): 27.23g Tris base (18.15g/100ml), 80ml deionized water, adjust to pH 8.8 with 6N HCL. Bring to total volume 150ml with deionized water.

0.5M Tris-HCI (PH 6.8): 6g Tris base, 60ml deionized water, adjust to pH 6.8 with 6N HCI and bring total volume to 100ml with deionized water.

Resolving Gel Buffer: 12.3 ml DD water, 9.9 ml 30% Acrylamide/ Bis solution, 7.5ml 1.5M Tris- Hcl, pH 8.8, 0.3ml 10% w/v SDS. Right before pouring the gel, add 150µl 10% APS (0.01g/ 100 µl) made fresh daily and l5 µl TEMED and swirl.

Stacking Gel Buffer: l8.3 ml DD water, 3.9 ml 30% Acrylamide/ Bis solution, 7.5ml 0.5M Tris-HCI, pH 6.8, 0.3 ml 10% w/v SDS. Right before pouring the gel, add l50µl % APS (0.01g/ 100 µl) made fresh daily and 30 µl TEMED and swirl.

10x TBS (Tris- buffered saline): 24.2g Tris base, 80g NaCI, adjust pH to 7.6 with HCl. Use at 1x TBS. Dissolve in l L of water.

Blocking Buffer: 1x TBS, 0.1 % tween 20, 5% w/v non-fat dry milk. Dissolved in water.

Primary Antibody Dilution Buffer: 2ml 10x TBS, 18ml water, 1.0g BSA, 20ul Tween-20.

Wash Buffer:TBS/T: 1x TBS and 0.1% Tween- 20.

10x Electrode Running Buffer: 15.15g Tris base, 72g Glycine, 5.0g SDS. Dissolve and bring volume to 500ml with DD water. Do not adjust pH with acid or base. Dilute 50ml of 10x stock with 450ml water before use.

Transfer Buffer: 25mM Tris base, 0.2M glycine, 20% methanol, dissolved in 800mL of water.